Lin28b regulation of early-life B lymphopoiesis. A model system to study how self-reactive B cells develop in early life.

Åkerstrand, Hugo

2023

Document Version:
Publisher's PDF, also known as Version of record

Lin28b regulation of early-life B lymphopoiesis

A model system to study how self-reactive B cells develop in early life

HUGO ÅKERSTRAND
MOLECULAR HEMATOLOGY | FACULTY OF MEDICINE | LUND UNIVERSITY

Printed by Media-Tryck, Lund 2023 NORDIC SWAN ECOLABEL 3041 0903

LUND UNIVERSITY

FACULTY OF MEDICINE

Department of Molecular Hematology

Lund University, Faculty of Medicine
Doctoral Dissertation Series 2023:89
ISBN 978-91-8021-429-2
ISSN 1652-8220

Lin28b regulation of early-life B lymphopoiesis

A model system to study how self-reactive B cells develop in early life

Hugo Åkerstrand

LUNDS UNIVERSITET

DOCTORAL DISSERTATION

Doctoral dissertation for the degree of Doctor of Philosophy (PhD) at the Faculty of Medicine at Lund University to be publicly defended on 20th of June at 09.00 in Segerfalkssalen, BMC A10, Lund, Sweden

Faculty opponent
Brian Rudd

Organization: LUND UNIVERSITY

Document name: **DOCTORAL DISSERTATION** **Date of issue:** 2023-06-20

Author: Hugo Åkerstrand **Sponsoring organization:**

Title and subtitle: *Lin28b* regulation of early-life B lymphopoiesis: a model system to study how self-reactive B cells develop in early life

Abstract: Antibody secretion by the B cell is an integral part of our immune system. Since our body contains millions of B cells expressing unique antibodies, together they afford an impressive range of antigen specificities and protection against pathogens. This diversity originates from molecular events during B cell development, which outputs mature B cells capable of recognizing foreign antigen while being tolerant towards self-antigen of the own body. However, there are exceptions to this central rule of immune tolerance and weakly self-reactive antibodies are abundant in the blood of healthy humans and mice. In the mouse, many of these self-reactive antibodies are produced by the B-1a subset of B cells, a rare cell type that was primarily generated in early-life and then maintain by self-renewal in adults. As such, the early-life origin of B-1a cells means that B cell development in early-life allows for a degree of self-reactivity, whereas self-reactivity is strictly counter selected in adults. Therefore, B-1a cell development makes for a handy gateway population to study self-reactive B cell development in early-life. An important advancement in our understanding of B-1a development was the identification of its dependence on LIN28B, an RNA-binding protein that exerts post-transcriptional gene regulation. The exact LIN28B mechanism in B cell progenitors has not been known and the subject matter of this thesis.

Given how self-reactive B cells are normally counter selected during B cell development, we hypothesized that LIN28B must instead enable positive selection of such self-reactive specificities. Indeed, by focusing on the Imm-B cell stage of development where self-reactivity is normally censored, we identified a subset that express the surface marker CD5, have elevated levels of BCR signalling, and develop into the B-1a subset. To identify the underlying mechanism, we explored the LIN28B mRNA interactome in B cell progenitors and identified binding of known LIN28B targets from studies outside of B cell development, including transcripts for ribosomal proteins. This led to the discovery of elevated protein synthesis as a novel hallmark of neonatal B cell development, being particularly elevated in the CD5 positive Imm-B subset. Importantly, B cell development during early-life crashes under a slight reduction in protein synthesis but becomes normal once the neonate matures and switches to producing adult type, CD5 negative Imm-B cells. Finally, we then explored how a LIN28B-mediated increase in glucose uptake might support B-1a cell development, by providing the cell with more biomass and ATP. This did indeed identify a LIN28B-dependent increase in glucose uptake by all the B cell progenitors but the impact on specifically B-1a development is still unclear and more work is necessary to fully understand any connection.

Taken together, our work establishes how LIN28B expression in early life augments B cell progenitor metabolism and facilitates positive selection of self-reactive CD5 positive Imm-B cells to produce the B-1a subset. Since LIN28B is capable of inducing positive selection of self-reactive clones that normally are negatively selected during B cell development, these findings are not only of interest to B-1a development but also for the understanding of the important central tolerance mechanism. In addition, insights during our studies indicate that LIN28B might affect development before the Imm-B cell stage to enable the output of CD5 positive Imm-B cells, which is an ongoing subject of investigation beyond this thesis work.

Key words: B cell development, LIN28B, positive selection, central tolerance, B-1a, metabolism

Language: English **ISSN:** 1652-8220

ISBN: 978-91-8021-429-2

Recipient's notes **Number of pages**: 65

Price Security classification

Lin28b regulation of early-life B lymphopoiesis

A model system to study how self-reactive B cells develop in early life

Hugo Åkerstrand

LUNDS
UNIVERSITET

Cover photo: Svetlana Soboleva

Faculty of Medicine
Department of Molecular Hematology

ISBN 978-91-8021-429-2
ISSN 1652-8220

Tryckt i Sverige av Media-Tryck, Lunds universitet
Lund 2023

Table of Contents

Original Papers and Manuscripts

List of publications included in the thesis

Paper I

Lin28b controls a neonatal to adult switch in B cell positive selection. Science Immunology, 2019; volume 4, issue 39.

Vanhee S., **Åkerstrand H.**, Kristiansen TA., Datta S., Montano G., Vergani S., Lang S., Ungerbäck J., Doyle A., Olsson K., Beneventi G., Jensen CT., Bellodi C., Soneji S., Sigvardsson M., Gyllenbäck EJ., and Yuan J.

Paper II

Enhanced protein synthesis is a defining requirement for neonatal B cell development.
Frontiers in Immunology, 2023; volume 14.

Åkerstrand H., Boldrin E., Montano G., Vanhee S., Olsson K., Krausse N., Vergani S., Cieśla M., Bellodi C., and Yuan J.

Paper III

Lin28b regulates glucose metabolism during neonatal B cell development. Manuscript, 2023.

Åkerstrand H., Boldrin E., Oburoglu L., Montano G., and Yuan J.

List of publications not included in the thesis

A self-sustaining layer of early-life-origin B cells drives steady-state IgA responses in the adult gut.
Immunity, 2022; volume 55, issue 10.

Vergani S., Muleta KG., Da Silva C., Doyle A., Kristiansen TA., Sodini S., Krausse N., Montano G., Kotarsky K., Nakawesi J., **Åkerstrand H.**, Vanhee S., Gupta SL., Bryder D., Agace WW., Lahl K., and Yuan J.

Transcriptomic analysis of functional diversity of human umbilical cord blood hematopoietic stem/progenitor cells in erythroid differentiation.
International Journal of Hematology, 2022; volume 115.
Soboleva S., **Åkerstrand H.**, and Miharada K.

Identification of potential chemical compounds enhancing generation of enucleated cells from immortalized human erythroid cell lines.
Communications Biology, 2021; volume 4.
Soboleva S., Kurita R., Ek F., **Åkerstrand H.**, Silvério-Alves R., Olsson R., Nakamura Y., and Miharada K.

Establishment of an immortalized human erythroid cell line sustaining differentiation potential without inducible gene expression system.
Human Cell, 2021; volume 35.
Soboleva S., Kurita R., Kajitani N., **Åkerstrand H.**, and Miharada K.

Comprehensive Proteomic Characterization of Ontogenic Changes in Hematopoietic Stem and Progenitor Cells.
Cell Reports, 2017; volume 21, issue 11.
Jassinskaja M., Johansson E., Kristiansen TA., **Åkerstrand H.**, Sjöholm K., Hauri S., Malmström J., Yuan J., and Hansson J.

Abbreviations

ALL	Acute lymphoblastic leukemia
BCR	B cell receptor
CSR	Class switch recombination
D	Diversity gene of the Ig locus
ELO B	Early-life origin B cell
FoB	Follicular B cell
HSC	Hematopoietic stem cell
HSPCs	Hematopoietic stem and progenitor cells
Ig	Immunoglobulin
IgH	Immunoglobulin heavy chain
IgK	Immunoglobulin kappa (κ)
IgL	Immunoglobulin light chain
iPSC	Induced pluripotent stem cell
IL-7	Interleukin 7
IL-7R	Interleukin 7 receptor
J	Joining gene of the Ig loci
MzB	Marginal zone B cell
mRNA	messenger RNA
miRNA	microRNA
NLS	Nucleolar localization signal
nAb	Natural antibody
PerC	Peritoneal cavity
PtC	Phosphatidylcholine
RNA	Ribonucleic acid
RAG	Recombination-activating gene
RSS	Recombination signal sequence
TCR	T cell receptor

TDT	Terminal deoxynucleotidyl transferase
TrB1a	Transitional B-1a progenitor
RBP	RNA-binding protein
V	Variable gene of the Ig loci

Grace is the beauty of form
under the influence of freedom.

Friedrich Schiller

Abstract

Antibody secretion by the B cell is an integral part of our immune system. Since our body contains millions of B cells expressing unique antibodies, together they afford an impressive range of antigen specificities and protection against pathogens. This diversity originates from molecular events during B cell development, which outputs mature B cells capable of recognizing foreign antigen while being tolerant towards the self-antigen of the own body. However, there are exceptions to this central rule of immune tolerance and weakly self-reactive antibodies are abundant in the blood of healthy humans and mice. In the mouse, many of these self-reactive antibodies are produced by the B-1a subset of B cells, a rare cell type that was primarily generated in early-life and then maintain by self-renewal in adults. As such, the early-life origin of B-1a cells means that B cell development in early-life allows for a degree of self-reactivity, whereas self-reactivity is strictly counter selected in adults. Therefore, B-1a cell development makes for a handy gateway population to study self-reactive B cell development in early-life. An important advancement in our understanding of B-1a development was the identification of its dependence on LIN28B, an RNA-binding protein that exerts post-transcriptional gene regulation. The exact LIN28B mechanism in B cell progenitors has not been known and the subject matter of this thesis.

Given how self-reactive B cells are normally counter selected during B cell development, we hypothesized that LIN28B must instead enable positive selection of such self-reactive specificities. Indeed, by focusing on the Imm-B cell stage of development where self-reactivity is normally censored, we identified a subset that express the surface marker CD5, have elevated levels of BCR signalling, and develop into the B-1a subset. To identify the underlying mechanism, we explored the LIN28B mRNA interactome in B cell progenitors and identified binding of known LIN28B targets from studies outside of B cell development, including transcripts for ribosomal proteins. This led to the discovery of elevated protein synthesis as a novel hallmark of neonatal B cell development, being particularly elevated in the CD5 positive Imm-B subset. Importantly, B cell development during early-life crashes under a slight reduction in protein synthesis but becomes normal once the neonate matures and switches to producing adult type, CD5 negative

Imm-B cells. Finally, we then explored how a LIN28B-mediated increase in glucose uptake might support B-1a cell development, by providing the cell with more biomass and ATP. This did indeed identify a LIN28B-dependent increase in glucose uptake by all the B cell progenitors but the impact on specifically B-1a development is still unclear and more work is necessary to fully understand any connection.

Taken together, our work establishes how LIN28B expression in early life augments B cell progenitor metabolism and facilitates positive selection of self-reactive CD5 positive Imm-B cells to produce the B-1a subset. Since LIN28B is capable of inducing positive selection of self-reactive clones that normally are negatively selected during B cell development, these findings are not only of interest to B-1a development but also for the understanding of the important central tolerance mechanism. In addition, insights during our studies indicate that LIN28B might affect development before the Imm-B cell stage to enable the output of CD5 positive Imm-B cells, which is an ongoing subject of investigation beyond this thesis work.

The unique early-life immune cells

The time around birth represents a unique immunological challenge. Following the absence of exposure to foreign antigen during development in the uterus, our immune system is suddenly faced by an explosion of antigens at birth and must quickly build up protection against a continuous invasion of pathogens. Interestingly, the immune cells at this critical time are functionally distinct from those that will later come to dominate the adult immune system. This functional distinction is well exemplified by the B cell lineage, the antibody producing component of our immune system. Early life B cells are enriched by 'innate-like' B cells, a designation made in reference to their similarity to the simple, germline encoded immune cells rather than being diverse and adaptive as the adult B lymphocytes (*1*). Their distinction is also manifested by different antigen specificities, where the adaptive B cell repertoire is diversified and unique to every individual but the innate-like B cell repertoire is semi-invariant and shared among unrelated individuals. Curiously, the invariant specificities of innate-like B cells recognize not only foreign antigen but also self-antigen, whereas adult B cells are strictly purged from self-reactivity to prevent autoimmune disease (*2*). This begs the question of how early-life development is different from the adult to enable development of self-reactive B cells? While the scientific community has been aware of this distinction for a long time (*3*), the underlying mechanism still needs further investigation.

The observation that early-life B cells were distinct from their adult counterpart laid the foundation for the 'layered immune system hypothesis', which posits how layers of distinct immune cells are produced by waves of distinct immune cell precursors over our lifetime (*4*). As many immune cells are long-lived, this is not only relevant for neonatal but also adult immunity. Indeed, while this thesis focuses on the B cell lineage (*5*), a layered immune system is also recognized for T cells (*6*) and macrophages (*7*).

An introduction to B cells in the human and mouse

The antigen specificity of a B cell depends on its B cell receptor (BCR), a membrane bound immunoglobulin (Ig) molecule that the B cell will also secrete as an antibody upon antigen recognition. To express a BCR, each B cell must recombine its Ig loci from a germline configuration into a functional gene capable of producing an Ig protein. This happens during B cell development, where pseudo-random recombination of different gene variants spread throughout the locus lays the foundation for a diverse BCR repertoire with different antigen specificities (*8*). As each B cell express a unique BCR with a unique antigen specificity, this affords an impressive breadth of antigen specificities that together provide a range of immunological protection. The mature B cell can later hone its antigen specificity by the process of somatic hypermutation or switch its antibody class to change what type of antibody-mediated immune response it will trigger. In total, there are five different Ig classes: IgA, IgD, IgE, IgG, and IgM.

Upon recognition of its antigen, the BCR triggers a complex network of signalling pathways that activates the B cell to promote differentiation, survival, and proliferation (*9*). Antigen binding by the BCR induces a conformational change that enables phosphorylation of immunoreceptor tyrosine-based activation motif (ITAM) residues on the coreceptors CD79A (also known as Igα) and CD79B (also known as Igβ). This leads to further phosphorylation and signal propagation through several components of the BCR signalling pathway, including splenic tyrosine kinase (SYK), B cell linker protein (BLNK), phospholipase Cγ2 (PLCγ2) and Bruton tyrosine kinase (BTK). Ultimately, this enables B cell activation by increasing the intracellular level of calcium and activation of several transcription factors. A much simplified schematic of BCR signalling with a focus on the relevant pathways for this thesis work is provided in Figure 1.

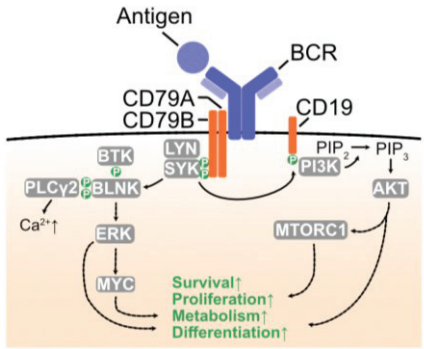

Figure 1. Simplified schematic of BCR signalling. Antigen binding induces a conformational change the enables phosphorylation of its coreceptors CD79A and CD79B. This is followed by phosphorylation of downstream components to propagate a signal that increases intracellular calcium levels and activity of transcription factors that ultimately promote survival, proliferation, metabolism, and differentiation.

Mature B cells can be divided into subsets based on their function (dependent on the BCR and additional receptors), tissue localization, and surface marker expression. In the mouse, they are broadly separated into the follicular B (FoB) cells, marginal zone B (MzB) cells, and the B-1 B cells. The non-B-1 B cells are sometimes collectively referred to as 'B-2' cells. Their function is non-redundant and only together do all the B cell subsets make up a complete B cell compartment (*10*).

The FoB subset is the most numerous in the body and they populate the follicles of the spleen from where they recirculate through the blood and lymph to B cell areas of the lymph nodes, bone marrow, and intestinal Peyer's patches. Long-term survival depends on recognition of its cognate antigen, otherwise the FoB cell will turn over after a few weeks of circulating in the periphery. Upon antigen recognition, they differentiate into either plasma blasts that secrete vast amounts of antibody or memory B cells that will be recalled upon future infection. In contrast to the FoB cells, the MzB and B-1 cells are instead long lived and spontaneously secrete antibody even without antigen stimulation (*11*). Together they provide a rapid response to particular antigen before the more specialized but slower response of FoB cells. The MzB cells populate the spleen where they line the B cell follicle and secrete IgM or class switched IgG to provide a first-line of defence against blood-borne pathogens. B-1 cells are rare in the spleen but the major B cell population in the serous cavities of the body (*12*). The B-1 subset function as a regulator of homeostasis by clearing dead cell debris and producing anti-inflammatory cytokines such as IL-10. The B-1 suset is

further separated based on CD5 expression into B-1a cells (CD5 positive) and B-1b cells (CD5 negative), with B-1a cells being primarily generated in early-life whereas B-1b cells are also produced in adulthood. While FoB and MzB cells are readily found in humans, the promiscuous CD5 expression on human B cells has foregone the identification of a human B-1a and its existence remains a controversial subject (*13*). Nevertheless, human B cells that are functionally similar to the murine B-1a have been identified (*14*) and argues that at least a functional equivalent also exists in humans.

Discovery of the B-1a subset

While antibody secretion is dramatically increased upon infection and activation of the B cells, a certain amount of antibody is constantly present in the blood of healthy individuals. For the IgM class, a significant proportion at steady-state consists of 'natural antibodies' (nAbs) that are spontaneously produced by B cells without the need of exogenous stimulation (*15*). Curiously, many of them recognize self-antigen in addition to foreign antigen, which is believed functionally important by providing immunity towards certain antigen and by helping to clear debris of dead cells from the body. Still, the existence of self-reactive specificities is curious given the danger of triggering an immune response towards the self.

In the mouse, many nAb specificities are conspicuously enriched within the B-1a subset. This subset was first discovered during pioneering work on the flow cytometer that identified a B cell subset expressing the pan T-cell antigen CD5 (also known as LY-1) (*3*). Soon thereafter it was realized that the B-1a cells are a functionally distinct subset that produce virtually all the nAb against a cryptic antigen on damaged red blood cells (*16*). Furthermore, we now know that B-1a cells are enriched by a broad range of self-antigen, including phosphatidylcholine (PtC) (*17*), bromelain treated red blood cells (*16*), thymocyte antigen (*18*), oxidized lipids (*19*), and annexin IV (*20*). In addition, B-1a cells also become enriched in certain mouse models of autoimmunity (*21-23*). As such, the B-1a subset represent a useful population in the mouse to study the general phenomena of self-reactive B cells.

A striking distinction of the B-1a subset is its unique BCR repertoire that endows reactivity towards self-antigen. The B-1a BCR repertoire is enriched for certain Ig genes, whereas Ig usage among B-2 cells is much more diverse. Such 'stereotyped' Ig usage is important for the recognition of self-antigen. For example, reactivity towards the cryptic antigen on damaged red blood cells (*16, 24*) is enriched for expression of certain Ig genes beyond a stochastic representation of their expression in the germline. Furthermore,

the same enriched Ig usage is repeatedly between unrelated individuals. As such, such antibodies are referred to as 'public clonotypes' and have been hardcoded into the immune repertoire over evolutionary time.

B-1a cells are generated early in life

Given their enrichment in stereotyped specificities against self-antigen and enrichment in autoimmune mouse models, the B-1a subset was a hot topic among B cell scientists at the end of the 1980's. Around this time, B cells were routinely generated and studied by transferring bone marrow from adult donor mice into recipient mice. As such, it was a surprising finding that adult bone marrow transfer failed in generating specifically the B-1a subset. Instead, transfer of neonatal bone marrow, spleen, or liver all output B-1a cells in the recipient (*25*). This indicated that B-1a cells in the adult had been generated in early-life and then maintained as mature cells in the periphery (*26*). Indeed, transplantation of the same immunophenotypically defined B cell progenitor (CD43+B220+THY1.2-, Pro-B cell) from fetal liver but not adult bone marrow generated B-1a cells in recipient mice (*27*). Two possible explanations were put forth to explain this: I) that the B-1a progenitor was short-lived and lost during ontogeny or II) that the B-1a progenitor remains in adulthood but is either dormant or produces B-2 cells instead.

Today we know that both short-lived and definitive progenitors contributes to the B-1a subset (*28*). Conventional B cells are ultimately produced by the hematopoietic stem cell (HSC), which first appear around day 10 of mouse embryonic development in the aorta, gonad, and mesonephros region (*29*). However, some HSC-independent B cell output precedes this time and B-1a potent progenitors are present in both day 8.5 para-aortic splanchnopleura (*30*) and day 9.5 yolk sac (*31*). These findings contributed to the idea that B-1a cells were generated from a 'primitive progenitor' during early-life instead of HSC-dependent lymphopoiesis. In line with this, B-1a cells can be isolated from *Cbfβ* mice that lack definitive HSCs (*32*) and two separate studies have reported on a fetal specific progenitor producing the B-1a subset (*33, 34*). On the other hand, previous work from our lab investigated changes in the HSC capacity to produce B-1a cells. By using cellular barcoding to link mature B cell output to an HSC origin, we found that fetal HSCs are initially B-1a potent but later switch into producing only the B-2 subset (*35*). A reconciliatory view acknowledges that B-1a cells are produced by both primitive progenitors and as a consequence of molecular differences in the hematopoietic stem and progenitor cells (HSPCs) across ontogeny (*36*). We recently investigated their relative

contribution by inducing stable expression of a fluorescent protein at specific ages and quantify labelled cell frequency among the total B-1a cells in the adult (*37*). This identified that the majority of B-1a cells are generated during the first two to three weeks post-birth, before a general switch of the HSPCs to an adult type hematopoiesis (*38*). Additionally, we also identified a previously unknown contribution of early-life origin (ELO) B cells to other B cell compartments, which we speculate to be functionally distinct during healthy immune responses or be the cell of origin in disease such as cancer.

Development of B cells

Ultimately, the goal of B cell development is to output an antibody producing mature B cell. The antibody consists of both a Ig heavy chain (IgH) and a light chain (IgL), which are encoded by separate loci. To produce an antibody secreting B cell, the B cell development revolves around recombining the Ig loci from their germline states into functional genes. The heavy chain locus is recombined first and once it is completed the IgL is initiated (*39, 40*). To enable Ig recombination, B cell development critically depends on expression of the Recombination-activating genes 1 and 2 (RAG1 and RAG2, herein collectively referred to as RAG) that recognize recombination signal sequences (RSS) flanking genes of the Ig locus to facilitate cutting out and recombining these gene segments (*41*). Each Ig locus consists of several gene copies that can be recombined, making it a pseudo-random process with a distinct recombination product in each developing B cell. However, many of these recombination products result in self-reactive BCRs that could develop into autoimmune disease were they to become expressed on a mature B cell (*42*). As such, B cell development is also actively pruned by negative selection against self-reactive specificities (*43*).

Given the negative selection against self-reactivity during B cell development, the existence of natural antibodies in general and the B-1a subset in particular are conspicuous exceptions to this central rule of B cell development: somehow self-reactive B-1a cells are allowed to develop in early-life. However, while adult B cell development has been extensively studied, **more work is needed to understand how early-life B cell development allows the development of self-reactive B-1a cells (Paper I-III)**.

Adult B cell development

The adult B cell progenitors ultimately originate from an HSC that has differentiated through progenitor stages of increasing lineage restriction (*44*). Commitment to the B cell lineage happens at the Pro-B stage and the expression of the transcription factor *Pax5* (*45*). Stepwise recombination of the B cell progenitor Ig loci then takes place at different stages of development. An overview of the different stages of bone marrow B cell development and Ig expression is outlined in Figure 2.

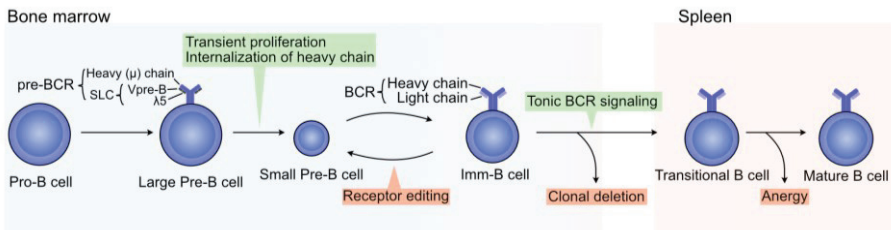

Figure 2. Overview of conventional B cell development. Immunoglobulin (Ig) heavy chain recombination finishes at the Pro-B cell stage, leading to expression of the pre-BCR and transition to the large Pre-B stage. Successful pairing of the IgH to the surrogate light chain leads to pre-BCR signaling that induces proliferation and licenses further development. At the subsequent small Pre-B cell stage, the heavy chain is internalized and the light chain locus recombined. Successful recombination and pairing of a heavy and light chain results in BCR expression. At the resulting Imm-B cell stage, the BCR is tested for self-reactivity that will result in receptor editing or clonal deletion. A low level of antigen-independent (tonic) BCR signaling induces developmental progression and the Imm-B cell transitions to the spleen for final maturation. This results in the output of a mature, antigen naïve B cell that turns over after a few weeks in the periphery if it doesn't encounter its antigen.

Recombination of the Ig heavy chain locus is completed at the Pro-B cell stage, whereas the light chain locus is kept in germline conformation. This depends on IL-7 signalling from the nearby stroma, which opens up the heavy chain locus accessibility (*46*) while maintaining the light chain locus in its germline conformation (*47*). Each heavy chain consists of a variable and constant region, where recombination of the variable region produces a functional exon upstream of the constant region exon and together they make a functional heavy chain gene. The recombined variable gene segment consists of a single variable (V_H), diverse (D_H), and joining (J_H) gene. This V(D)J recombination achieves a wide diversity of antigen specificities by pseudo-random recombination of slightly different V_H, D_H, and J_H gene copies that are spread throughout the heavy chain locus (*48*). The heavy chain is further diversified by random N-nucleotides additions to the junctures of the recombined locus, which is facilitated by the Terminal deoxynucleotidyl transferase (TDT) enzyme (*49*).

Successful V(D)J recombination and expression of the heavy chain marks the next developmental stage and the cell is now referred to as a 'Pre-B'. As the light chain hasn't been recombined yet, the functionality of the recombined heavy chain is instead tested by pairing it to the surrogate light chain (SLC) that consists of two germline encoded proteins, VpreB and λ5 (*50, 51*). These two proteins have considerable sequence homology to the light chain (*52, 53*) and together with the heavy chain they make up the 'pre-BCR' that, with the help of the necessary co-receptors, signal in a similar way to a mature BCR upon antigen recognition (*54*). As a consequence of pre-BCR signalling, recombination of the heavy chain stops (*55, 56*) and, in combination with IL-7 signalling, the Pre-B cell proliferates (*57-59*). In effect, this expands a B cell progenitor that has successfully recombined and expressed a functional heavy chain protein.

The proliferation ends up spending the cellular biomass and the cell goes from being a proliferative large Pre-B cell to a quiescent small Pre-B cell. At this progenitor stage, the heavy chain gets internalized and pre-BCR signalling stops. At the same time, the cell moves away from IL-7 producing stroma and downregulates its expression of the IL-7 receptor (*60*). Collectively, this relieves both the suppression of RAG protein and opens up the light chain locus for recombination. As for the heavy chain, the Ig light chain consists of a constant and a variable segment where pseudo-random recombination of different V_L and J_L gene copies produces a variable region that further diversifies the antigen specificity. The recombined IgL gets paired with the IgH and the cell now express a mature BCR. The cell is now referred to as an immature B cell ('Imm-B') and can be identified by surface expression of its BCR in the form of a membrane bound IgM. As for pre-BCR signalling, BCR signalling once again turns off RAG protein expression and light chain recombination (*61, 62*).

The reactivity of the BCR is now tested at what is referred to as 'the central tolerance checkpoint' that gauges the BCR signalling strength to censor further development of self-reactive clones (*63*). This is an important checkpoint, with up to 50% of all the newly recombined BCRs being poly-reactive and achieving an unacceptably high BCR signalling that block their continued development (*42*). Instead, a new round of light chain recombination is initiated in a process referred to as 'receptor editing' (*64, 65*). The light chain is encoded by two separate loci that are referred to as kappa (κ) and lambda (λ), which allows for several attempts of light chain recombination. First the kappa locus is recombined then the lambda (*66*). Several receptor editing attempts are attempted or, given continued failure in generating a tolerable BCR, the clone will eventually undergo 'clonal deletion' (*67-70*). The high frequency of self-reactive clones underscores the importance of this checkpoint to avoid development of self-reactive BCRs

that could result in rampant immune responses against ubiquitous self-antigen, such as reactivity against DNA (*71*). Indeed, central tolerance is defect in the autoimmune diseases Systemic lupus erythematosus (*72*) and Rheumatoid arthritis (*73*).

A certain degree of antigen-independent BCR signalling (so called 'tonic signalling') indicates that the mature BCR is functional yet not self-reactive and allows for developmental progression (*74*). This induces Imm-B cell transition from the bone marrow and into the spleen for final maturation. The progenitor is now referred to as a 'transitional B cell progenitor' and express both surface IgM and IgD to achieve the necessary BCR signalling to finalize the development (*75*). Self-reactive clones that escaped central tolerance can also be tolerized at this stage by becoming anergic (*76*). The cell is now mature and referred to as an antigen naïve B cell. B cell development throughout life produces a stream of naïve B cells that will continuously turn over unless they get stimulated by their cognate antigen.

Distinctions of early-life B cell development

In contrast to B-2 restricted development during adult life, early-life B development also efficiently produce B-1a cells. While the mechanism is still not known, there are distinctions of early-life B cell progenitors that could be linked to B-1a development (summarized in Table 1). Definitively saying that these age-dependent differences are hallmark features specifically for B-1a development has been hampered by the fact that B-2 cells are also produced in early-life and we have no way of separating a B-1a progenitor from a B-2 progenitor. However, this resolution is now improving with the identification of a rare B-1 progenitor in the adult bone marrow (*77*) and a B-1a progenitor in the spleen (*78*). Still, **identifying a definitive B-1a cell progenitor in the bone marrow would be a significant step towards identifying the molecular underpinning of B-1a development (Paper I).**

Table 1 Selected differences between adult and early-life B progenitors that might be connected to B-1a development

Progenitor	Feature	Adult	Early-life	References
Pro-B	IL-7 signaling	Dependent	Less dependent	(*38, 79, 80*)
Pro-B	TDT expression	Present	Absent	(*81, 82*)
Pro-B	Light chain recombination	Germline	Premature recombination	(*83*)
Large Pre-B	Development of B-1a enriched heavy chains with a poor SLC pairing	Inefficient	Efficient	(*84-86*)
Large Pre-B	pre-BCR signalling	Induces development	Blocks development	(*84, 87*)
Splenic transitional progenitor	Capacity of producing B-1a cells	Absent	CD5 positive subset produces B-1a cells	(*78*)

Clues on B-1a development in early-life

The mature B-1a cells are enriched for certain IgH chains (*88-90*) that are critical for their reactivity against self-antigen. Studies using transgenic mice that express such 'B-1a enriched' heavy chains (*84, 85, 91-93*) or BCRs with artificial self-reactivity (*94-96*) have clearly demonstrated that self-reactive B cell development is permitted in early life but blocked in adults. Since heavy chain gene expression in Pro-B cells follows the expression in germline (*97, 98*), it argues B-1a enrichment of specific heavy chain genes is not due to changes in Ig locus accessibility but rather the result of B cell development.

An interesting distinction of the B-1a enriched V_H11 (*84*), V_H81X (*85*), and V_H12 (*86*) is their poor pairing to the SLC. Such an inefficient pairing could be important for development of self-reactive BCRs given that SLC-knockout mice have an increased frequency of self-reactive B cells (*99*). However, given that the pre-BCR induces developmental progression in adults, it is not clear how early-life development overcomes the lack of a pre-BCR signal. One possible explanation has been provided by the Skok laboratory, who linked premature light chain recombination in fetal liver Pro-B cells to B-1a development (*83*). Such premature recombination produces a mature BCR already in the Pro-B cell and circumvents the need of the SLC and pre-BCR checkpoint. An opposing explanation instead suggests that pre-BCR signalling is actually negative for early life B cell development, rather

than positive as in the adult (*84, 87*). This surprising finding, reported by two separate groups, found that strong signalling from a transgenic BCR blocked development at the pre-BCR checkpoint in early life whereas it licensed development in adults. According to this model, the poor SLC pairing of B-1a enriched heavy chains would instead be beneficial by not inducing a pre-BCR signal at all.

Following the pre-BCR checkpoint, the self-reactive BCR must now overcome the central tolerance checkpoint at the Imm-B cell stage. Indeed, development of self-reactive Imm-B cells is only allowed in early-life and is negatively selected in the adult (*92-94*). The Imm-B cell negative selection depends on self-antigen recognition to induce BCR signalling, as was elegantly proven by the Hardy and Hayakawa lab (*95*). Their study used Ig transgenic mice reactive to the ubiquitous Thy-1 antigen, a specificity that normally is enriched in the B-1a subset (*18*). Enrichment of Thy-1 positive B-1a cells in the PerC was in line with an intact early-life B cell development. In contrast, adult B cell development was blocked but could be rescued by abrogating the BCR signalling if the mouse was crossed onto a Thy-1 antigen knockout background. Interestingly, this B cell development resulted in FoB cells rather than B-1a. While this seems puzzling given the normal B-1a enrichment of this specificity, it is in line with BCR signalling levels dictating lineage commitment (*100*). Especially studies from the Rajewsky lab have convincingly proven that BCR signalling dictates B cell lineage choice, where a weak BCR signal yields B-2 cells and strong BCR signal B-1a cells (*101*). As in the study on Thy-1 knockout mice, the lineage commitment only depends on BCR signal strength and not what the actual antigen is. This was shown by mimicking a strong BCR signal in heavy chain knockout mice, by crossing *IgH* knockout mice with a constitutively active *Lmp2a*. LMP2A activates the same signalling pathway as an activated BCR and thereby achieved BCR signalling in the absence of an actual BCR. A strong BCR signal yielded B-1a cells (*101*). Finally, they also showed that a mature B-2 cell can be forced to become a phenotypic B-1a cell by switching out its own BCR for that of a B-1a (*102*). Collectively, these findings prove that the B-1a identity is essentially linked to the levels of BCR signalling. Indeed, BCR signalling is directly linked to CD5 levels on B cells from both human (*103*) and mouse (*104*), where it regulates BCR signalling strength (*105*).

These findings have spurred a debate whether B-1a cells are ‘born’ of a separate lineage from the B-2 or ‘made’ from high BCR signalling clones of a common lineage (*106*). This issue is still not resolved but regardless of which is true the fact remains that the self-reactive BCRs capable of becoming a B-1a only develop in early-life.

Metabolism during B cell development: a potential role for B-1a development?

The B-1a cell is distinctly more metabolic active compared to the B-2 cell, including an increased glucose uptake and metabolism (*107*). This difference is, at least in part, a consequence of active BCR signalling by the self-reactive B-1a, since BCR signalling regulates B cell metabolism during a normal antigen response and becomes elevated in autoimmune disease (*108*). Since the BCR gets expressed already at the Imm-B cell stage, it is reasonable to believe that glucose metabolism increases already at this stage of B-1a development. In line with this, it was recently suggested that limiting glucose metabolism during adult B cell development results in too low ATP levels to support a self-reactive BCR, thereby constituting a natural barrier against autoimmune disease and oncogenic transformation (*109, 110*). However, **whether glucose metabolism is naturally elevated during B-1a development in early-life needs to be investigated (Paper III) (Figure 3).**

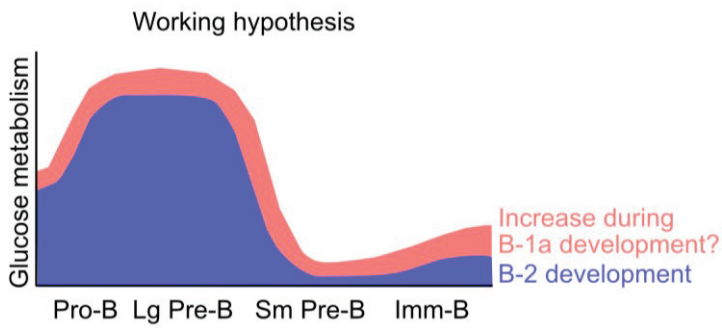

Figure 3. Working hypothesis on increased glucose metabolism during B-1a development. Illustration of the shifting levels of glucose metabolism during B cell development and a hypothesized difference in its absolute level between B-2 development (blue) and B-1a development (red). Glucose metabolism peaks around the pre-BCR checkpoint at the large Pre-B cell stage and is relatively low in the subsequent small Pre-B and Imm-B cell stages. An increased glucose metabolism would yield more ATP to support the energy demands of self-reactive clones.

Knowledge on the regulation of B cell progenitor metabolism is limited (*111*). The progenitors go from being relatively large and proliferative (the Pro-B and large Pre-B stages) to becoming small and quiescent (the small Pre-B and Imm-B stages), which is matched by changes in their overall metabolism. Glycolysis peaks around the pre-BCR checkpoint to support the proliferative burst in response to pre-BCR signalling, akin to antigen activation of a mature B cell (*112-114*). High level of glucose metabolism at this stage is important and development becomes blocked upon treatment with the glucose inhibitor 2-DOG (*115*). Molecularly, regulation of B cell

progenitor metabolism depends on PI3K signalling to control the activity of both Mechanistic target of Rapamycin complex 1 (mTORC1) and c-MYC (*116, 117*). In turn, PI3K signalling depends on IL-7 signalling at the Pro-B and large Pre-B stages (*118*) and BCR signalling from the pre-BCR on large Pre-B cells (*119*) or mature BCR on Imm-B cells (*120*). Additionally, the second mTOR containing complex (mTORC2) is also activated by PI3K signalling and regulates metabolism during B cell development by activating c-MYC and mTORC1 (*121, 122*).

Although maintaining active mTORC1 and c-MYC signalling is critical for B cell development, there is also an upper limit to how much is tolerated and strong mTORC1 activation results in a block at the pre-BCR checkpoint (*119*). This is due to an upper threshold on how much mTORC1 activation the progenitor can handle, which is set by the antagonistic AMPK. Similarly, the same block at the pre-BCR checkpoint can be activated by deleting *Pten* to increased PI3K signalling (*123*).

Age-dependent differences with a connection to B-1a cells

Ultimately, underlying molecular differences that distinguish a B-1a progenitor from a B-2 progenitor must explain how self-reactive cells are allowed to develop. There are many known mouse models with gene modifications that specifically affect B-1a cells. Given its importance, it is not surprising that a plethora of mouse models that positively or negatively regulate BCR signalling has increased or decreased number of B-1a cells, respectively (*124*). However, given how mature B-1a cells undergo BCR dependent clonal expansion (*125*) and most mouse models represent constitutive alterations to their BCR signalling, they lack the resolution to say if development was affected in addition to mature cell expansion. Still, a knockout mouse model for the transcription factor *Bhlhe41* connects B-1a development and BCR signalling, since it lacks both mature B-1a cells and their CD5 positive splenic progenitor (*126*).

An important distinction that shapes the BCR repertoire in early-life is the inactivity of *Dntt* that encodes the TDT enzyme, which adds non-templated nucleotides to the heavy chain to diversify the BCR repertoire (*81, 82*). As such, the BCR repertoire within the B-1a subset lacks N-nucleotide additions in contrast to the B-2 cells. Its lack is important for B-1a cell function, with enforced TDT expression altering BCR specificities and negatively affecting the B-1a mediated response to *Streptococcus pneumoniae* (*127*). In addition, a lack of N-nucleotides additions to the heavy chain also affects development by favoring homologous recombination of certain gene segments and skews the VDJ recombination during early-life (*128*). Indeed, a similar mechanism

also plays a role for the invariant T cell receptor (TCR) repertoire during early life (*129*). However, *Dntt* deficiency is not in itself enough to drive B-1a development (*82, 130*).

There are also studies implicating certain B cell lineage factors in B-1a development. More B-1a (and MzB) cells were produced in a mouse model with *Ebf1* overexpression, which is an essential factor for B cell development (*131*). As mature B-1a cells from *Ebf1* knockout mice had lower BCR signalling, it is not clear if the effect was on mature cells or development. Additionally, knockout of another B cell lineage factor *Pu1* favors development of B-1 cells (*132*). Such independence from *Pu1* has also been reported for a rare B-1 progenitor in adult bone marrow (*133*).

But arguably the strongest factor known to affect B-1a development is the RNA-binding protein LIN28B (*134*). It was first identified in a screen for determinants of early-life HSPCs and, remarkably, re-introduces B-1a development upon ectopic expression in the adult. As such, **understanding the *Lin28b* program holds key insights for understanding B-1a development (Paper I-III).**

Lin28b regulation of B cell development

LIN28B is an RNA-binding protein (RBP) that post-transcriptionally regulates specific mRNA and non-coding RNA that express its cognate RNA-recognition motif. The mammalian genome harbors two paralogs (*Lin28a* and *Lin28b*, herein collectively referred to as *Lin28*) that are functionally redundant by sharing the same cold-shock domains and CCHC zinc finger motifs (*135*). Since LIN28B also express a nucleolar localization signal (NLS), its subcellular localization can be shifted and affect what RNA targets are available.

Lin28a was first discovered outside of mammals, in a study that screened the worm *Caenorhabditis elegans* for genes affecting its developmental timing. Loss of *Lin28a* led to premature development and stage-specific events being skipped (*136*). A similar role was later identified in mammals, with high levels of expression at the initiation of embryonic development that goes down during ontogeny (*137, 138*). Conversely, enforced expression when *Lin28* is normally downregulated impedes maturation and the acquisition of an adult phenotype (*139*). Remarkably, in addition with a defined set of transcription factors, *Lin28* is even capable of reverting back a terminally differentiated cell into an 'embryonic like stem cell state', also known as an induced pluripotent stem cell (iPSC) (*140*). Such inappropriate expression of LIN28 can be detrimental, with it being sufficient to induce various cancers in mice (*141-145*) and it is frequently identified in cancer patients (*146, 147*). Thus, LIN28 are powerful oncofetal proteins that have been evolutionarily conserved to regulate early-life development.

Lin28b is a master-regulator of early-life hematopoiesis

Endogenous *Lin28b* expression during human and mouse early-life hematopoiesis was first identified in a search for molecular determinants of fetal HSPCs relative to their adult counterparts (*134*). The early-life is a time of distinctly different hematopoiesis compared to the adult, including an expansion of the HSCs, increased erythroid output, and an output of functionally distinct T and B cells by their respective progenitors. Remarkably, ectopic LIN28 in adult HSPCs re-initiate many aspects of early-life hematopoiesis including an output of B-1a and γδ T cells (*134*), HSC self-renewal (*148*), platelet development and function (*149, 150*), development of regulatory T cells (*151*), an output of functionally distinct CD8 positive T cells (*152*), development of the innate-like natural killer T cells (*153*), and increased erythropoiesis (*154-156*). As such, endogenous *Lin28b* expression during early life is a master regulator of its unique hematopoiesis. While studies have focused on the mouse and the information on the LIN28 effect in human is more sparse, human fetus HSPCs, but not adult, also express *Lin28b* (*134*) where it is required for γδ T cell development in the fetal thymus (*157*).

Multi-faceted RNA regulation by LIN28

The post-transcriptional regulation by LIN28 affect translation of mRNA into protein primarily through two separate mechanisms: by reducing the level of let-7 microRNA (miRNA) family and direct binding of mRNA to influence translation (outlined in Figure 4).

miRNA is a class of short (~21 nucleotides) RNA that negatively regulate translation through sequence complementarity between its ‘seed sequence’ and the target mRNA (*158*). The mammalian genome contains twelve let-7 family members that are functionally redundant by sharing a common seed sequence and, thus, mRNA targets (*159*). Like all miRNA, let-7 biogenesis begins with its transcription in the nucleus to generate the intermediary pri-let-7 miRNA. The pri-let-7 forms a hairpin structure by folding back on itself which allows binding and further processing by the microprocessor (*160*), resulting in pre-let-7 miRNA that is exported to cytoplasm for final maturation and regulation of target mRNA (*161*). LIN28 recognize and bind to let-7 precursors in both the nucleus and cytoplasm, which sabotages development and lowers the level of mature let-7 (*162-169*). Conversely,

mature let-7 recognize and negatively regulate *Lin28* (*170*), resulting in a bistable switch that controls developmental timing (*171*).

In addition to sabotaging let-7 maturation, LIN28 also directly bind and regulate the translation of thousands of mRNA by shuttling them to ribosomes, different components of the translation machinery, or processing bodies (*156, 172-174*). Such a post-transcriptional regulation has been reported in several different cell types where translation increased or decreased seemingly dependent on the specific mRNA target (*156, 175-184*). Collectively, these studies have identified a common *Lin28* program across various cell types in regulating central processes to all cells, including the cell cycle, glucose metabolism, mRNA splicing, and the ribosome.

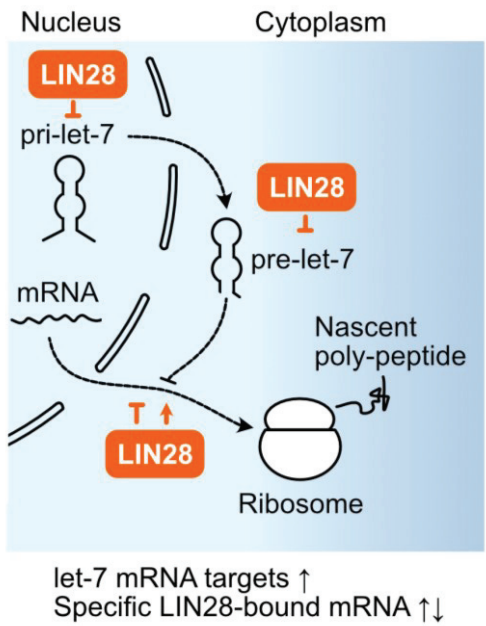

Figure 4 Overview of post-transcriptional regulation by LIN28B. The precursor of the let-7 microRNA can be developmentally blocked by LIN28B in both the nucleus and cytoplasm, ultimately resulting in decreased level of mature let-7 and increased expression of let-7 target genes. Additionally, LIN28B also binds and directly regulates specific mRNA that results in increased or decreased translation.

LIN28B-RNA targets during B cell development

The vast LIN28-RNA interactome complicates identification of the critical target(s) for B cell development. As the different B cell progenitor stages are marked by transcriptional changes (*185*), it is possible that LIN28B targets also change during development. Furthermore, even when cells share the expression of a LIN28 target, its role is not necessarily shared between the cells. This is exemplified by LIN28B regulation of HMGA2 expression, which controls HSC expansion but on its own cannot induce B-1a development (*148*). Additionally, the preferential RNA targets are also affected by post-translational modification of LIN28 in response to ERK signalling (*186*). As such, the complex post-transcriptional regulation by LIN28 should be studied in the specific cell type of interest and under as close to physiological conditions as possible.

So far, the LIN28B targets during B cell development remain incompletely understood but enforced expression of let-7 miRNA in the early-life B cell progenitors negatively impacts the frequency of B-1a cells (*187*). By focusing on the overlapping LIN28B and let-7 dependent changes in the Pro-B transcriptome, the study identified that the transcription factor ARID3A (also known as BRIGHT) could phenocopy the LIN28B increase in B-1a cell number upon ectopic expression in adults. ARID3A might affect different stages of development, as it has previously been shown to regulate both the IgH locus accessibility in progenitors (*188*) and downregulate BCR signalling in mature B cells (*189*). Thus, ARID3A seems to be yet another link between BCR signalling and the B-1a subset (*124*). The authors proposed that LIN28B increases ARID3A to keep BCR signalling levels in self-reactive Imm-B cells to a lower level that avoids activation of the central tolerance checkpoint, but more work is necessary. In addition, **direct LIN28B regulation of mRNA independently of let-7 might also contribute to B cell development and needs to be further investigated (Paper II).**

Glucose metabolism: a major point of regulation for LIN28

Studies across widely different cell types have repeatedly identified the same mechanism in LIN28 favoring increased glucose metabolism and cell growth (*190*). Through glucose metabolism, LIN28 influence such various processes as embryonic development (*137*), tissue repair (*191*), conversion of stem

cells to primed pluripotency (*176*), and cancer stemness and metastasis (*192*). However, **an effect on glucose metabolism during B cell development is currently unknown (Paper III).**

The LIN28 effect on glucose metabolism has been well studied through the IGF2/Insulin-PI3K-mTOR signalling pathway, where several points of regulation exist. LIN28 binds the mRNA to increase translation of *Igf2* (*173*) while repression of let-7 results in increased signalling by regulating several pathway components, including *Igf1r*, *Insr*, *Irs2*, *Akt2*, *Rictor*, and *Tsc1* (*193-195*). Additionally, a more tenuous finding also linked control over glucose metabolism to the let-7 dependent regulation of the long non-coding RNA H19 (*196*). Apart from PI3K signalling, let-7 also regulates the other major metabolic signalling pathways that will ultimately result in increased glucose metabolism, including RAS (*197*), c-MYC (*198*) and mTORC1 (*194, 195*).

Glucose is metabolized to generate ATP through oxidative phosphorylation and glycolysis, thereby providing the energy which is essential to a cell (*199*). LIN28 facilitates glucose metabolism into ATP by increasing the abundance of several enzymes controlling oxidative phosphorylation (e.g. NDUFB3 and NDUFB8) (*176, 191*) and through let-7 dependent regulation of glycolysis through *Pdk1* (*200*). Repression of let-7 has also been reported to increase glucose and glutamine metabolism in mature B cells during a T cell independent immune response, through regulation of Hexokinase 2, glutamine transporter *Slc1a5*, and Glutaminase (*201*). Alternatively, glucose might be funnelled into other metabolic pathways other than those that generate ATP. For example, glucose can be funnelled into the pentose phosphate pathway (PPP) to generate NADPH and ultimately aid in nucleotide synthesis (*199*).

Thesis aims

The overarching aim of this thesis work has been to explore how LIN28B controls development of self-reactive B-1a cells. To this end, the papers aim to:

- Identify whether LIN28B enables positive selection of self-reactive Imm-B cells (Paper I).

- Identify novel LIN28B mechanisms during B cell development by exploring the direct mRNA interactome in B cell progenitors (Paper II).

- Specifically investigate the role of glucose metabolism during B-1a development (Paper III), a well-studied LIN28 target outside of B cell development.

Summaries of included papers

Paper I

This thesis work followed up on the remarkable finding that LIN28B as a single factor can re-initiate B-1a development from adult HSPCs (*134*). Given the long standing debate whether B-1a cells are generated from definitive or primitive B cell progenitors (*202*), this finding was naturally met by critical questions and concerns including whether the LIN28B induced B-1a cells were functional equivalent to normal B-1a cells and whether LIN28B actually induced development in the adult or just expanded mature B-1a cells. Therefore, an important next step was to prove that LIN28B induces definitive B-1a development, a task complicated by the fact that no surface marker was known to distinguish a bone marrow B-1a progenitor from a B-2 progenitor. We reasoned that one such marker could be CD5, the defining marker of the mature B-1a cell. Indeed, a recent publication at the start of my thesis work had identified a B-1a potent splenic progenitor by a combination of surface markers including CD5 (*78*). As CD5 levels had been shown to correlate with TCR affinity for self-antigen (*203*), we hypothesized that CD5 expression would also correlate with BCR affinity in a similar way and that LIN28B induction of B-1a development would be marked by an increase in BCR signalling and CD5 expression.

We first established that CD5 expression on wildtype B-1a cells correlated with their level of self-reactivity. Indeed, by separating the mature B-1 subset based on CD5 expression we found a positive correlation between CD5 expression and antigen-dependent clonal dominance, including enrichment of the known B-1a specificity against the self-antigen phosphatidylcholine (PtC). We therefore used CD5 expression as a surrogate marker for self-reactivity during B cell development. This identified CD5 expression on a subset of neonatal Imm-B cells, including all the ones reactive to PtC. Conversely, only background levels of CD5 expression was detected on adult Imm-B cells. Furthermore, by analyzing neonatal mice with different levels of endogenous *Lin28b*, we also found that the frequency of the CD5 positive subset followed the expression level of *Lin28b*. Conversely, ectopic re-expression of LIN28B in adulthood induced a CD5 positive Imm-B subset.

By transferring the CD5 positive or negative Imm-B cells from a LIN28B induced mouse into separate recipients, we confirmed that the B-1a cells were only made from the CD5 positive Imm-B cells. Furthermore, LIN28B seemed to increase positive selection of developing B cells, with an increased number of unique, mature B cells following LIN28B induced B cell development. We then explored the underlying mechanism by RNA-sequencing analysis of LIN28B induced Imm-B cells, which identified a clear upregulation in the CD19/PI3K/c-MYC signalling pathway. Indeed, ectopic LIN28B was capable of rescuing B cell development in *Cd19* deficient mice. Finally, we confirmed the validity of studying LIN28B induced B-1a cells as they were functionally equivalent to normal B-1a cells. Collectively, this paper makes it clear that LIN28B induces B-1a cell development through positive selection of an Imm-B cell subset marked by active BCR signalling and CD5 expression.

Paper II

In addition to establishing its induction of B-1a development, parallel investigations in paper II focused on identifying the LIN28B targets in B cell progenitors. At the start of the thesis work, only one publication had described the LIN28B RNA interactome during B cell development and it had focused on let-7 dependent regulation of *Arid3a*, which on its own increases the number of B-1a cells (*187*). Still, LIN28B can bind to thousands of RNA targets and we reasoned that let-7 independent regulation might also contribute to LIN28B induced B-1a development. For example, previous studies outside of B cell development had focused on LIN28B regulating the translation of specific mRNA to bolster energy metabolism and proliferation (*190*). Theoretically, such an increase in cellular fitness during B cell development could support the energy demands of a self-reactive BCR.

To investigate the direct RNA targets of LIN28B during B cell development, we expanded primary B cell progenitors *ex vivo* to have sufficient material for deep sequencing of LIN28B-coimmunoprecipitated mRNA (RIP-SEQ). This identified the commonly identified LIN28B targets, including binding to transcripts encoding ribosomal proteins, regulators of oxidative phosphorylation, and regulators of mRNA splicing. We chose to focus on LIN28B induced changes in ribosomal content and through this identified a LIN28B dependent increase in protein synthesis during the later stages of bone marrow B cell development (the small Pre-B and Imm-B cells). In particular, it was the CD5 positive Imm-B cell subset that had the highest rate of protein synthesis. In contrast, LIN28B do not increase protein

synthesis in the upstream Pro-B and large Pre-B cell stages, which rather depend on IL-7 signalling to control protein synthesis rates. Titrating down IL-7 *ex vivo* identified a slight increase in protein synthesis upon LIN28B induction. Importantly, we then identified how neonatal B cell development relies on increased protein synthesis rates and crashes under even a slight reduction in its maximum rate, whereas B cell development in the same mouse becomes normalized once the mouse reaches 19 days post-birth and switch to producing B-2 cells (*38*). As such, this work identifies increased protein synthesis as a novel hallmark of early-life B lymphopoiesis.

Paper III

Finally, we have also devoted special attention to the common LIN28B mechanism of increasing glucose metabolism (*190*). This is an important point of regulation that impacts embryonic development (*137*), tissue repair (*191*), conversion of stem cells to primed pluripotency (*176*), and cancer stemness and metastasis (*192*). An effect on B cell development could also be important, as increased glucose metabolism during B-1a cell development could elevate ATP levels to support the self-reactive BCR (*204*). However, any age-dependent increase in glucose metabolism downstream of LIN28B and its importance during B-1a development was unknown at the beginning of this thesis work and needed to be investigated.

In the preliminary work presented in paper III, we identified a LIN28B dependent increase in glucose uptake by all the B cell progenitors that followed endogenous *Lin28b* expression in neonates or ectopic LIN28B in adults. In order to investigate its importance, we turned to *ex vivo* cultured B cell progenitors where we could measure the effect on B-1a cell development by analyzing the frequency of CD5 positive Imm-B cells after titrating the glucose availability in the cell culture media. Interestingly, this identified that CD5 positive Imm-B cells dominate the LIN28B induced Imm-B cell pool *ex vivo*, being much more frequent than what is normally seen *in vivo*. However, titration of the available glucose did not affect the frequency of CD5 positive Imm-B cells *ex vivo*. Instead, it did reduce the frequency of Pro-B cells in LIN28B induced cultures. It is currently not clear if the *ex vivo* culture faithfully captures a potential glucose dependence *in vivo* and more work is necessary. Additionally, the LIN28B effect on glucose metabolism is not clear, given that glucose uptake increased across all stages of development but ATP levels only increased at the Imm-B cell stage.

General Discussion and Future Directions

Our work establishes CD5 expression and BCR signalling at the Imm-B cell stage as a novel hallmark of B-1a cell development in early-life, which is reintroduced upon ectopic LIN28B expression (paper I-II). In contrast, CD5 negative Imm-B cells have none or low BCR signalling and do not develop into the B-1a subset. As such, our findings are in line with previous publications implicating the level of BCR signalling dictating cell fate (*101*) with LIN28B enabling the development of clones with high enough BCR signalling to become a B-1a cell. While previous work focused on the mature cells (*124*), we now show that high BCR signalling is achieved already during development of the Imm-B cell.

This positions neonatal B cell development in the mouse closer to T lymphocytes that express CD5 and depend on recognition of self-antigen during their development (*205*). During T cell development, CD5 expression fine tunes the levels of TCR signalling for positive selection of self-reactive TCRs (*206, 207*) and, as with neonatal B cell development, CD5 expression is higher during the increased output of self-reactive TCRs in early-life (*208*). As such, tapping in on the knowledge on positive selection during T cell development might hold novel insights for development of self-reactive BCRs in early life.

While the LIN28B program in B cell progenitors still needs to be resolved in full, one key factor has been identified in let-7 dependent regulation of ARID3A that on its own phenocopies LIN28B (*187, 209*). However, the underlying mechanism and whether ARID3A on its own increases CD5 expression and BCR signalling in Imm-B cells needs to be investigated. Additionally, another interesting lead to follow up is the transcription factor BHLHE41 that regulates B-1a cell development by facilitating the mRNA transcription in response to BCR signalling (*126*) and is upregulated in LIN28B induced Imm-B cells (*210*). Together, these three factors might achieve the necessary BCR signalling to enable B-1a development. Their interdependence could be interrogated by crossing *Lin28b* inducible mice

onto *Arid3a* and/or *Bhlhe41* null background and measure CD5 levels on the Imm-B cells.

Another important finding to follow up is how high level of BCR signalling is tolerated by CD5 positive Imm-B cells, as it normally results in negative selection during conventional B cell development (*43*). As such, direct comparison of CD5 positive and negative Imm-B cells will be informative not only for B-1a development but will also deepen the knowledge on the important but incompletely understood central tolerance checkpoint (*63*).

Speculations on the (LIN28B) mechanisms in neonatal B cell progenitors

Our analysis of the LIN28B mRNA interactome in Paper II identified an enrichment in transcripts encoding ribosomal proteins, components of the oxidative phosphorylation pathway, and mRNA splicing. While we chose to focus on the ribosome and protein synthesis, the other pathways (and single genes that were not captured by the gene ontology analysis) might well contribute to B-1a development in so far unknown ways. Additionally, we have not proven that the LIN28B binding of certain ribosomal protein coding transcripts actually underlies an increased protein synthesis rate. Indeed, LIN28B regulates protein synthesis in small Pre-B and Imm-B cells, while the RIP-SEQ was done primarily on the Pro-B and large Pre-B cells. It is possible that LIN28B increases specific ribosomal proteins to achieve their 'extra ribosomal functions', which will be unique to each individual ribosomal protein. One such candidate is *Rpl22l1* that was bound by LIN28B in *ex vivo* cultured B cell progenitors and is known to control B- and T-cell development without having an effect on global protein synthesis rates (*211*). In addition, an emerging concept is the idea of a 'specialized ribosome' where a distinct ribosome composition facilitates the preferential translation of certain mRNA (*212*). Perhaps such a specialized ribosome is enforced by LIN28B, although this point is highly speculative.

Why does early-life B cell development rely on a high rate of protein synthesis?

In Paper II we find that the mild reduction in global protein synthesis rates of the $Rpl24^{BST/WT}$ mouse model (*213*) crashes neonatal but not adult B lymphopoiesis. The underlying mechanism was not resolved, but it does not

seem to be due to increased sensitivity as a consequence of increased proliferation in early life, as neonatal or LIN28B induced progenitors were not proliferating in a strikingly different way (Paper II and own unpublished data). However, we do have an additional observation that allows for speculation.

While measuring the levels of c-MYC expression in neonatal B cell progenitors over the weeks following birth, we noticed how increased c-MYC expression perfectly overlaps with the time of sensitivity to reduced protein synthesis rates (own unpublished data). As the c-MYC expression naturally wanes and eventually reaches an adult level during the first weeks post-birth, so did the sensitivity to protein synthesis. This is in line with a previous study that showed how the same $Rpl24^{BST/WT}$ mouse model negatively impacts c-MYC driven B cell leukemia, by reducing the protein synthesis rate to a low level that interfered with translation of specific mRNA (*214*). The translation of a specific mRNA depends on several factors, including the availability of free ribosomes, the transcript propensity for associating with the ribosome (and other important co-factors), and the efficiency by which a specific mRNA is then translated into a protein (*215*). As such, the increased sensitivity of neonatal B cell progenitors to reduced protein synthesis rates could be a result of their increased c-MYC activity, which increases the overall mRNA levels and, thus, competition for available ribosomes. Given such a model, reducing protein synthesis in neonates will be detrimental when competition for ribosomes is relatively high, whereas the lower competition for ribosomes in adult B cell progenitors is still manageable. In line with such a mechanism, the erythroid lineage crashes under reduce protein synthesis as a result of failed translation of a specific subset of critical genes (*216*).

Does LIN28B regulation of glucose metabolism matter, for B-1a development and beyond?

From our work in Paper III, it is still not clear if the LIN28B increase in glucose metabolism holds any importance for B-1a development and the CD5 positive Imm-B cells, given that titrating down the glucose levels in the cell culture media did not decrease the frequency of CD5 positive Imm-B cells *ex vivo* (Paper III). However, it is possible that this experimental approach lacks the resolution to identify the true impact on the CD5 positive Imm-B cells, given that the *ex vivo* culture is not well-suited to study an effect on this developmental stage and that even a titrated glucose availability might still saturate the glucose uptake of the Imm-B cell. Instead, it is still possible that the increased glucose uptake *in vivo* might result in the increased ATP

levels we identified in LIN28B induced Imm-B cells, perhaps to support increased levels of BCR signalling. More work is necessary, for example by titrating down glucose from a more physiological level or investigation of glucose metabolism in B cell progenitors *in vivo*.

In addition, our finding that LIN28B increases glucose uptake into the B cell progenitor might hold importance outside of B-1a development. For example, the risk of developing Acute lymphoblastic leukemia (ALL) is increased during early-life (*217*) and B-ALL depends on an increased glucose metabolism (*218*). Additionally, LIN28B increased glucose metabolism might affect mature neonatal B cells in addition to the progenitors, as was previously shown to be the case for neonatal T cells (*219*).

Could LIN28B mediate positive selection through an indirect effect on non-let-7 miRNA?

In addition to gene regulation through let-7 and direct mRNA binding, an interesting mechanism by which LIN28B might enable positive selection of self-reactive BCRs could be through an indirect effect on other miRNA.

miRNA are post-transcriptional regulators that repress specific mRNA targets through sequence complementarity to their specific 'seed sequence'. To repress their target mRNA, miRNA must first be loaded into the DICER complex. As this complex is expressed at a limiting rate, competition between different miRNA for binding the DICER complex also indirectly regulates the activity of other miRNA. As such, when LIN28B reduces the expression levels of let-7 it also removes a part of the competition and indirectly increase the activity of other miRNA (*220*).

Such an effect might be important for positive selection of self-reactive Imm-B cells, for example through increased activity of miR-148 (*221*) and miR-17~92 (*222*) that both regulate PI3K signalling and positive selection. Indeed, while LIN28B overexpression in Imm-B cells leads to increased expression of let-7 targets, there is also a clear decreased expression of many other miRNA targets, including miR-148 (Figure 5).

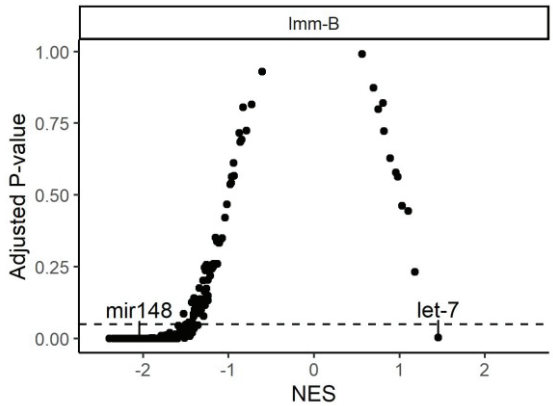

Figure 5. Gene set enrichment analysis (GSEA) for miRNA targets in Imm-B cells (data from Paper I). Normalized enrichment score (NES) is calculated as LIN28B over control Imm-B cells (i.e. a positive value means that the gene set is increased in LIN28B induced Imm-B cells and vice versa). Adjusted P-value of 0.05 is indicated by the dashed line. The let-7 and miR148 gene sets are annotated. miR17~92 was not available in the used gene set collection.

Does LIN28B affect the Pro-B or large Pre-B stages of development?

One interesting observation from our work in Paper I & II was how the LIN28B effect was primarily observed in the small CD5 positive subset that upregulated BCR signalling and metabolism. Still, the majority of Imm-B cells remain CD5 negative, do not achieve high signalling through their BCR, and remain metabolically quiescent, even when inducible LIN28B is abundantly expressed by both CD5 positive and CD5 negative cells. Thus, LIN28B cannot make just any Imm-B cell become CD5 positive. Instead, LIN28B may enable the CD5 subset by I) having a direct effect on some Imm-B cells and/or II) enabling CD5 output by affecting the preceding development. To identify the timing of the LIN28B effect, we measured the B-1a cell output after 'turning on' or 'turning off' LIN28B induction at distinct stages of development, by transferring progenitors between doxycycline fed and non-doxycycline fed mice (Paper I). By transferring uninduced Imm-B cells from a non-doxycycline fed tet-Lin28b mouse to a doxycycline fed recipient, we found that inducing LIN28B at the Imm-B cell stage did not yield B-1a cells. Transferring Pro-B cells from a doxycycline

fed tet-Lin28b mouse to a non-doxycycline fed recipient found that turning off LIN28B at the Pro-B cell stage failed to generate B-1a cells. This is indicating that LIN28B has a necessary effect at the Pro-B cell stage or the subsequent pre-BCR checkpoint for B-1a development.

Does LIN28B enable pre-BCR independent development?

Given how the pre-BCR checkpoint plays a role in censoring self-reactive B cell development (*99*), it is possible that LIN28B circumvents the pre-BCR checkpoint to output self-reactive, CD5 positive Imm-B cells. In line with this, the γδ T cell subset can develop without the pre-TCR (*223*) and their development further depends on LIN28B (*134*). A LIN28B effect on the pre-BCR checkpoint is currently not known and subject to ongoing research in the Yuan lab.

More than one possible mechanism might explain how LIN28B would allow pre-BCR independent B cell development, and they need not be mutually exclusive. LIN28B might enable premature light chain recombination in Pro-B cells to circumvent the pre-BCR checkpoint, as has been described during fetal liver B-1a development (*83*). In line with this, LIN28B enables a degree of IL-7 independent B cell development (*134*) that could allow premature light chain recombination (*47, 224*). Additionally, LIN28B might circumvent the pre-BCR checkpoint by enabling development of pre-BCR independent heavy chains (*84-86*), perhaps by supplying the same signal that is necessary for development. This notion is consistent with LIN28B rescuing the deficient BCR signalling in *Cd19* knockout mice, through its direct increase in PI3K signalling activity (Paper I). Additionally, perhaps ARID3A also plays a role in this since its overexpression on a V_H11 transgenic background (i.e. a poor SLC pairing heavy chain) increased the frequency of Imm-B cells, although it is not clear whether this was due to an effect on the pre-BCR checkpoint (*209*).

Identifying a separation between B-1a and B-2 development before CD5 expression at the Imm-B cell stage

Investigation into whether LIN28B affects development before the Imm-B cell stage is complicated by the lack of any surface marker (including CD5) to separate out a B-1a progenitor from a B-2 progenitor. As a result, prospective analysis of Pro-B and Pre-B cells using bulk analysis suffers from poor resolution since the B-1a progenitors are diluted out by B-2 progenitors. Single cell analysis is becoming more available and will ultimately overcome this issue and allow for prospective analysis. For

example, combined RNA- and VDJ-sequencing analysis could provide information on BCR signalling levels in tet-Lin28b and neonatal Pre-B cells. Another prospective single-cell approach could investigate the level of light chain locus accessibility (i.e. premature light chain recombination) in tet-Lin28b and neonatal Pro-B cells.

In the meanwhile, an additional approach could take advantage of the fact that CD5 positive Imm-B cells become increasingly enriched over the days when LIN28B inducible progenitors are cultured *ex vivo* (Paper III). As such, repeated sampling of the same culture over the days could help identify any increasing effect that correlates with frequency of CD5 positive Imm-B cells (e.g. light chain recombination in Pro-B cells).

LIN28B induced B-1a cells: 'made or born'?

Finally, LIN28B induction of B-1a cell development in adult mice also provides some new insights for the old discussion whether a B-1a cell is 'born' from a separate lineage or 'made' from a B-2 cell with high BCR signalling (*106*). While B-2 cells can indeed be coaxed into becoming a B-1a in a BCR-dependent manner (*102*), it is not known whether LIN28B induction in adults re-activates a B-1a potent progenitor or enable high BCR signalling during B-2 development.

Mature LIN28B induced B-1a cells are polyclonal instead of enriched for the usual B-1a repertoire that develops in early life (*187*), in line with LIN28B enabling positive selection of any self-reactive BCR. Indeed, LIN28B also enables development in adult Ig-HEL mice that are forced to express a specific self-reactive BCR during development (*210*). Still, by using barcode labelling of progenitors to track their progeny, previous work from our lab found that LIN28B induced B-1a output originates from a subset of all the progenitors (*35*). This hints at a hidden layer of complexity where not all B cell progenitors are the same and perhaps ectopic LIN28B only allows B-1a development from a subset of progenitors, hypothetically the same subset that originally produced B-1a cells in early-life.

To explore this interesting possibility, one could yet again take advantage of the fact that CD5 positive Imm-B cells become increasingly enriched when LIN28B inducible progenitors are cultured *ex vivo* (Paper III). By barcode labelling single Pro-B cells before *ex vivo* expansion, the barcode heterogeneity among the Pro-B cell pool can be compared to the barcode representation among CD5 positive Imm-B cells. For example, following five days in culture of barcode labelled Pro-B cells the CD5 positive Imm-B cells will dominate over CD5 negative Imm-B cells. If the barcode

representation among the Pro-B cells is restricted to a few clones, it would imply that the high frequency of CD5 positive Imm-B cells *ex vivo* originate from the enrichment of a B-1a biased Pro-B cell. If instead the Pro-B cell enrichment is polyclonal (i.e. diverse barcode representation), it can be cross compared to the barcode representation among CD5 positive Imm-B cells to see if only a few B-1a biased Pro-B cells yielded all of the CD5 positive Imm-B cells (Figure 6).

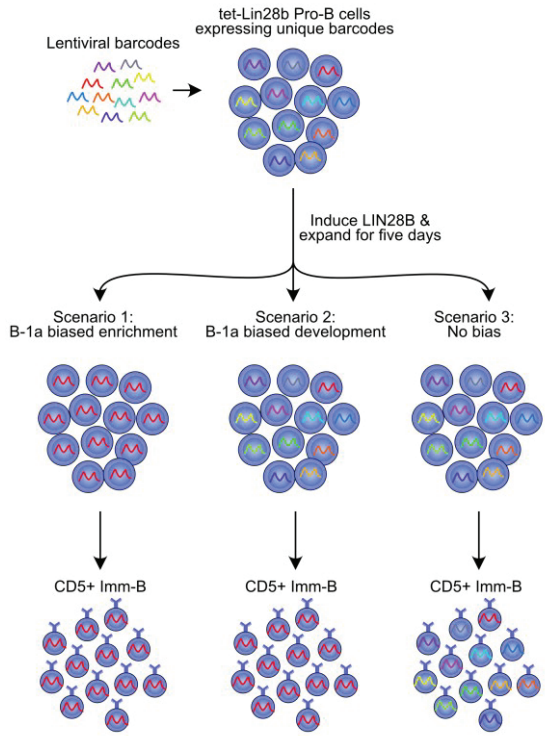

Figure 6. Experiment idea for investigating B-1a enrichment ex vivo. Barcode experiment to investigate whether high levels of CD5 positive Imm-B cells *ex vivo* is due to enrichment of a B-1a biased Pro-B cell (scenario 1), B-1a biased development (scenario 2), or without any such bias (scenario 3).

Populärvetenskaplig sammanfattning

Varenda vuxen person som genomlevde COVID-19-pandemin känner nog till ordet ’antikropp’: den ’osynliga barriären’ mot viruset som mättes och diskuterades i tid och otid. Men vad är egentligen en antikropp? En antikropp är en mikroskopisk molekyl som utsöndras av en B-cell (en typ av immuncell) när cellen känner igen ett specifikt ’antigen’, alltså en struktur på t.ex. COVID-19 viruset. För att upptäcka ifall kroppen har blivit infekterad så uttrycker varje B-cell sin antikropp utanpå cellens yta. Till exempel vid en COVID-19 infektion, när viruset finns i närheten och känns igen av en B-cell så binds det in av B-cellen och resulterar i en massiv utsöndring av dess antikropp. I kroppen finns miljontals av olika B-celler som uttrycker olika antikroppar mot olika antigen som uttrycks på virus, bakterier, osv. Tillsammans utgör alla dessa specificiteter mot olika antigen den ’osynliga barriären’ som skyddar oss mot infektioner.

Hur kan kroppen producera miljontals av olika antikroppar? Vilken antikropp en B-cell uttrycker bestäms först under dess utveckling till att bli en mogen B-cell. Det är en komplex genetisk process som resulterar i att en unik antikropp uttrycks av varje B cell, ifall allting går som det ska. Men ibland går det fel och då kan farliga B-celler som reagerar på kroppens egna antigen utvecklas, t.ex. hos personer med autoimmuna sjukdomar. Därför regleras B-cellsutvecklingen mycket noggrant för att motverka sådana ’självreaktiva’ B-celler. Men B-cellsutveckling ter sig lite annorlunda under olika stadier i livet och trots risken att utveckla autoimmunsjukdom så tillåts faktiskt självreaktiva B-celler att utvecklas under det tidiga levnadsstadiet. Hur genetisk reglering tillåter utvecklingen av självreaktiva B-celler i nyfödda möss är utgångspunkten för denna avhandling.

För att studera genetisk reglering av B-cellsutvecklingen hos nyfödda så använder vi oss av möss där vi kan påtvinga B-cellerna att uttrycka proteinet LIN28B. Vi har tidigare bevisat att LIN28B kontrollerar B-cellsutvecklingen tidigt i livet, men inte till fullo förstått hur det fungerar. Genom att studera B-cellsutvecklingen med LIN28B har vi nu kunnat påvisa att det här proteinet möjliggör utvecklingen av B-celler som kan reagera på kroppens egna antigen

(Artikel 1). Molekylärt så möjliggör LIN28B det genom att reglera uttrycket av olika gener. Vi har kartlagt vilka gener som binds av LIN28B och genom detta identifierat att LIN28B reglerar cellens syntes av protein. Protein är viktiga molekyler som utför olika funktioner i cellen och bildas kontinuerligt av en cell. Vi har nu visat att protein bildas snabbare under nyföddas B-cellsutveckling än vad det gör under vuxnas. Ökningen är viktig och om vi delvis begränsar hur mycket protein som kan bildas så kraschar nyföddas B-cellsutveckling men den fungerar som normalt i vuxna möss (Artikel 2). Slutligen så har vi också studerat hur LIN28B påverkar metabolismen av glukos under B-cellsutvecklingen. Glukos är en sockerart som bryts ned av cellen för att frigöra energi och för att bli omvandlad till andra typer av molekyler som cellen behöver. Vi hypotiserade att glukos-metabolismen skulle vara förhöjd under B-cellsutvecklingen hos nyfödda för att tillgodose den extra energi som de självreaktiva B-cellerna kommer behöva. Vi kunde visa att B-cellsutvecklingen hos nyfödda tog upp mer glukos men det är fortfarande oklart ifall detta resulterar i mer energi (Artikel 3).

Genom våra insikter har vi bidragit med bättre förståelse för hur B-cellsutvecklingen fungerar. Genom att studera normal B-cellsutveckling kommer vi bättre kunna förstå vad som går fel när en person drabbas av t.ex. en autoimmunsjukdom eller cancer i dessa celler. Dessutom tror vi att vissa av de B-celler som utvecklades när vi var barn finns kvar hos oss som vuxna där de spelar en specifik roll för vårat immunförsvar genom att uttrycka unika antikroppar. Sammantaget hoppas vi att vårat arbete i förlängningen kommer bidra med en bättre förståelse om hur B-celler utvecklas, hur nyföddas B-celler bidrar till immunförsvaret, och vad som går fel vid t.ex. uppkomsten av cancer.

Acknowledgements

Too many people have been a part of my PhD to remember everyone: a big thanks to all of you who made these years enjoyable! You know who you are!

Of course, this PhD wouldn't have been possible without my PI **Joan Yuan**. Thank you Joan, for your supervision during all these years! Thank your for teaching me the scientific process, for being such a passionate and inspirational scientist, and for providing a creative and positive work environment! Thank you also to my co-supervisor **Jenny Pyl-Hansson** for being such a great person and supportive colleague! Thank you to my second co-supervisor **Mikael Sigvardson** who helped in creating and managing an inspiring and fun environment at B12! Thank you to all the present and past Yuan group members: **Stijn, Giorgia, Trine, Karin, Elena, Niklas, Selene, Stefano, Elin, Alex, Sneha, Sebak.** You have all been great colleagues and made it fun to spend time in the lab! A special thanks to all the experts who have helped me in one way or another during the PhD: **Zhi, Anna, Teia, Sam, Pillai, Beata, Shamit, Stefan, Leal, Maciej, Roberto, Mattias.**

Thank you to all the other colleagues and friends who I have had the pleasure of spending time with during my PhD: **Cote, Roberto, Abdul Ghani, Erin, Jonas, Ania, Maciej, Giulia, Filipo, Magda, Nico, Sandy, Mateusz, Phuong, Sudip, Maria, Kristyna, Mikael, Mojqan, Parashar, Rebecca, Ram, Johan, Oskar, Sandro, Dimitra, Hongzhe, Hooi Ching, Isabel, Dang, Gladys, Johanna, Tina, Alexandra, Ariana, Sara, Rasmus, Roshanak, Ouyang, Mo, Qinyu, Juliane, Leal, Roger, Chaos Accelerator, Ludwig, Yang, Ineke, Natsumi, Melissa, Hooi Min, Els, Valli, Shubh, Kristijonas, Alexandra, Gabriella, Rita, Olga, Fabio, Cristiana, Sara, Maria, Sarah, Taha, Alexander, Sandra, Pavan, Sofia, Simon, Anna, Aurelie, Kiyoka, Agathees, Ilana, Alya, Kenichi, Cristian, Johan, Stefan, Göran, Ewa, Kees-Jan, David, Charlotta, Jonas, Niels-Bjarne, Filipe, Stefan, Mattias, Christine**, **Maria, Helena, Olga, Mina, Linda, Marie, Kristin, Gerd.** Thank you for providing a great work environment, for scientific discussions and ideas, for the good times at parties and pub hangs, floorball, sauna (and Jonas-fit), dinners, trips, and everything else!

Thank you to family and friends: **Hampus, Annika, Per, Sigrid, Katarina, Nils, Oleg, Liubov, Georgij, Gustaf, Ulla, Sven, Nina, Johanna, Kalle, Ullis, Peder, Lars, Tussan, Kristina, Thomas, Kalle, Oscar, Stina, Linnea, Trond, Axel, Frida, Johan, Ninni, Marianne, Jan, Cilla, Mats, Caroline, Claes, Mette, Viktor, Victor, Patrik, Rickard, and all the rest of my friends!** Thank you for all the good times and for always being there!

Finally, thank you **Svetlana**, who has been by my side throughout this whole PhD and my constant partner and support. No one else will ever fully understand what this PhD actually means except me and you! I am so happy we did it together and I cannot wait to continue on new adventures. Thank you for everything you give me and for more things than words can put on a paper! Älskar dig!

References

1. A. Bendelac, M. Bonneville, J. F. Kearney, Autoreactivity by design: innate B and T lymphocytes. *Nat Rev Immunol* **1**, 177-186 (2001).
2. F. Melchers, Checkpoints that control B cell development. *J Clin Invest* **125**, 2203-2210 (2015).
3. K. Hayakawa *et al.*, Ly-1 B cells: functionally distinct lymphocytes that secrete IgM autoantibodies. *Proc Natl Acad Sci U S A* **81**, 2494-2498 (1984).
4. L. A. Herzenberg, L. A. Herzenberg, Toward a layered immune system. *Cell* **59**, 953-954 (1989).
5. R. Elsaid, J. Yang, A. Cumano, The influence of space and time on the establishment of B cell identity. *Biomed J* **42**, 209-217 (2019).
6. C. Tabilas, N. L. Smith, B. D. Rudd, Shaping immunity for life: Layered development of CD8(+) T cells. *Immunol Rev*, (2023).
7. E. G. Perdiguero, F. Geissmann, The development and maintenance of resident macrophages. *Nat Immunol* **17**, 2-8 (2016).
8. K. Rajewsky, Clonal selection and learning in the antibody system. *Nature* **381**, 751-758 (1996).
9. R. C. Rickert, New insights into pre-BCR and BCR signalling with relevance to B cell malignancies. *Nat Rev Immunol* **13**, 578-591 (2013).
10. D. Allman, S. Pillai, Peripheral B cell subsets. *Curr Opin Immunol* **20**, 149-157 (2008).
11. F. Martin, J. F. Kearney, Marginal-zone B cells. *Nat Rev Immunol* **2**, 323-335 (2002).
12. N. Baumgarth, The double life of a B-1 cell: self-reactivity selects for protective effector functions. *Nat Rev Immunol* **11**, 34-46 (2011).
13. J. Dirks, D. Viemann, N. Beyersdorf, C. Hartel, H. Morbach, Insights into B-cell ontogeny inferred from human immunology. *Eur J Immunol*, e2250116 (2023).
14. D. O. Griffin, N. E. Holodick, T. L. Rothstein, Human B1 cells in umbilical cord and adult peripheral blood express the novel phenotype CD20+ CD27+ CD43+ CD70. *J Exp Med* **208**, 67-80 (2011).
15. C. Gronwall, J. Vas, G. J. Silverman, Protective Roles of Natural IgM Antibodies. *Front Immunol* **3**, 66 (2012).

16. R. R. Hardy, C. E. Carmack, S. A. Shinton, R. J. Riblet, K. Hayakawa, A single VH gene is utilized predominantly in anti-BrMRBC hybridomas derived from purified Ly-1 B cells. Definition of the VH11 family. *J Immunol* **142**, 3643-3651 (1989).
17. T. J. Mercolino, L. W. Arnold, L. A. Hawkins, G. Haughton, Normal mouse peritoneum contains a large population of Ly-1+ (CD5) B cells that recognize phosphatidyl choline. Relationship to cells that secrete hemolytic antibody specific for autologous erythrocytes. *J Exp Med* **168**, 687-698 (1988).
18. K. Hayakawa, C. E. Carmack, R. Hyman, R. R. Hardy, Natural autoantibodies to thymocytes: origin, VH genes, fine specificities, and the role of Thy-1 glycoprotein. *J Exp Med* **172**, 869-878 (1990).
19. M. Y. Chou *et al.*, Oxidation-specific epitopes are dominant targets of innate natural antibodies in mice and humans. *J Clin Invest* **119**, 1335-1349 (2009).
20. L. Kulik *et al.*, Pathogenic natural antibodies recognizing annexin IV are required to develop intestinal ischemia-reperfusion injury. *J Immunol* **182**, 5363-5373 (2009).
21. V. Manohar, E. Brown, W. M. Leiserson, T. M. Chused, Expression of Lyt-1 by a subset of B lymphocytes. *J Immunol* **129**, 532-538 (1982).
22. R. R. Hardy, K. Hayakawa, J. Haaijman, L. A. Herzenberg, B-cell subpopulations identified by two-colour fluorescence analysis. *Nature* **297**, 589-591 (1982).
23. C. L. Sidman, L. D. Shultz, R. R. Hardy, K. Hayakawa, L. A. Herzenberg, Production of immunoglobulin isotypes by Ly-1+ B cells in viable motheaten and normal mice. *Science* **232**, 1423-1425 (1986).
24. C. A. Pennell, K. M. Sheehan, P. H. Brodeur, S. H. Clarke, Organization and expression of VH gene families preferentially expressed by Ly-1+ (CD5) B cells. *Eur J Immunol* **19**, 2115-2121 (1989).
25. K. Hayakawa, R. R. Hardy, L. A. Herzenberg, L. A. Herzenberg, Progenitors for Ly-1 B cells are distinct from progenitors for other B cells. *J Exp Med* **161**, 1554-1568 (1985).
26. K. Hayakawa, R. R. Hardy, A. M. Stall, L. A. Herzenberg, L. A. Herzenberg, Immunoglobulin-bearing B cells reconstitute and maintain the murine Ly-1 B cell lineage. *Eur J Immunol* **16**, 1313-1316 (1986).
27. R. Hardy, K. Hayakawa, Generation of Ly-1 B cells from developmentally distinct precursors. Enrichment by stromal-cell culture or cell sorting. *Ann N Y Acad Sci* **651**, 99-111 (1992).
28. E. Montecino-Rodriguez, K. Dorshkind, The layered development of mouse B and T Cells. *Immunol Rev*, (2022).
29. A. Medvinsky, E. Dzierzak, Definitive hematopoiesis is autonomously initiated by the AGM region. *Cell* **86**, 897-906 (1996).

30. I. E. Godin, J. A. Garcia-Porrero, A. Coutinho, F. Dieterlen-Lievre, M. A. Marcos, Para-aortic splanchnopleura from early mouse embryos contains B1a cell progenitors. *Nature* **364**, 67-70 (1993).
31. M. Yoshimoto *et al.*, Embryonic day 9 yolk sac and intra-embryonic hemogenic endothelium independently generate a B-1 and marginal zone progenitor lacking B-2 potential. *Proc Natl Acad Sci U S A* **108**, 1468-1473 (2011).
32. M. Kobayashi *et al.*, Functional B-1 progenitor cells are present in the hematopoietic stem cell-deficient embryo and depend on Cbfbeta for their development. *Proc Natl Acad Sci U S A* **111**, 12151-12156 (2014).
33. E. E. Ghosn *et al.*, Fetal Hematopoietic Stem Cell Transplantation Fails to Fully Regenerate the B-Lymphocyte Compartment. *Stem Cell Reports* **6**, 137-149 (2016).
34. A. E. Beaudin *et al.*, A Transient Developmental Hematopoietic Stem Cell Gives Rise to Innate-like B and T Cells. *Cell Stem Cell* **19**, 768-783 (2016).
35. T. A. Kristiansen *et al.*, Cellular Barcoding Links B-1a B Cell Potential to a Fetal Hematopoietic Stem Cell State at the Single-Cell Level. *Immunity* **45**, 346-357 (2016).
36. T. A. Kristiansen, S. Vanhee, J. Yuan, The influence of developmental timing on B cell diversity. *Curr Opin Immunol* **51**, 7-13 (2018).
37. S. Vergani *et al.*, A self-sustaining layer of early-life-origin B cells drives steady-state IgA responses in the adult gut. *Immunity* **55**, 1829-1842 e1826 (2022).
38. K. Kikuchi, M. Kondo, Developmental switch of mouse hematopoietic stem cells from fetal to adult type occurs in bone marrow after birth. *Proc Natl Acad Sci U S A* **103**, 17852-17857 (2006).
39. F. Young *et al.*, Influence of immunoglobulin heavy- and light-chain expression on B-cell differentiation. *Genes Dev* **8**, 1043-1057 (1994).
40. E. Spanopoulou *et al.*, Functional immunoglobulin transgenes guide ordered B-cell differentiation in Rag-1-deficient mice. *Genes Dev* **8**, 1030-1042 (1994).
41. D. Jung, C. Giallourakis, R. Mostoslavsky, F. W. Alt, Mechanism and control of V(D)J recombination at the immunoglobulin heavy chain locus. *Annu Rev Immunol* **24**, 541-570 (2006).
42. H. Wardemann *et al.*, Predominant autoantibody production by early human B cell precursors. *Science* **301**, 1374-1377 (2003).
43. E. Meffre, H. Wardemann, B-cell tolerance checkpoints in health and autoimmunity. *Curr Opin Immunol* **20**, 632-638 (2008).
44. S. Zandi, D. Bryder, M. Sigvardsson, Load and lock: the molecular mechanisms of B-lymphocyte commitment. *Immunol Rev* **238**, 47-62 (2010).

45. S. L. Nutt, B. Heavey, A. G. Rolink, M. Busslinger, Commitment to the B-lymphoid lineage depends on the transcription factor Pax5. *Nature* **401**, 556-562 (1999).
46. A. E. Corcoran, A. Riddell, D. Krooshoop, A. R. Venkitaraman, Impaired immunoglobulin gene rearrangement in mice lacking the IL-7 receptor. *Nature* **391**, 904-907 (1998).
47. S. Malin *et al.*, Role of STAT5 in controlling cell survival and immunoglobulin gene recombination during pro-B cell development. *Nat Immunol* **11**, 171-179 (2010).
48. S. Tonegawa, Somatic generation of antibody diversity. *Nature* **302**, 575-581 (1983).
49. S. Gilfillan, C. Benoist, D. Mathis, Mice lacking terminal deoxynucleotidyl transferase: adult mice with a fetal antigen receptor repertoire. *Immunol Rev* **148**, 201-219 (1995).
50. H. Karasuyama, A. Kudo, F. Melchers, The proteins encoded by the VpreB and lambda 5 pre-B cell-specific genes can associate with each other and with mu heavy chain. *J Exp Med* **172**, 969-972 (1990).
51. D. Kitamura *et al.*, A critical role of lambda 5 protein in B cell development. *Cell* **69**, 823-831 (1992).
52. N. Sakaguchi, F. Melchers, Lambda 5, a new light-chain-related locus selectively expressed in pre-B lymphocytes. *Nature* **324**, 579-582 (1986).
53. A. Kudo, F. Melchers, A second gene, VpreB in the lambda 5 locus of the mouse, which appears to be selectively expressed in pre-B lymphocytes. *EMBO J* **6**, 2267-2272 (1987).
54. C. Eschbach *et al.*, Efficient generation of B lymphocytes by recognition of self-antigens. *Eur J Immunol* **41**, 2397-2403 (2011).
55. U. Grawunder *et al.*, Down-regulation of RAG1 and RAG2 gene expression in preB cells after functional immunoglobulin heavy chain rearrangement. *Immunity* **3**, 601-608 (1995).
56. M. C. Nussenzweig *et al.*, Allelic exclusion in transgenic mice that express the membrane form of immunoglobulin mu. *Science* **236**, 816-819 (1987).
57. F. Ramadani *et al.*, The PI3K isoforms p110alpha and p110delta are essential for pre-B cell receptor signaling and B cell development. *Sci Signal* **3**, ra60 (2010).
58. R. H. Amin, M. S. Schlissel, Foxo1 directly regulates the transcription of recombination-activating genes during B cell development. *Nat Immunol* **9**, 613-622 (2008).
59. J. J. Limon, D. A. Fruman, Akt and mTOR in B Cell Activation and Differentiation. *Front Immunol* **3**, 228 (2012).
60. M. R. Clark, M. Mandal, K. Ochiai, H. Singh, Orchestrating B cell lymphopoiesis through interplay of IL-7 receptor and pre-B cell receptor signalling. *Nat Rev Immunol* **14**, 69-80 (2014).

61. L. Verkoczy *et al.*, Basal B cell receptor-directed phosphatidylinositol 3-kinase signaling turns off RAGs and promotes B cell-positive selection. *J Immunol* **178**, 6332-6341 (2007).
62. M. Llorian, Z. Stamataki, S. Hill, M. Turner, I. L. Martensson, The PI3K p110delta is required for down-regulation of RAG expression in immature B cells. *J Immunol* **178**, 1981-1985 (2007).
63. D. Nemazee, Mechanisms of central tolerance for B cells. *Nat Rev Immunol* **17**, 281-294 (2017).
64. M. Hertz, D. Nemazee, BCR ligation induces receptor editing in IgM+IgD- bone marrow B cells in vitro. *Immunity* **6**, 429-436 (1997).
65. D. Gay, T. Saunders, S. Camper, M. Weigert, Receptor editing: an approach by autoreactive B cells to escape tolerance. *J Exp Med* **177**, 999-1008 (1993).
66. P. A. Hieter, S. J. Korsmeyer, T. A. Waldmann, P. Leder, Human immunoglobulin kappa light-chain genes are deleted or rearranged in lambda-producing B cells. *Nature* **290**, 368-372 (1981).
67. D. Nemazee, K. Buerki, Clonal deletion of autoreactive B lymphocytes in bone marrow chimeras. *Proc Natl Acad Sci U S A* **86**, 8039-8043 (1989).
68. D. A. Nemazee, K. Burki, Clonal deletion of B lymphocytes in a transgenic mouse bearing anti-MHC class I antibody genes. *Nature* **337**, 562-566 (1989).
69. S. B. Hartley *et al.*, Elimination from peripheral lymphoid tissues of self-reactive B lymphocytes recognizing membrane-bound antigens. *Nature* **353**, 765-769 (1991).
70. S. B. Hartley *et al.*, Elimination of self-reactive B lymphocytes proceeds in two stages: arrested development and cell death. *Cell* **72**, 325-335 (1993).
71. C. Chen *et al.*, The site and stage of anti-DNA B-cell deletion. *Nature* **373**, 252-255 (1995).
72. S. Yurasov *et al.*, Defective B cell tolerance checkpoints in systemic lupus erythematosus. *J Exp Med* **201**, 703-711 (2005).
73. J. Samuels, Y. S. Ng, C. Coupillaud, D. Paget, E. Meffre, Impaired early B cell tolerance in patients with rheumatoid arthritis. *J Exp Med* **201**, 1659-1667 (2005).
74. J. G. Monroe, ITAM-mediated tonic signalling through pre-BCR and BCR complexes. *Nat Rev Immunol* **6**, 283-294 (2006).
75. F. Loder *et al.*, B cell development in the spleen takes place in discrete steps and is determined by the quality of B cell receptor-derived signals. *J Exp Med* **190**, 75-89 (1999).
76. C. C. Goodnow *et al.*, Altered immunoglobulin expression and functional silencing of self-reactive B lymphocytes in transgenic mice. *Nature* **334**, 676-682 (1988).
77. E. Montecino-Rodriguez, H. Leathers, K. Dorshkind, Identification of a B-1 B cell-specified progenitor. *Nat Immunol* **7**, 293-301 (2006).

78. G. K. Pedersen *et al.*, B-1a transitional cells are phenotypically distinct and are lacking in mice deficient in IkappaBNS. *Proc Natl Acad Sci U S A* **111**, E4119-4126 (2014).
79. L. Erlandsson *et al.*, Impaired B-1 and B-2 B cell development and atypical splenic B cell structures in IL-7 receptor-deficient mice. *Eur J Immunol* **34**, 3595-3603 (2004).
80. D. G. Hesslein, S. Y. Yang, D. G. Schatz, Origins of peripheral B cells in IL-7 receptor-deficient mice. *Mol Immunol* **43**, 326-334 (2006).
81. Y. S. Li, K. Hayakawa, R. R. Hardy, The regulated expression of B lineage associated genes during B cell differentiation in bone marrow and fetal liver. *J Exp Med* **178**, 951-960 (1993).
82. S. Gilfillan, A. Dierich, M. Lemeur, C. Benoist, D. Mathis, Mice lacking TdT: mature animals with an immature lymphocyte repertoire. *Science* **261**, 1175-1178 (1993).
83. J. B. Wong *et al.*, B-1a cells acquire their unique characteristics by bypassing the pre-BCR selection stage. *Nat Commun* **10**, 4768 (2019).
84. R. Wasserman *et al.*, A novel mechanism for B cell repertoire maturation based on response by B cell precursors to pre-B receptor assembly. *J Exp Med* **187**, 259-264 (1998).
85. G. H. Kline *et al.*, Pre-B cell receptor-mediated selection of pre-B cells synthesizing functional mu heavy chains. *J Immunol* **161**, 1608-1618 (1998).
86. C. Tatu, J. Ye, L. W. Arnold, S. H. Clarke, Selection at multiple checkpoints focuses V(H)12 B cell differentiation toward a single B-1 cell specificity. *J Exp Med* **190**, 903-914 (1999).
87. G. C. Bosma, Y. Chang, H. Karasuyama, M. J. Bosma, Differential effect of an Ig mu transgene on development of pre-B cells in fetal and adult SCID mice. *Proc Natl Acad Sci U S A* **96**, 11952-11957 (1999).
88. A. B. Kantor, C. E. Merrill, L. A. Herzenberg, J. L. Hillson, An unbiased analysis of V(H)-D-J(H) sequences from B-1a, B-1b, and conventional B cells. *J Immunol* **158**, 1175-1186 (1997).
89. U. C. Tornberg, D. Holmberg, B-1a, B-1b and B-2 B cells display unique VHDJH repertoires formed at different stages of ontogeny and under different selection pressures. *EMBO J* **14**, 1680-1689 (1995).
90. R. M. Perlmutter, J. F. Kearney, S. P. Chang, L. E. Hood, Developmentally controlled expression of immunoglobulin VH genes. *Science* **227**, 1597-1601 (1985).
91. F. Martin, X. Chen, J. F. Kearney, Development of VH81X transgene-bearing B cells in fetus and adult: sites for expansion and deletion in conventional and CD5/B1 cells. *Int Immunol* **9**, 493-505 (1997).

92. L. W. Arnold, C. A. Pennell, S. K. McCray, S. H. Clarke, Development of B-1 cells: segregation of phosphatidyl choline-specific B cells to the B-1 population occurs after immunoglobulin gene expression. *J Exp Med* **179**, 1585-1595 (1994).
93. B. Rowley, L. Tang, S. Shinton, K. Hayakawa, R. R. Hardy, Autoreactive B-1 B cells: constraints on natural autoantibody B cell antigen receptors. *J Autoimmun* **29**, 236-245 (2007).
94. H. Ferry, T. L. Crockford, J. C. Leung, R. J. Cornall, Signals from a self-antigen induce positive selection in early B cell ontogeny but are tolerogenic in adults. *J Immunol* **176**, 7402-7411 (2006).
95. K. Hayakawa *et al.*, Positive selection of anti-thy-1 autoreactive B-1 cells and natural serum autoantibody production independent from bone marrow B cell development. *J Exp Med* **197**, 87-99 (2003).
96. K. Hayakawa *et al.*, Positive selection of natural autoreactive B cells. *Science* **285**, 113-116 (1999).
97. E. ten Boekel, F. Melchers, A. G. Rolink, Changes in the V(H) gene repertoire of developing precursor B lymphocytes in mouse bone marrow mediated by the pre-B cell receptor. *Immunity* **7**, 357-368 (1997).
98. J. Ye, S. K. McCray, S. H. Clarke, The transition of pre-BI to pre-BII cells is dependent on the VH structure of the mu/surrogate L chain receptor. *EMBO J* **15**, 1524-1533 (1996).
99. R. A. Keenan *et al.*, Censoring of autoreactive B cell development by the pre-B cell receptor. *Science* **321**, 696-699 (2008).
100. T. Kreslavsky, J. B. Wong, M. Fischer, J. A. Skok, M. Busslinger, Control of B-1a cell development by instructive BCR signaling. *Curr Opin Immunol* **51**, 24-31 (2018).
101. S. Casola *et al.*, B cell receptor signal strength determines B cell fate. *Nat Immunol* **5**, 317-327 (2004).
102. R. Graf *et al.*, BCR-dependent lineage plasticity in mature B cells. *Science* **363**, 748-753 (2019).
103. R. A. Miller, J. Gralow, The induction of Leu-1 antigen expression in human malignant and normal B cells by phorbol myristic acetate (PMA). *J Immunol* **133**, 3408-3414 (1984).
104. Y. Z. Cong, E. Rabin, H. H. Wortis, Treatment of murine CD5- B cells with anti-Ig, but not LPS, induces surface CD5: two B-cell activation pathways. *Int Immunol* **3**, 467-476 (1991).
105. G. Bikah, J. Carey, J. R. Ciallella, A. Tarakhovsky, S. Bondada, CD5-mediated negative regulation of antigen receptor-induced growth signals in B-1 B cells. *Science* **274**, 1906-1909 (1996).
106. G. Haughton, L. W. Arnold, A. C. Whitmore, S. H. Clarke, B-1 cells are made, not born. *Immunol Today* **14**, 84-87; discussion 87-91 (1993).

107. A. J. Clarke, T. Riffelmacher, D. Braas, R. J. Cornall, A. K. Simon, B1a B cells require autophagy for metabolic homeostasis and self-renewal. *J Exp Med* **215**, 399-413 (2018).
108. I. G. A. Raza, A. J. Clarke, B Cell Metabolism and Autophagy in Autoimmunity. *Front Immunol* **12**, 681105 (2021).
109. L. N. Chan *et al.*, Metabolic gatekeeper function of B-lymphoid transcription factors. *Nature* **542**, 479-483 (2017).
110. G. Xiao *et al.*, B-Cell-Specific Diversion of Glucose Carbon Utilization Reveals a Unique Vulnerability in B Cell Malignancies. *Cell* **173**, 470-484 e418 (2018).
111. S. Urbanczyk *et al.*, Regulation of Energy Metabolism during Early B Lymphocyte Development. *Int J Mol Sci* **19**, (2018).
112. F. J. Dufort *et al.*, Cutting edge: IL-4-mediated protection of primary B lymphocytes from apoptosis via Stat6-dependent regulation of glycolytic metabolism. *J Immunol* **179**, 4953-4957 (2007).
113. C. A. Doughty *et al.*, Antigen receptor-mediated changes in glucose metabolism in B lymphocytes: role of phosphatidylinositol 3-kinase signaling in the glycolytic control of growth. *Blood* **107**, 4458-4465 (2006).
114. A. Caro-Maldonado *et al.*, Metabolic reprogramming is required for antibody production that is suppressed in anergic but exaggerated in chronically BAFF-exposed B cells. *J Immunol* **192**, 3626-3636 (2014).
115. H. Kojima *et al.*, Differentiation stage-specific requirement in hypoxia-inducible factor-1alpha-regulated glycolytic pathway during murine B cell development in bone marrow. *J Immunol* **184**, 154-163 (2010).
116. T. N. Iwata *et al.*, Conditional Disruption of Raptor Reveals an Essential Role for mTORC1 in B Cell Development, Survival, and Metabolism. *J Immunol* **197**, 2250-2260 (2016).
117. S. Zhang *et al.*, Constitutive reductions in mTOR alter cell size, immune cell development, and antibody production. *Blood* **117**, 1228-1238 (2011).
118. H. Zeng *et al.*, Discrete roles and bifurcation of PTEN signaling and mTORC1-mediated anabolic metabolism underlie IL-7-driven B lymphopoiesis. *Sci Adv* **4**, eaar5701 (2018).
119. H. Park *et al.*, Disruption of Fnip1 reveals a metabolic checkpoint controlling B lymphocyte development. *Immunity* **36**, 769-781 (2012).
120. A. C. Donahue, D. A. Fruman, Distinct signaling mechanisms activate the target of rapamycin in response to different B-cell stimuli. *Eur J Immunol* **37**, 2923-2936 (2007).
121. M. Li *et al.*, Sin1/mTORC2 regulate B cell growth and metabolism by activating mTORC1 and Myc. *Cell Mol Immunol* **16**, 757-769 (2019).
122. A. S. Lazorchak *et al.*, Sin1-mTORC2 suppresses rag and il7r gene expression through Akt2 in B cells. *Mol Cell* **39**, 433-443 (2010).

123. S. Shojaee *et al.*, PTEN opposes negative selection and enables oncogenic transformation of pre-B cells. *Nat Med* **22**, 379-387 (2016).
124. R. Berland, H. H. Wortis, Origins and functions of B-1 cells with notes on the role of CD5. *Annu Rev Immunol* **20**, 253-300 (2002).
125. Y. Yang *et al.*, Distinct mechanisms define murine B cell lineage immunoglobulin heavy chain (IgH) repertoires. *Elife* **4**, e09083 (2015).
126. T. Kreslavsky *et al.*, Essential role for the transcription factor Bhlhe41 in regulating the development, self-renewal and BCR repertoire of B-1a cells. *Nat Immunol* **18**, 442-455 (2017).
127. C. L. Benedict, J. F. Kearney, Increased junctional diversity in fetal B cells results in a loss of protective anti-phosphorylcholine antibodies in adult mice. *Immunity* **10**, 607-617 (1999).
128. A. J. Feeney, Predominance of VH-D-JH junctions occurring at sites of short sequence homology results in limited junctional diversity in neonatal antibodies. *J Immunol* **149**, 222-229 (1992).
129. Y. Zhang *et al.*, The role of short homology repeats and TdT in generation of the invariant gamma delta antigen receptor repertoire in the fetal thymus. *Immunity* **3**, 439-447 (1995).
130. K. Hayakawa *et al.*, B lymphocyte developmental lineages. *Ann N Y Acad Sci* **815**, 15-29 (1997).
131. B. Vilagos *et al.*, Essential role of EBF1 in the generation and function of distinct mature B cell types. *J Exp Med* **209**, 775-792 (2012).
132. M. Ye, O. Ermakova, T. Graf, PU.1 is not strictly required for B cell development and its absence induces a B-2 to B-1 cell switch. *J Exp Med* **202**, 1411-1422 (2005).
133. E. Montecino-Rodriguez *et al.*, Distinct Genetic Networks Orchestrate the Emergence of Specific Waves of Fetal and Adult B-1 and B-2 Development. *Immunity* **45**, 527-539 (2016).
134. J. Yuan, C. K. Nguyen, X. Liu, C. Kanellopoulou, S. A. Muljo, Lin28b reprograms adult bone marrow hematopoietic progenitors to mediate fetal-like lymphopoiesis. *Science* **335**, 1195-1200 (2012).
135. Y. Nam, C. Chen, R. I. Gregory, J. J. Chou, P. Sliz, Molecular basis for interaction of let-7 microRNAs with Lin28. *Cell* **147**, 1080-1091 (2011).
136. V. Ambros, H. R. Horvitz, Heterochronic mutants of the nematode Caenorhabditis elegans. *Science* **226**, 409-416 (1984).
137. G. Shinoda *et al.*, Fetal deficiency of lin28 programs life-long aberrations in growth and glucose metabolism. *Stem Cells* **31**, 1563-1573 (2013).
138. E. G. Moss, L. Tang, Conservation of the heterochronic regulator Lin-28, its developmental expression and microRNA complementary sites. *Dev Biol* **258**, 432-442 (2003).

139. E. G. Moss, R. C. Lee, V. Ambros, The cold shock domain protein LIN-28 controls developmental timing in C. elegans and is regulated by the lin-4 RNA. *Cell* **88**, 637-646 (1997).
140. J. Yu *et al.*, Induced pluripotent stem cell lines derived from human somatic cells. *Science* **318**, 1917-1920 (2007).
141. A. Urbach *et al.*, Lin28 sustains early renal progenitors and induces Wilms tumor. *Genes Dev* **28**, 971-982 (2014).
142. L. H. Nguyen *et al.*, Lin28b is sufficient to drive liver cancer and necessary for its maintenance in murine models. *Cancer Cell* **26**, 248-261 (2014).
143. J. J. Molenaar *et al.*, LIN28B induces neuroblastoma and enhances MYCN levels via let-7 suppression. *Nat Genet* **44**, 1199-1206 (2012).
144. S. H. Beachy *et al.*, Enforced expression of Lin28b leads to impaired T-cell development, release of inflammatory cytokines, and peripheral T-cell lymphoma. *Blood* **120**, 1048-1059 (2012).
145. C. E. King *et al.*, LIN28B promotes colon cancer progression and metastasis. *Cancer Res* **71**, 4260-4268 (2011).
146. S. R. Viswanathan *et al.*, Lin28 promotes transformation and is associated with advanced human malignancies. *Nat Genet* **41**, 843-848 (2009).
147. J. Balzeau, M. R. Menezes, S. Cao, J. P. Hagan, The LIN28/let-7 Pathway in Cancer. *Front Genet* **8**, 31 (2017).
148. M. R. Copley *et al.*, The Lin28b-let-7-Hmga2 axis determines the higher self-renewal potential of fetal haematopoietic stem cells. *Nat Cell Biol* **15**, 916-925 (2013).
149. T. A. Kristiansen *et al.*, Developmental cues license megakaryocyte priming in murine hematopoietic stem cells. *Blood Adv* **6**, 6228-6241 (2022).
150. M. C. Stolla *et al.*, Lin28b regulates age-dependent differences in murine platelet function. *Blood Adv* **3**, 72-82 (2019).
151. Y. Bronevetsky, T. D. Burt, J. M. McCune, Lin28b Regulates Fetal Regulatory T Cell Differentiation through Modulation of TGF-beta Signaling. *J Immunol* **197**, 4344-4350 (2016).
152. J. Wang *et al.*, Fetal and adult progenitors give rise to unique populations of CD8+ T cells. *Blood* **128**, 3073-3082 (2016).
153. L. A. Pobezinsky *et al.*, Let-7 microRNAs target the lineage-specific transcription factor PLZF to regulate terminal NKT cell differentiation and effector function. *Nat Immunol* **16**, 517-524 (2015).
154. Y. T. Lee *et al.*, LIN28B-mediated expression of fetal hemoglobin and production of fetal-like erythrocytes from adult human erythroblasts ex vivo. *Blood* **122**, 1034-1041 (2013).
155. R. G. Rowe *et al.*, Developmental regulation of myeloerythroid progenitor function by the Lin28b-let-7-Hmga2 axis. *J Exp Med* **213**, 1497-1512 (2016).

156. A. Basak *et al.*, Control of human hemoglobin switching by LIN28B-mediated regulation of BCL11A translation. *Nat Genet* **52**, 138-145 (2020).
157. P. Tieppo *et al.*, The human fetal thymus generates invariant effector gammadelta T cells. *J Exp Med* **217**, (2020).
158. D. P. Bartel, Metazoan MicroRNAs. *Cell* **173**, 20-51 (2018).
159. S. Roush, F. J. Slack, The let-7 family of microRNAs. *Trends Cell Biol* **18**, 505-516 (2008).
160. T. A. Nguyen *et al.*, Functional Anatomy of the Human Microprocessor. *Cell* **161**, 1374-1387 (2015).
161. M. Ha, V. N. Kim, Regulation of microRNA biogenesis. *Nat Rev Mol Cell Biol* **15**, 509-524 (2014).
162. S. R. Viswanathan, G. Q. Daley, R. I. Gregory, Selective blockade of microRNA processing by Lin28. *Science* **320**, 97-100 (2008).
163. A. Rybak *et al.*, A feedback loop comprising lin-28 and let-7 controls pre-let-7 maturation during neural stem-cell commitment. *Nat Cell Biol* **10**, 987-993 (2008).
164. M. A. Newman, J. M. Thomson, S. M. Hammond, Lin-28 interaction with the Let-7 precursor loop mediates regulated microRNA processing. *RNA* **14**, 1539-1549 (2008).
165. I. Heo *et al.*, Lin28 mediates the terminal uridylation of let-7 precursor MicroRNA. *Mol Cell* **32**, 276-284 (2008).
166. J. P. Hagan, E. Piskounova, R. I. Gregory, Lin28 recruits the TUTase Zcchc11 to inhibit let-7 maturation in mouse embryonic stem cells. *Nat Struct Mol Biol* **16**, 1021-1025 (2009).
167. J. E. Thornton, H. M. Chang, E. Piskounova, R. I. Gregory, Lin28-mediated control of let-7 microRNA expression by alternative TUTases Zcchc11 (TUT4) and Zcchc6 (TUT7). *RNA* **18**, 1875-1885 (2012).
168. I. Heo *et al.*, Mono-uridylation of pre-microRNA as a key step in the biogenesis of group II let-7 microRNAs. *Cell* **151**, 521-532 (2012).
169. E. Piskounova *et al.*, Lin28A and Lin28B inhibit let-7 microRNA biogenesis by distinct mechanisms. *Cell* **147**, 1066-1079 (2011).
170. B. J. Reinhart *et al.*, The 21-nucleotide let-7 RNA regulates developmental timing in Caenorhabditis elegans. *Nature* **403**, 901-906 (2000).
171. V. Ambros, MicroRNAs and developmental timing. *Curr Opin Genet Dev* **21**, 511-517 (2011).
172. J. Jin *et al.*, Evidence that Lin28 stimulates translation by recruiting RNA helicase A to polysomes. *Nucleic Acids Res* **39**, 3724-3734 (2011).
173. A. Polesskaya *et al.*, Lin-28 binds IGF-2 mRNA and participates in skeletal myogenesis by increasing translation efficiency. *Genes Dev* **21**, 1125-1138 (2007).

174. E. Balzer, E. G. Moss, Localization of the developmental timing regulator Lin28 to mRNP complexes, P-bodies and stress granules. *RNA Biol* **4**, 16-25 (2007).
175. S. Wang *et al.*, Enhancement of LIN28B-induced hematopoietic reprogramming by IGF2BP3. *Genes Dev* **33**, 1048-1068 (2019).
176. J. Zhang *et al.*, LIN28 Regulates Stem Cell Metabolism and Conversion to Primed Pluripotency. *Cell Stem Cell* **19**, 66-80 (2016).
177. M. Hafner *et al.*, Identification of mRNAs bound and regulated by human LIN28 proteins and molecular requirements for RNA recognition. *RNA* **19**, 613-626 (2013).
178. R. Graf *et al.*, Identification of LIN28B-bound mRNAs reveals features of target recognition and regulation. *RNA Biol* **10**, 1146-1159 (2013).
179. M. L. Wilbert *et al.*, LIN28 binds messenger RNAs at GGAGA motifs and regulates splicing factor abundance. *Mol Cell* **48**, 195-206 (2012).
180. J. Cho *et al.*, LIN28A is a suppressor of ER-associated translation in embryonic stem cells. *Cell* **151**, 765-777 (2012).
181. S. Peng *et al.*, Genome-wide studies reveal that Lin28 enhances the translation of genes important for growth and survival of human embryonic stem cells. *Stem Cells* **29**, 496-504 (2011).
182. P. Missios *et al.*, LIN28B alters ribosomal dynamics to promote metastasis in MYCN-driven malignancy. *J Clin Invest* **131**, (2021).
183. B. Xu, K. Zhang, Y. Huang, Lin28 modulates cell growth and associates with a subset of cell cycle regulator mRNAs in mouse embryonic stem cells. *RNA* **15**, 357-361 (2009).
184. M. Eldeeb *et al.*, A fetal tumor suppressor axis abrogates MLL-fusion-driven acute myeloid leukemia. *Cell Rep* **42**, 112099 (2023).
185. R. D. Lee *et al.*, Single-cell analysis identifies dynamic gene expression networks that govern B cell development and transformation. *Nat Commun* **12**, 6843 (2021).
186. K. M. Tsanov *et al.*, LIN28 phosphorylation by MAPK/ERK couples signalling to the post-transcriptional control of pluripotency. *Nat Cell Biol* **19**, 60-67 (2017).
187. Y. Zhou *et al.*, Lin28b promotes fetal B lymphopoiesis through the transcription factor Arid3a. *J Exp Med* **212**, 569-580 (2015).
188. D. Lin *et al.*, Bright/ARID3A contributes to chromatin accessibility of the immunoglobulin heavy chain enhancer. *Mol Cancer* **6**, 23 (2007).
189. C. Schmidt *et al.*, Signalling of the BCR is regulated by a lipid rafts-localised transcription factor, Bright. *EMBO J* **28**, 711-724 (2009).
190. N. Shyh-Chang, G. Q. Daley, Lin28: primal regulator of growth and metabolism in stem cells. *Cell Stem Cell* **12**, 395-406 (2013).

191. N. Shyh-Chang *et al.*, Lin28 enhances tissue repair by reprogramming cellular metabolism. *Cell* **155**, 778-792 (2013).
192. C. Chen *et al.*, Targeting LIN28B reprograms tumor glucose metabolism and acidic microenvironment to suppress cancer stemness and metastasis. *Oncogene* **38**, 4527-4539 (2019).
193. A. N. Dubinsky *et al.*, Let-7 coordinately suppresses components of the amino acid sensing pathway to repress mTORC1 and induce autophagy. *Cell Metab* **20**, 626-638 (2014).
194. H. Zhu *et al.*, The Lin28/let-7 axis regulates glucose metabolism. *Cell* **147**, 81-94 (2011).
195. R. J. Frost, E. N. Olson, Control of glucose homeostasis and insulin sensitivity by the Let-7 family of microRNAs. *Proc Natl Acad Sci U S A* **108**, 21075-21080 (2011).
196. Y. Gao *et al.*, The H19/let-7 double-negative feedback loop contributes to glucose metabolism in muscle cells. *Nucleic Acids Res* **42**, 13799-13811 (2014).
197. S. M. Johnson *et al.*, RAS is regulated by the let-7 microRNA family. *Cell* **120**, 635-647 (2005).
198. V. B. Sampson *et al.*, MicroRNA let-7a down-regulates MYC and reverts MYC-induced growth in Burkitt lymphoma cells. *Cancer Res* **67**, 9762-9770 (2007).
199. M. G. Vander Heiden, L. C. Cantley, C. B. Thompson, Understanding the Warburg effect: the metabolic requirements of cell proliferation. *Science* **324**, 1029-1033 (2009).
200. X. Ma *et al.*, Lin28/let-7 axis regulates aerobic glycolysis and cancer progression via PDK1. *Nat Commun* **5**, 5212 (2014).
201. S. Jiang, W. Yan, S. E. Wang, D. Baltimore, Let-7 Suppresses B Cell Activation through Restricting the Availability of Necessary Nutrients. *Cell Metab* **27**, 393-403 e394 (2018).
202. R. R. Hardy, K. Hayakawa, Perspectives on fetal derived CD5+ B1 B cells. *Eur J Immunol* **45**, 2978-2984 (2015).
203. H. S. Azzam *et al.*, CD5 expression is developmentally regulated by T cell receptor (TCR) signals and TCR avidity. *J Exp Med* **188**, 2301-2311 (1998).
204. M. Muschen, Metabolic gatekeepers to safeguard against autoimmunity and oncogenic B cell transformation. *Nat Rev Immunol* **19**, 337-348 (2019).
205. N. Vrisekoop, J. P. Monteiro, J. N. Mandl, R. N. Germain, Revisiting thymic positive selection and the mature T cell repertoire for antigen. *Immunity* **41**, 181-190 (2014).
206. A. Tarakhovsky *et al.*, A role for CD5 in TCR-mediated signal transduction and thymocyte selection. *Science* **269**, 535-537 (1995).
207. H. S. Azzam *et al.*, Fine tuning of TCR signaling by CD5. *J Immunol* **166**, 5464-5472 (2001).

208. M. Dong *et al.*, Alterations in the Thymic Selection Threshold Skew the Self-Reactivity of the TCR Repertoire in Neonates. *J Immunol* **199**, 965-973 (2017).
209. K. Hayakawa *et al.*, Crucial Role of Increased Arid3a at the Pre-B and Immature B Cell Stages for B1a Cell Generation. *Front Immunol* **10**, 457 (2019).
210. X. Xu *et al.*, An ontogenetic switch drives the positive and negative selection of B cells. *Proc Natl Acad Sci U S A* **117**, 3718-3727 (2020).
211. S. P. Fahl *et al.*, Loss of Ribosomal Protein Paralog Rpl22-like1 Blocks Lymphoid Development without Affecting Protein Synthesis. *J Immunol* **208**, 870-880 (2022).
212. S. Xue, M. Barna, Specialized ribosomes: a new frontier in gene regulation and organismal biology. *Nat Rev Mol Cell Biol* **13**, 355-369 (2012).
213. E. R. Oliver, T. L. Saunders, S. A. Tarle, T. Glaser, Ribosomal protein L24 defect in belly spot and tail (Bst), a mouse Minute. *Development* **131**, 3907-3920 (2004).
214. M. Barna *et al.*, Suppression of Myc oncogenic activity by ribosomal protein haploinsufficiency. *Nature* **456**, 971-975 (2008).
215. E. W. Mills, R. Green, Ribosomopathies: There's strength in numbers. *Science* **358**, (2017).
216. R. K. Khajuria *et al.*, Ribosome Levels Selectively Regulate Translation and Lineage Commitment in Human Hematopoiesis. *Cell* **173**, 90-103 e119 (2018).
217. S. P. Hunger, C. G. Mullighan, Acute Lymphoblastic Leukemia in Children. *N Engl J Med* **373**, 1541-1552 (2015).
218. T. Liu *et al.*, Glucose transporter 1-mediated glucose uptake is limiting for B-cell acute lymphoblastic leukemia anabolic metabolism and resistance to apoptosis. *Cell Death Dis* **5**, e1470 (2014).
219. C. Tabilas *et al.*, Cutting Edge: Elevated Glycolytic Metabolism Limits the Formation of Memory CD8(+) T Cells in Early Life. *J Immunol* **203**, 2571-2576 (2019).
220. F. E. Tan *et al.*, A Transcriptome-wide Translational Program Defined by LIN28B Expression Level. *Mol Cell* **73**, 304-313 e303 (2019).
221. A. Gonzalez-Martin *et al.*, The microRNA miR-148a functions as a critical regulator of B cell tolerance and autoimmunity. *Nat Immunol* **17**, 433-440 (2016).
222. D. Benhamou *et al.*, A c-Myc/miR17-92/Pten Axis Controls PI3K-Mediated Positive and Negative Selection in B Cell Development and Reconstitutes CD19 Deficiency. *Cell Rep* **16**, 419-431 (2016).
223. H. J. Fehling, A. Krotkova, C. Saint-Ruf, H. von Boehmer, Crucial role of the pre-T-cell receptor alpha gene in development of alpha beta but not gamma delta T cells. *Nature* **375**, 795-798 (1995).

224. M. Mandal *et al.*, Epigenetic repression of the Igk locus by STAT5-mediated recruitment of the histone methyltransferase Ezh2. *Nat Immunol* **12**, 1212-1220 (2011).

Paper I

LYMPHOCYTES

Lin28b controls a neonatal to adult switch in B cell positive selection

Stijn Vanhee[1], Hugo Åkerstrand[1], Trine Ahn Kristiansen[1], Sebak Datta[1], Giorgia Montano[1], Stefano Vergani[1], Stefan Lang[2], Jonas Ungerbäck[3], Alexander Doyle[1], Karin Olsson[1], Giulia Beneventi[4], Christina T. Jensen[3], Cristian Bellodi[4], Shamit Soneji[2], Mikael Sigvardsson[3,5], Elin Jaensson Gyllenbäck[1], Joan Yuan[1]*

The ability of B-1 cells to become positively selected into the mature B cell pool, despite being weakly self-reactive, has puzzled the field since its initial discovery. Here, we explore changes in B cell positive selection as a function of developmental time by exploiting a link between CD5 surface levels and the natural occurrence of self-reactive B cell receptors (BCRs) in BCR wild-type mice. We show that the heterochronic RNA binding protein Lin28b potentiates a neonatal mode of B cell selection characterized by enhanced overall positive selection in general and the developmental progression of $CD5^+$ immature B cells in particular. Lin28b achieves this by amplifying the CD19/PI3K/c-Myc positive feedback loop, and ectopic Lin28b expression restores both positive selection and mature B cell numbers in $CD19^{-/-}$ adult mice. Thus, the temporally restricted expression of *Lin28b* relaxes the rules for B cell selection during ontogeny by modulating tonic signaling. We propose that this neonatal mode of B cell selection represents a cell-intrinsic cue to accelerate the de novo establishment of the adaptive immune system and incorporate a layer of natural antibody-mediated immunity throughout life.

INTRODUCTION

Whereas T cell development relies on self-peptide–major histocompatibility complex (MHC) ligand-mediated positive selection to effectively contribute to host defense (*1*), B cell function is not similarly constrained and adult immature B (ImmB) cells are purged for self-antigen reactivity even at low binding affinities (*2*, *3*). Instead, developmental progression of newly formed ImmB cells carrying innocuous B cell receptors (BCRs) relies on ligand-independent tonic signaling mediated by the BCR and CD19 (*4*–*7*). Defying this censorship of self-reactivity are B-1 cells, an innate-like B cell subset harboring an oligoclonal and weakly self-reactive repertoire, which is excluded from germinal center reaction and is responsible for a functionally distinct layer of antibody-mediated immunity through the secretion of protective natural antibodies (*8*). Their positive selection was elegantly demonstrated using an anti-thymocyte autoantigen-specific BCR transgenic model, in which the presence of the Thy-1 self-antigen was a prerequisite for the establishment of transgene-positive $CD5^+$ B-1 cells of this naturally occurring specificity (*9*). In the near two decades that followed this discovery, the basis for the ability of B-1 cells to escape central tolerance and undergo positive selection has remained unresolved.

Considering the predominant early-life origin of $CD5^+$ B-1 cells, it is conceivable that B cell positive selection stringency may be temporally controlled during ontogeny. Transgenic expression of BCRs directed against self-antigens such as phosphatidylcholine (PtC) are efficiently incorporated into the neonatal B cell repertoire while being excluded in favor of endogenous BCRs in the adult (*9*–*12*). However, although the use of BCR transgenic models has been instrumental in unveiling unique aspects of B-1 cell selection, conclusions were limited to a few B-1–restricted antigen specificities in a non-physiological setting. To date, the underlying molecular mechanisms for such a putative ontogenic switch in B cell selection remain unknown.

Lin28b is a mammalian paralog of the heterochronic RNA binding protein Lin28, first described in *Caenorhabditis elegans* to block the biogenesis of the let-7 family of microRNAs (miRNAs) and thereby control the timing of developmental events (*13*). We have previously shown that Lin28b exhibits a fetal restricted expression pattern during murine hematopoiesis and that ectopic expression in the adult promotes key aspects of fetal-like lymphopoiesis, including the efficient production of $CD5^+$ B-1 cells (*14*, *15*). Since then, additional evidence from the lymphoid, erythroid, and megakaryocyte lineages has cemented the role of Lin28b as a multilineage molecular switch for fetal hematopoiesis (*16*–*20*). However, the requirement for endogenous Lin28b during early-life B lymphopoiesis has not been explored.

CD5 is a negative regulator of antigen receptor signaling and was first identified as a surface molecule expressed on human T cells and B chronic lymphoblastic leukemia cells (*21*). Parallel observations in mice and men established a positive correlation between the frequency of $CD5^+$ B cells and antibody polyreactivity (*22*). More recently, it was shown in antigen receptor transgenic mice that CD5 levels reflect the degree of self-antigen reactivity in T and B cells (*9*, *23*–*26*). In this study, we use surface CD5 levels to interrogate ontogenic changes in B cell positive selection in BCR wild-type (WT) mice. Our results demonstrate that B cell positive selection is temporally controlled during ontogeny by endogenous *Lin28b* by amplifying a previously reported positive feedback loop involving CD19 and c-Myc (*27*–*29*). Thus, Lin28b acts as a cell-intrinsic enhancer of overall ImmB cell positive selection, including the efficient developmental progression of weakly self-reactive B-1 cells early in life.

[1]Developmental Immunology Unit, Division of Molecular Hematology, Department of Laboratory Medicine, Lund Stem Cell Center, Lund University, 22242 Lund, Sweden. [2]Computational Genomics Unit, Division of Molecular Hematology, Department of Laboratory Medicine, Lund Stem Cell Center, Lund University, 22242 Lund, Sweden. [3]Molecular Lymphopoiesis Unit, Division of Molecular Hematology, Department of Laboratory Medicine, Lund Stem Cell Center, Lund University, 22242 Lund, Sweden. [4]RNA and Stem Cell Biology Unit, Division of Molecular Hematology, Department of Laboratory Medicine, Lund Stem Cell Center, Lund University, 22242 Lund, Sweden. [5]Department of Clinical and Experimental Medicine, Linköping University, 58185 Linköping, Sweden.
*Corresponding author. Email: joan.yuan@med.lu.se

RESULTS

Establishing a positive correlation between CD5 expression and self-reactivity in BCR WT B-1 cells

The murine adult B-1 cell compartment displays a range of CD5 surface levels, with those originating from fetal liver (FL) hematopoietic stem and progenitor cells (HSPCs) displaying the most surface expression. Although B-1 cells can mature in low numbers from adult HSPCs (*30*–*32*), these exhibit markedly lower surface CD5 expression (Fig. 1A) (*33*). Thus, we reasoned that uncovering the significance and developmental control of B cell CD5 levels would be critical in understanding the ontogenic switch in B cell output, leading to reduced B-1 cell generation. Although CD5 expression has been linked to self-reactivity in BCR transgenic models, this link has not been empirically established in a nontransgenic BCR setting. To this end, we took advantage of the high degree of self-antigen–driven clonal dominance in the murine B-1 compartment as a measure of self-reactivity and analyzed the BCR repertoires of sorted $CD5^{hi}$, $CD5^{int}$, $CD5^{low}$, and $CD5^{neg}$ peritoneal cavity B-1 cells from WT adult C57BL/6 mice (Fig. 1B). The successful separation based on CD5 surface levels was confirmed by fluorescence-activated cell sorting (FACS) analysis (Fig. 1C). Subsequent *IgHM* BCR repertoire sequencing analysis (VDJseq; see data file S2) demonstrated a correlation between increasing CD5 expression and CDR3 clonal dominance (Fig. 1D). This was quantified by the inequality index (Gini coefficient) of clonal representation (Fig. 1E). In addition, we observed a gradual increase in the representation of IGHV-11 and IGHV-12 gene segment usage, known to primarily encode the self-reactive specificity against PtC (Fig. 1F). This observation is consistent with FACS data displaying increasing PtC liposome reactivity with rising CD5 levels (Fig. 1G). Consistent with the superior ability of fetal HSPCs to generate $CD5^+$ B-1 cells (Fig. 1A) and the lack of terminal deoxynucleotidyl transferase (TdT) expression during fetal life (*34*), the presence of N-nucleotide additions inversely correlated with CD5 levels (Fig. 1H). These data establish that surface CD5 expression correlates with B cell self-reactivity and early ontogeny, providing a practical readout for self-reactivity in a non-BCRtg setting.

Lin28b potentiates an elevated mode of positive selection unique to neonatal mice

During adult B cell development in WT mice at steady state, CD5 expression is restricted to self-reactive transitional B cells in the spleen doomed for anergy and exclusion from the long-lived B cell pool (*25*). This is in contrast to the T cell lineage, where reactivity toward self-peptide–MHC complex is a desirable feature and CD5 is developmentally induced during positive selection in the $CD4^+CD8^+$ double-positive thymocyte stage (*23*, *24*). Considering that $CD5^+$ B-1 cells are allowed to mature early in life, we hypothesized that neonatal self-reactive $CD5^+$ ImmB cells would be positively selected into the mature B cell pool, analogous to $CD4^+CD8^+$ double-positive thymocytes, rather than being purged from the naïve B cell repertoire. In line with this hypothesis, we found that both the median fluorescence intensity (MFI) and the spread in surface CD5 levels as measured by interquartile range (IQR) were elevated as neonatal bone marrow (NBM) pre-B cells entered the IgM^+CD93^+ ImmB cell stage (Fig. 2A and fig. S1A). This emergence of $CD5^{hi}$ cells was apparent in the neonate but not adult ImmB cells and coincides with the timing of central tolerance establishment (*35*). Although only present at low frequencies (0.45 ± 0.25%) among neonatal ImmB cells, PtC-reactive cells reside within this $CD5^{hi}$ fraction (Fig. 2B), suggesting that

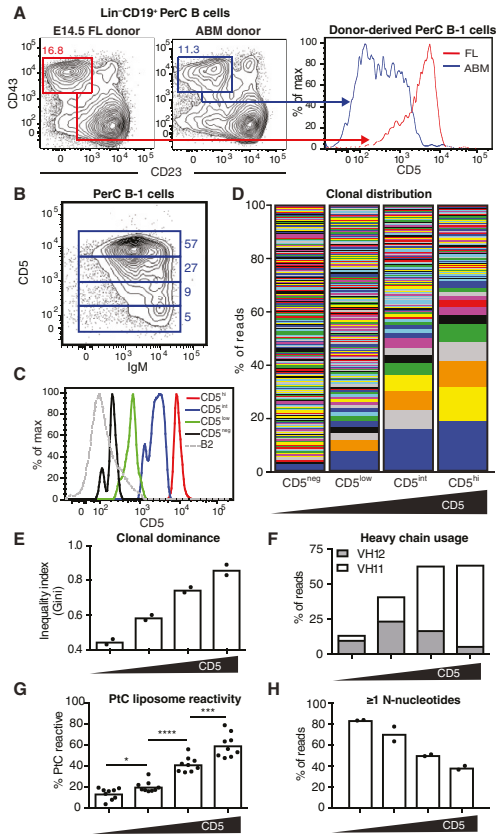

Fig. 1. Establishing a positive correlation between CD5 expression and self-reactivity in BCR WT B-1 cells. (**A**) Flow cytometric analysis of peritoneal cavity (PerC) B cells 16 weeks after transplantation of E14.5 FL or ABM $Lin^-Sca1^+cKit^+$ (LSK) HSPCs into lethally irradiated $CD45.1^+CD45.2^+$ congenic recipients. Lineage panel for E14.5 FL LSK: $Ter119^-B220^-Gr1^-CD3e^-$; ABM LSK: $Ter119^-B220^-Gr1^-CD11b^-CD3e^-$; PerC B cells: $Ter119^-Gr1^-CD3e^-$. (**B**) $CD5^{neg}$, $CD5^{low}$, $CD5^{int}$, and $CD5^{hi}$ gating strategy for WT adult PerC B-1 cells ($Lin^-CD19^+CD43^+CD23^-$). (**C**) Histogram overlay showing post sort analysis of the populations defined in (B). (**D**) Relative distribution of IgHM CDR3 sequences as determined by high-throughput VDJseq of the indicated populations. (**E**) Gini index of IgHM CDR3 sequence reads in sorted $CD5^{neg}$, $CD5^{low}$, $CD5^{int}$, and $CD5^{hi}$ populations (left to right). (**F**) Stacked bar graph indicates the combined frequency of IGHV-11 (white) and IGHV-12 (gray) containing IgHM CDR3 sequence reads. (**G**) Frequency of PtC liposome–reactive cells in the indicated B-1 populations as assessed by FACS. $*P \leq 0.05$, $***P \leq 0.001$, $****P \leq 0.0001$ ($n = 9$ from three experiments). (**H**) Frequency of CDR3 containing ≥1 N-nucleotide additions at the N1 and N2 junctions combined. VDJseq data (B to F and H) are representative of two biological and technical replicates.

CD5 levels are induced during B cell maturation on the basis of self-reactivity. The neonatal specific expression of CD5 on ImmB cells was mirrored by the presence of $CD5^+$ transitional T1 cells in the neonatal

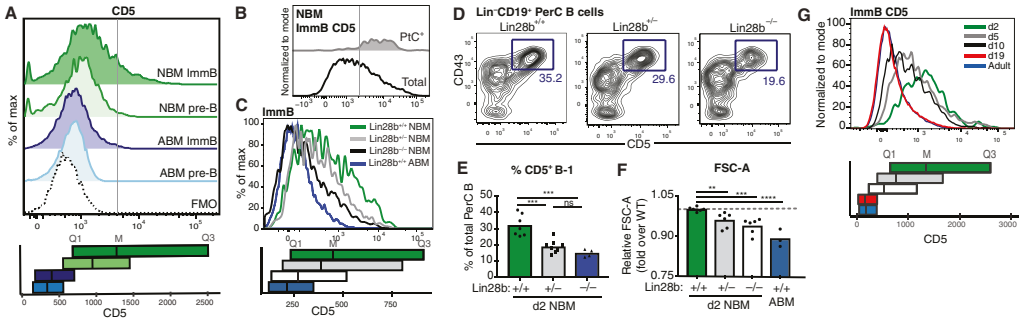

Fig. 2. Lin28b promotes the positive selection of CD5$^+$ ImmB cells in neonatal mice. (**A**) Representative histogram overlay of CD5 surface expression on 2-day-old NBM and 4-month-old ABM small pre-B (Lin$^-$CD19$^+$CD93$^+$IgM$^-$CD43$^-$CD24^{high}FSC^{low}) and ImmB cells (ImmB) (Lin$^-$CD19$^+$CD93$^+$IgM$^+$CD24^{high}). Lower panel shows the CD5 fluorescence intensity IQRs of the same populations. Q1, 25th percentile; Q3, 75th percentile; M, median; FMO, fluorescence minus one staining control. (**B**) CD5 levels on PtC liposome–reactive and total ImmB cells from 2-day-old WT NBM. (**C**) Histogram overlay of CD5 levels on 2-day-old NBM and ABM of the indicated genotypes. Lower panel shows the CD5 IQR. (**D**) Representative FACS plots showing the frequency of PerC CD5$^+$ B-1 cells from 10-day-old mice. (**E**) Quantification of data shown in (D) ($n = 4$ to 7 from three experiments). (**F**) Quantification of relative forward scatter (FSC-A) of ImmB from mice of the indicated genotypes and ages. Data are shown as a value relative to the FSC-A of a representative Lin28b$^{+/+}$ 2-day-old sample ($n = 3$ to 7 from three experiments). ns, not significant. $^{**}P \leq 0.01$, $^{***}P \leq 0.001$, $^{****}P \leq 0.0001$. (**G**) Representative histogram overlays of CD5 surface expression on WT BM ImmB of the indicated ages.

but not adult spleen (fig. S1B) known to be destined for the B-1 lineage (*36*). Considering the link between CD5 expression and BCR self-reactivity, these results are consistent with an increase in the tolerated spectrum of self-reactive specificities and an age-restricted licensing of an enhanced mode of positive selection in neonatal ImmB cells.

We and others have previously established Lin28b as a molecular switch capable of reinitiating fetal-like hematopoiesis including B-1 cell output (*14*, *15*, *20*). However, these data were exclusively based on ectopic expression of either Lin28a or Lin28b. To investigate whether endogenous Lin28b is required for the maturation of CD5$^+$ B-1 cells during neonatal life, we analyzed *Lin28b*$^{-/-}$ neonatal mice (*37*). We found that Lin28b deficiency led to decreased CD5 MFI and IQR in the ImmB compartment in a dose-dependent manner (Fig. 2C), resulting in the subsequent reduction of CD5$^+$ transitional T1 B cells in the spleen (fig. S1C) and mature CD5$^+$ B-1 cell output in the peritoneal cavity (Fig. 2, D and E). Furthermore, we observed a positive correlation between increased Lin28b dosage and ImmB cell size as measured by forward scatter (Fig. 2F), a hallmark of B cell positive selection (*6*). These data suggest that permissiveness toward CD5$^+$ ImmB cells and developmental progression of CD5$^+$ B-1 cells rely on endogenous *Lin28b* in neonatal mice. In line with this notion, we observed a postnatal decline in ImmB cell surface CD5 levels that coincides with the timing of the attenuation in *Lin28b* mRNA expression in hematopoietic stem cells (*15*) and becomes indistinguishable from the levels in adult ImmB cells by day 19 of age (Fig. 2G). We conclude that Lin28b expression early in life potentiates an elevated mode of positive selection characterized by the tolerance of CD5$^+$ ImmB cells and the output of CD5$^+$ B-1 cells during the first weeks of life.

Ectopic expression of Lin28b is sufficient to augment overall B cell positive selection in adult mice

To address whether ectopic Lin28b expression during adult B cell maturation is sufficient for potentiating the generation of CD5$^+$ ImmB cells, we put tet-Lin28b mice (*38*) on a doxycycline (DOX) diet for a minimum of 10 days. Lin28b transgene expression resulted in a potent increase in CD5 MFI and IQR upon pre-B to ImmB cell transition (Fig. 3A). Increased CD5 levels were accompanied by a tet-Lin28b–induced increase in ImmB cell size (Fig. 3B) and the emergence of CD5$^+$ transitional T1 cells in the spleen (fig. S1D), consistent with the neonatal mode of enhanced positive selection (*6*, *36*). Despite the observed increase in cell size, we did not observe apparent changes in the percentage of replicating cells among tet-Lin28b pre-B and ImmB cells (fig. S2, A and D), consistent with a modest increase in cellular anabolism. To track the maintenance of CD5 expression in the periphery, we adoptively transferred the 20% highest and lowest CD5-expressing ImmB cells from DOX-treated tet-Lin28b mice into individual non–DOX-treated Rag1KO recipients. Three weeks after adoptive transfer, CD5 levels were largely maintained in most donor-derived mature B cells, demonstrating that CD5$^+$ ImmB cells are predisposed to give rise to CD5$^+$ B-1 cells in a cell-intrinsic manner (Fig. 3, C to E). Furthermore, PtC-reactive specificities exclusively derived from the CD5$^+$ donor population (Fig. 3F), consistent with CD5 marking self-reactive ImmB cells.

To establish at which B cell developmental stage Lin28b is required to mediate efficient CD5$^+$ B-1 cell output, we adoptively transferred pro-B, pre-B, or ImmB cells from untreated tet-Lin28b donor mice into DOX-fed Rag1KO recipients (fig. S3A). CD5$^+$ B-1 cell output was most efficient when transgene expression is initiated at the pro-B cell stage and declined when initiated later at the pre-B and ImmB stages (fig. S3B). We subsequently performed the reverse experiment in which tet-Lin28b transgene expression in DOX-treated donor mice was turned off at different stages of B cell differentiation upon adoptive transfer into non–DOX-treated Rag1KO recipients. Our results demonstrate that cessation of Lin28b transgene expression before the ImmB stage is detrimental to developmental progression of progenitors destined for the CD5$^+$ B-1 fate (fig. S3B). Although there is a delay in transgene expression/cessation after transfer, these data firmly establish a need for Lin28b expression during the central tolerance checkpoint of B cell maturation (fig. S3C).

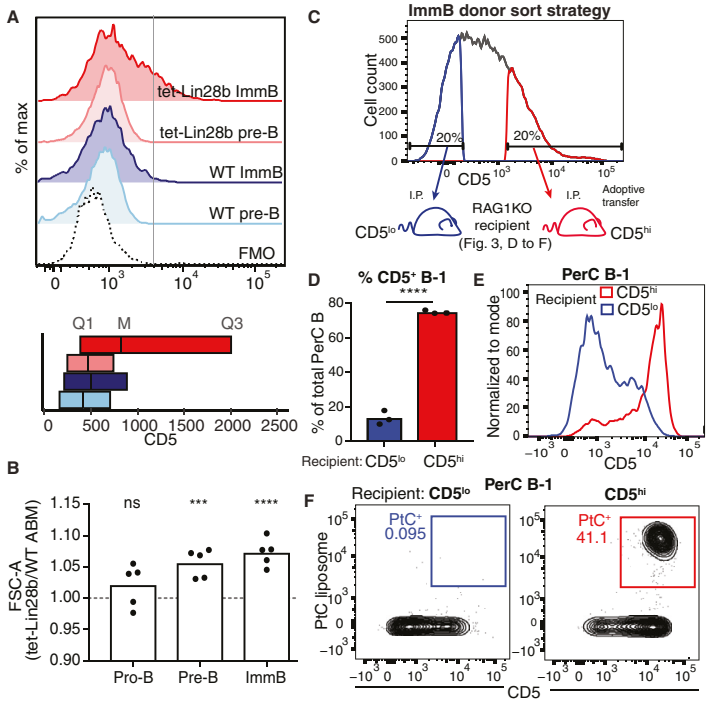

Fig. 3. Ectopic expression of Lin28b is sufficient to support enhanced B cell positive selection in the adult. (**A**) Representative histogram overlay of CD5 surface expression on ABM small pre-B cells and ImmB cells from tet-Lin28b and WT ABM mice fed a DOX diet for at least 10 days. Lower panel shows the CD5 IQR of the populations in the upper panel. (**B**) Quantification of relative FSC-A of pro-B, pre-B, and ImmB cells from tet-Lin28b ABM. The ratio of tet-Lin28b/WT cells from each experiment was calculated and plotted ($n = 5$ from three experiments). Statistics of the ratios against the value 1 were performed. ***$P \leq 0.001$, ****$P \leq 0.0001$. (**C**) Sort strategy for isolation of the 20% highest and lowest CD5-expressing ABM ImmB cells from DOX-fed tet-Lin28b mice. Sorted cells were transplanted intraperitoneally (I.P.) into untreated RAG1KO recipient mice on a normal diet. (**D**) Frequency of PerC CD5$^+$ B-1 cells 3 weeks after transplantation ($n = 3$ from two experiments). (**E**) Representative CD5 surface expression on PerC B-1 cells 3 weeks after transplantation. (**F**) Representative PtC liposome reactivity of PerC B-1 cells.

To quantitatively test whether the efficiency of B cell positive selection is enhanced by Lin28b, we measured mature B cell output by single-cell lineage tracing of preselection pro-B cells using lentiviral cellular barcoding (*15*, *39*). Adult bone marrow (ABM) pro-B cells were FACS-sorted from uninduced tet-Lin28b mice and transduced with a lentiviral library (Barcode-GFP-LV) encoding high-complexity DNA barcodes (Fig. 4A) (*40*). After transduction, the cells were divided into two equal halves that were adoptively transferred into Rag1KO recipients fed either DOX or normal diet. Green fluorescent protein–positive (GFP$^+$) mature B cells were isolated from the recipient spleen 2 weeks after transfer and analyzed for unique barcode content as a measure of relative selection efficiency (fig. S4, A to E). The number of unique progenitors that contributed to mature B cells was significantly increased upon ectopic Lin28b expression (Fig. 4, B and C). Barcode read frequency analysis did not reveal any unbalanced clonal expansion over the course of the experiment (Fig. 4B). Because barcode labeling efficiency was directly comparable, our finding is consistent with an increase in progeny:precursor ratio and thereby selection efficiency. In addition, both splenic mature B-1 and follicular B-2 cells from DOX-treated recipients displayed increased CD5 levels (Fig. 4, D and E). These data are reminiscent of previous observations that the majority of B cells in the human fetal spleen and cord blood are CD5$^+$ (*41*–*43*) and implicate Lin28b in the mechanism underlying this developmentally restricted expression pattern. We conclude that Lin28b augments overall B cell positive selection, including selection into the B-1 lineage.

To track the kinetics of developmental progression through the central tolerance checkpoint in the presence or absence of tet-Lin28b transgene expression in vivo, we pulsed DOX-fed tet-Lin28b and WT adult mice with a single dose of 5-ethynyl-2′-deoxyuridine (EdU) and assessed labeled B cells after 2, 24, 48, 72, and 96 hours of chase (Fig. 4F). Whereas initial labeling efficiency of IgM$^-$ B cell progenitors was comparable, labeled tet-Lin28b cells displayed accelerated progression through the B cell developmental stages and emergence into the splenic transitional T1 stage. Together, our data demonstrate that Lin28b promotes overall positive selection efficiency, leading to accelerated developmental progression of bone marrow egress.

Lin28b promotes B cell positive selection by amplifying the CD19/PI3K/c-Myc feedback loop

To explore the molecular pathway by which Lin28b regulates B cell positive selection, we performed RNA sequencing (RNA-seq) analysis of DOX-fed tet-Lin28b and WT ABM ImmB cells (see data file S3). Differential gene expression analysis identified an increase in the expression of several previously known Lin28b/let-7 target genes (e.g., *Igf2bp3*, *Myc*, and *Lin28b* itself) (Fig. 5A) as well as increased *Cd5* and *Nr4a1* (Nur77) transcript levels (Fig. 5B), consistent with enhanced self-reactivity (Fig. 3) (*44*). Unsupervised gene set enrichment analysis (GSEA) of the hallmark gene set collection from the Molecular Signature Database (*45*) identified c-Myc–induced targets as the top up-regulated molecular signature upon tet-Lin28b transgene expression (Fig. 5, C and D, and fig. S5). let-7 and interferon-γ response target genes served as positive and negative controls of our GSEAs, respectively (Fig. 5D). In line with this, we observed a consistent increase in *Myc* mRNA and protein levels upon ectopic tet-Lin28b expression in ABM ImmB cells (Fig. 5, E and F). This finding is consistent with previous reports establishing c-Myc as a let-7 target that is derepressed upon Lin28b expression (*46*–*48*).

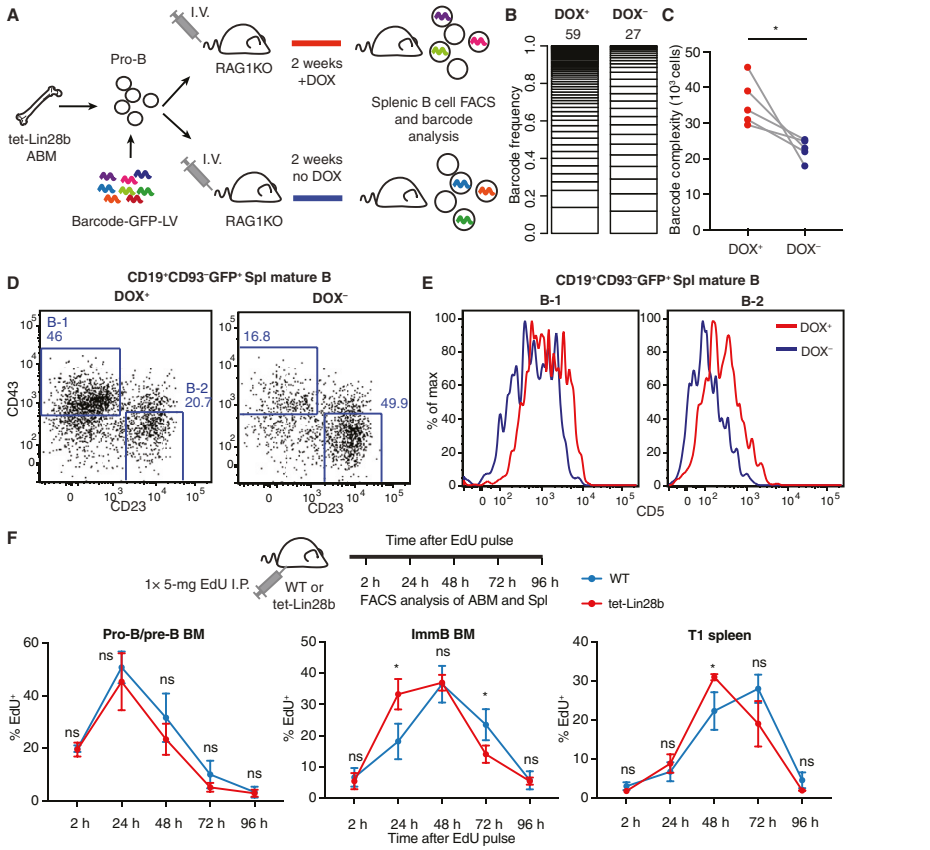

Fig. 4. Lin28b alters the efficiency of overall B cell selection. (**A**) Schematic showing the cellular barcoding setup of pro-B cells. Tet-Lin28b pro-B cells (1×10^5) ($Lin^-CD19^+IgM^-CD93^+cKit^+CD43^+CD24^{lo}CD25^-$) were sorted from untreated mice and transduced with Barcode-GFP-LV. Transduced cells were divided into two equal parts that were individually adoptively transferred into DOX-fed and untreated Rag1KO recipients, respectively. Barcode representation of mature splenic B cell progeny ($CD19^+CD93^-GFP^+$) was assessed 2 weeks after adoptive transfer. I.V., intravenously. (**B**) Stacked bars show representative read frequencies of individual barcodes retrieved. Number on top of bars indicates the number of unique barcodes detected in both PCR technical replicates (for details, see fig. S3). (**C**) Enumeration of barcodes retrieved ($n = 5$ from two experiments). Significance was tested using a paired t test. (**D**) Representative dot plots showing splenic mature B cells 2 weeks after transfer. (**E**) Histogram overlay shows representative CD5 expression of splenic mature B-1 ($GFP^+CD19^+CD93^-CD43^+CD23^-$) and follicular B-2 subsets ($GFP^+CD19^+CD93^-CD43^-CD23^+$). (**F**) Kinetics of EdU label progression during B cell development after administration of a single pulse of EdU into tet-Lin28b and WT mice fed a DOX diet for at least 10 days before labeling. Labeling of the indicated populations at the indicated time points was assessed by FACS ($n = 3$ to 5 per data point from two to three experiments). Error bars show the SD of the mean. *$P \leq 0.05$.

Next, to assess whether c-Myc protein levels are controlled by endogenous *Lin28b* during neonatal B cell maturation, we performed intracellular FACS staining (Fig. 5G). We observed an elevated level of c-Myc protein in WT neonatal ImmB cells compared with their adult counterparts. This elevated c-Myc expression is decreased in neonatal $Lin28b^{-/+}$ and $Lin28b^{-/-}$ ImmB cells in a dose-dependent fashion. Immunoblotting of total neonatal splenic lysates also confirmed reduced c-Myc expression in $Lin28b^{-/-}$ mice (Fig. 5H). In line with this finding, RNA-seq analyses of sorted neonatal ImmB cells revealed a depletion of c-Myc target genes among $Lin28b^{-/-}$ compared with WT mice (Fig. 5I) (see data file S4). Thus, Lin28b critically maintains an elevated level of c-Myc protein levels and function during neonatal B cell maturation.

To assess whether transgenic c-Myc overexpression mediates increased positive selection, we analyzed ImmB cells of precancerous Eu-Myc transgenic mice. Our findings demonstrate decreased λ light chain usage (fig. S6, A and B), increased cell size (fig. S6C), and a trend, although not significant, toward increased surface CD5 expression

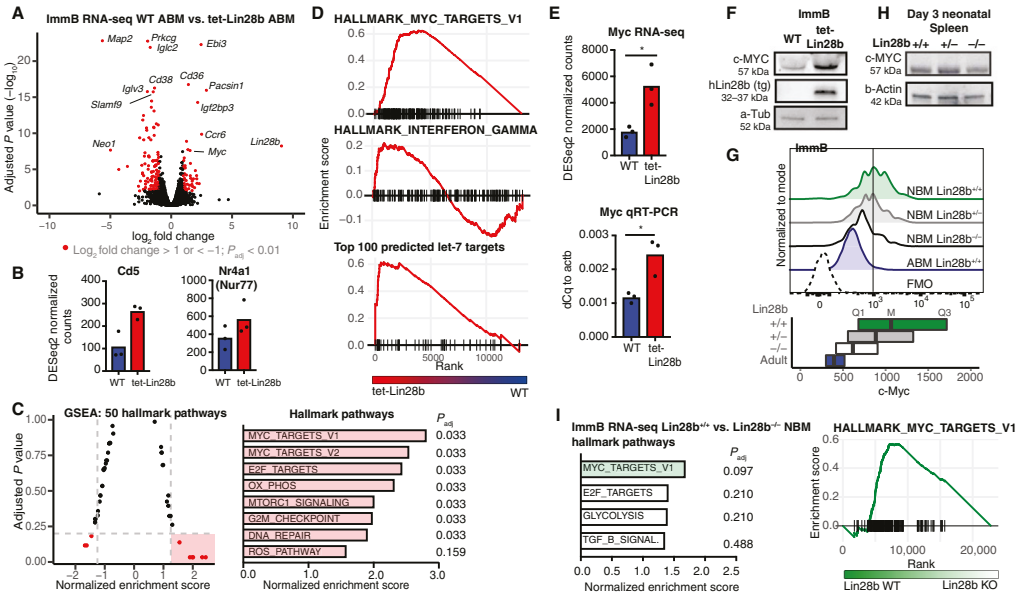

Fig. 5. Lin28b promotes B cell positive selection by activating the c-Myc transcriptional program. (**A**) RNA-seq of sorted ABM ImmB cells from WT and tet-Lin28b mice after 2 weeks of DOX diet ($n = 3$). Volcano plot shows differential gene expression analysis (DESeq). (**B**) Normalized DESeq counts for the indicated genes. (**C**) Unsupervised GSEA for significantly enriched gene sets among the hallmark gene set collection from the Molecular Signature Database (*45*) (left) and top enriched gene sets (right). (**D**) Leading edge plots show enrichment analysis of the indicated gene sets. Top 100 predicted let-7 targets are extracted from TargetScan7.2 (*83*). (**E**) Normalized DESeq counts and qPCR analysis of *Myc* transcript levels in ABM ImmB cells from WT or tet-Lin28b mice ($n = 3$). (**F**) Western blot analysis of c-Myc and Lin28b transgene protein levels in sorted ABM ImmB cells. (**G**) Histogram showing c-Myc protein expression as measured by intracellular FACS in 3-day-old NBM and ABM ImmB cells from the indicated genotypes. (**H**) Western blot analysis showing c-Myc protein expression in 3-day-old NBM and spleen cells from the indicated genotypes. (**I**) RNA-seq of WT ($n = 3$) and *Lin28b*$^{-/-}$ ($n = 4$) 3-day-old NBM. Left: Top enriched hallmark gene sets. Right: Leading edge plot showing a depletion of c-Myc targets in Lin28b-deficient ImmB cells based on DESeq analysis.

(fig. S6, D and E), consistent with increased positive selection and a partial recapitulation of tet-Lin28b–induced B cell maturation. We also observed a marked increase in CD19 surface expression on Eu-Myc ImmB cells, consistent with the previously reported CD19/c-Myc positive feedback loop (fig. S6F) (*28*). We did not, however, detect any reactivation of endogenous *Lin28b* expression as has been reported in several human and murine tumor models (fig. S6, G and H) (*49*, *50*). Together, our evidence suggests that c-Myc is a key mediator of Lin28b-mediated positive selection. It is important to note that c-Myc is not the only downstream mediator of Lin28b. We observed several other significantly enriched molecular signatures in our GSEA (Fig. 5C and fig. S5)—including E2F, oxidative phosphorylation, and mammalian target of rapamycin complex 1 (MTORC1) signaling—consistent with previous reports of Lin28b action (*38*, *47*, *51*).

Previous studies have implicated c-Myc as a key mediator of the CD19/PI3K (phosphatidylinositol 3-kinase) signaling pathway that critically controls ImmB cell positive selection and mature B cell survival (*27*–*29*, *52*–*54*). *CD19*$^{-/-}$ mice display reduced c-Myc protein levels (*28*), extensive receptor editing and developmental arrest of ImmB cells (*5*–*7*), as well as decreased peripheral B cell numbers and B-1 cell representation (*55*–*57*). We crossed the tet-Lin28b transgene onto a *CD19*$^{-/-}$ background (*56*) to test whether Lin28b-induced Myc expression can genetically rescue the observed defects in *CD19*$^{-/-}$ mice. After a 3-week DOX treatment, we observed a near-complete rescue of splenic B cell numbers in tet-Lin28b transgenic *CD19*$^{-/-}$ mice (Fig. 6, A and B) as well as a partial rescue of B-1 cell representation (figs. S6, I to K). FACS analysis of *CD19*$^{-/-}$ ImmB cells revealed the expected characteristics of impaired positive selection—including decreased CD5 levels, enhanced λ:κ light chain usage ratio (Fig. 6, C to E), and reduced ImmB cell representation (fig. S6L). These defects were also restored to normal adult levels by tet-Lin28b expression. These results demonstrate a potent ability of Lin28b to functionally compensate for CD19 during B cell selection and maintenance.

To assess whether tet-Lin28b expression up-regulates c-Myc expression in CD19$^{-/-}$ mice, we performed Western blot analyses. c-Myc protein in total splenic B cells increased upon tet-Lin28b transgene expression. In addition, Lin28b also augmented the PI3K signaling pathway in CD19$^{+/+}$ and CD19$^{-/-}$ mice as measured by phospho-PDK1, phospho-GSK3b, and phospho-S6 (Fig. 6, F and G), consistent with a previously reported role for Lin28b in the positive regulation of the PI3K/MTORC1 signaling pathway (*38*), as well as our own RNA-seq analyses (Fig. 5C). We conclude that Lin28b promotes B cell positive selection at least in part through the amplification of a previously reported c-Myc/PI3K positive feedback loop (*27*–*29*).

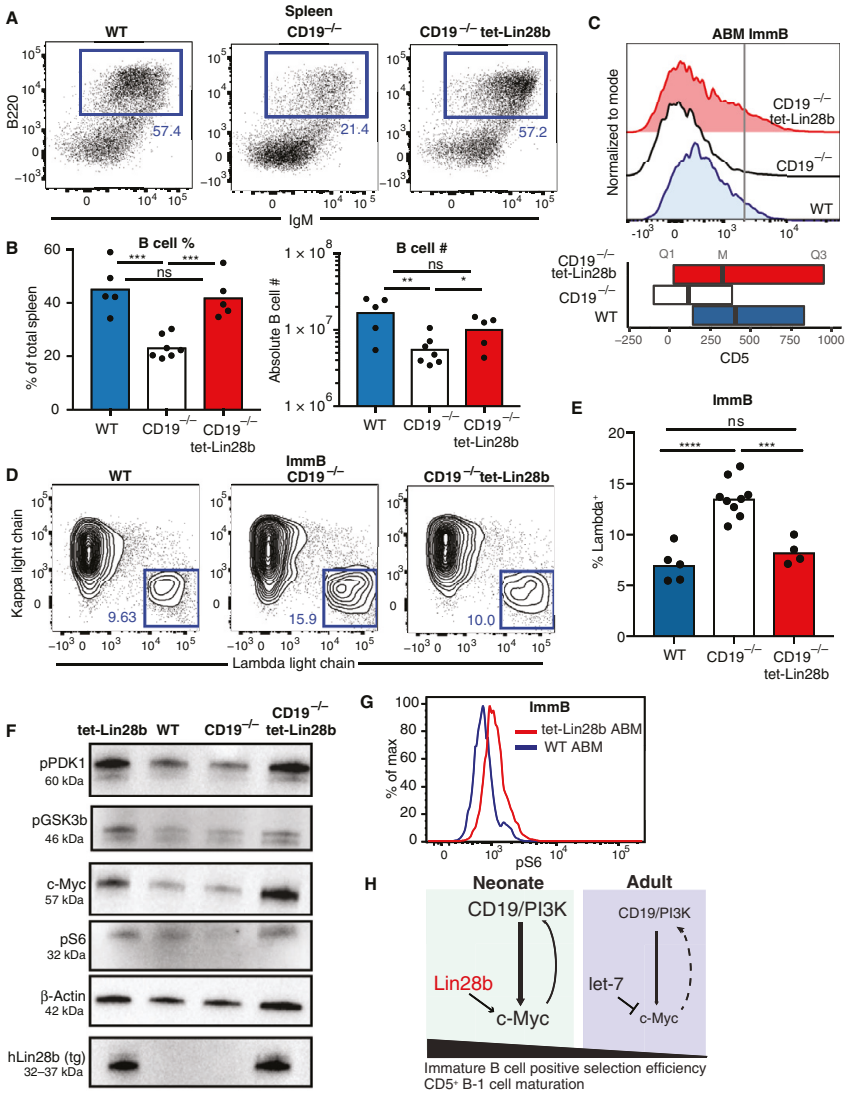

Fig. 6. Ectopic Lin28b functionally replaces CD19 in B cell development and maintenance. (**A**) Representative FACS plots showing frequency of splenic B cell adult mice of the indicated genotypes fed a DOX diet for 3 weeks ($n = 5$ to 7 from three experiments). (**B**) Quantification (left) and absolute B cell numbers (right) in spleen of mice from (A). (**C**) CD5 levels on ABM ImmB cells from (A). (**D**) Representative plots of κ and λ light chain usage in ABM ImmB cells. (**E**) Quantification of (D) ($n = 4$ to 9 from three experiments). (**F**) Representative Western blot of pPDK1, pGSK3b, c-Myc, human Lin28b (tg-Lin28b), pS6, and β-actin levels in magnetically lineage-depleted ($CD3^-Gr1^-CD11b^-Ter119^-$) splenic B cells ($n \geq 3$). (**G**) Representative histogram of pS6 levels in ABM ImmB cells from WT and tet-Lin28b mice ($n \geq 3$). (**H**) Proposed CD19/c-Myc/Lin28b positive feedback loop in neonatal and adult mice.

Lin28b-induced positive selection in the adult produces fully functional CD5$^+$ B-1 cells

To assess the functionality of CD5$^+$ B-1 cells induced by tet-Lin28b–mediated positive selection in the adult, we compared their in vivo and in vitro effector functions with natural CD5$^+$ B-1 cells found in unperturbed adult WT mice ($_n$B-1). To this end, we first established a transplantation-based model system that circumvents a critical pitfall of previous approaches (*14*, *20*), in which constitutive overexpression of Lin28a/b in mature B-1 cells failed to resolve developmental effects on positive selection from those on mature B-1 cell maintenance and function. Donor tet-Lin28b ABM HSPCs were DOX-treated for 4 weeks to allow for a transient wave of fetal-like CD5$^+$ B-1 cell ($_{L28}$B-1) output upon transfer into preconditioned Rag1KO recipient mice (Fig. 7A). WT FL and ABM Lin$^-$Sca1$^+$cKit$^+$ (LSK) HSPCs were similarly transplanted, yielding $_{FL}$B-1 and $_{ABM}$B-1 control populations, respectively. Donor-derived B-1 cells were analyzed after a 12-week chase period during which DOX treatment was removed. We confirmed the cessation of ectopic Lin28b protein expression and the subsequent decline of ongoing B-1 maturation (fig. S7, A and B), which mimics the natural down-regulation of endogenous *Lin28b* during postnatal life (*14*, *17*). Whereas WT ABM HSPCs produced a low frequency of CD5$^+$ B-1 cells, transient Lin28b expression resulted in the long-term reconstitution of $_{L28}$B-1 cells with a similar CD5 expression profile as $_n$B-1 cells (Fig. 7, B and C, and fig. S7, C to E). To more rigorously assess the long-term survival of $_{L28}$B-1 cells in the absence of ABM influx, a hallmark of B-1 cell biology (*58*), we performed competitive transfer of FACS-sorted test B-1 cell subsets at a 1:2 ratio with $_n$B-1 congenic competitor cells into Rag1KO mice. At 12 weeks after transfer, the $_{L28}$B-1 cells displayed long-term fitness comparable with $_{FL}$B-1 and $_n$B-1 cells (Fig. 7D). In contrast, $_{ABM}$B-1 cells were markedly outnumbered by competitor cells. Thus, continuous Lin28b expression is not required for the bone marrow–independent long-term maintenance of $_{L28}$B-1 cells in the periphery. Instead, our data suggest that the initial Lin28b-dependent mode of B-1 cell selection is the main predictive parameter of longevity. The stability of surface CD5 levels closely mirrored our observations of peripheral maintenance. While $_{L28}$B-1 cells maintained their CD5 levels long term, the remaining $_{ABM}$B-1 cells, initially sorted for CD5 positivity, displayed a lower CD5 expression profile at the time of analysis (Fig. 7E). Corroborating these data, CD5 levels on $_{ABM}$B-1 cells were destabilized upon in vitro lipopolysaccharide (LPS) stimulation but remained constant on $_{L28}$B-1 and $_n$B-1 cells (fig. S7F). We conclude that the long-term fitness and stability in CD5 expression critically depend on the Lin28b-mediated mode of positive selection.

One hallmark of B-1 cells is their semi-invariant repertoire stemming from the lack of TdT expression early in life (*34*). To address the diversity of the $_{L28}$B-1 BCR repertoire, we performed VDJseq of the immunoglobulin heavy chain repertoire. Our results demonstrate that $_{L28}$B-1 cells, like $_{ABM}$B-1 cells, exhibit high junctional diversity (Fig. 7F). These results are in line with the observation that Lin28b does not abrogate TdT expression in ABM pro-B cells (fig. S7G) and is consistent with a previous report based on constitutive Lin28b overexpression (*20*). Thus, we conclude that Lin28b allows for the positive selection of a highly diverse repertoire of CD5$^+$ ImmB cells and that germline-encoded specificities prevalently used early in life are not a prerequisite for neonatal-like B cell positive selection or long-lived B-1 cell fate.

Last, we assessed IgM and interleukin-10 (IL-10) secretion as two important B-1 effector functions. Our results show that both $_{L28}$B-1 and $_{ABM}$B-1 isolated from the spleen cells are capable of spontaneous IgM secretion by enzyme-linked immunospot (ELISPOT) assay. Furthermore, IL-10 production upon in vitro LPS stimulation of both $_{L28}$B-1 and $_{ABM}$B-1 was comparable with $_n$B-1 and $_{FL}$B-1 levels (fig. S7, H and I). We conclude that Lin28b-dependent positive selection produces functionally competent B-1 cells and is a prerequisite for the B-1 signature characteristics of long-term survival and stable CD5 expression. However, the Lin28b-dependent mode of positive selection is not required for other critical innate-like functional properties such as IL-10 production and spontaneous IgM secretion (Fig. 7G) (*8*).

DISCUSSION

In this study, we demonstrate that the early-life restricted expression pattern of Lin28b potentiates an enhanced mode of B cell positive selection during a limited window of time. Numerous studies have previously cemented a role for Lin28b as a multilineage master regulator of fetal-like hematopoiesis (*14*, *16*–*20*). Our finding that Lin28b promotes positive selection by amplifying a positive feedback loop involving CD19 and c-Myc represents a highly B lineage–specific mode of Lin28b action. CD19 overexpression has previously been demonstrated to enhance positive selection, B-1 cell numbers, and autoantibody production by shifting the selection criteria for newly formed B cells (*55*, *59*, *60*). Thus, the ability of Lin28b to replace CD19-mediated tonic signaling during B cell maturation represents a cell-intrinsic mechanism of altering the threshold for B cell selection early in life and positions the Lin28b/let-7 axis among a growing list of miRNA-dependent modes to fine-tune the PI3K pathway and B cell selection (*29*, *61*, *62*).

Our results suggest that the proto-oncogene c-Myc, which promotes B lymphomagenesis through the CD19/PI3K pathway (*28*, *63*), is one key mediator of Lin28b action in B cells. In addition to being a let-7 target that is derepressed upon Lin28 expression (*46*–*49*), the *Myc* transcript was recently found to be bound by Lin28b, which may result in stabilization of the transcript (*64*). These findings are consistent with a conserved functional synergy between Lin28b, itself a c-Myc transcriptional target, and c-Myc during normal development, induced pluripotent stem cell reprogramming, as well as oncogenic transformation. Previously, another let-7 target, Arid3a, was shown to be ontogenically controlled by Lin28b (*20*) and to promote B-1 cell output, in part, through up-regulation of Myc expression (*65*). These findings implicate Arid3a as an additional player in the molecular network controlling the neonatal mode of positive selection. Many questions remain as to how Lin28b achieves enhanced B cell positive selection including to what extent death by neglect and negative selection is suppressed and how Lin28b deploys let-7–dependent versus let-7–independent mechanisms. Lin28b-positive (*66*) and CD5-positive (*67*) subtypes of pediatric acute lymphoblastic leukemias have been independently described and highlight the need to dissect whether or not endogenous Lin28b is complicit with c-Myc in the oncogenesis of B cell cancers.

Previously, the topic of B-1 cell selection has mainly been studied through the narrow lens of a small number of germline-encoded BCR specificities using BCR transgenic mice. Here, we used several innovative approaches to tackle this question in BCR WT mice. First, we establish CD5 FACS analysis as a useful tool for studying ImmB cell positive selection in general and neonatal mice in particular. Second, our use of cellular barcoding represents a suitable method for quantifying

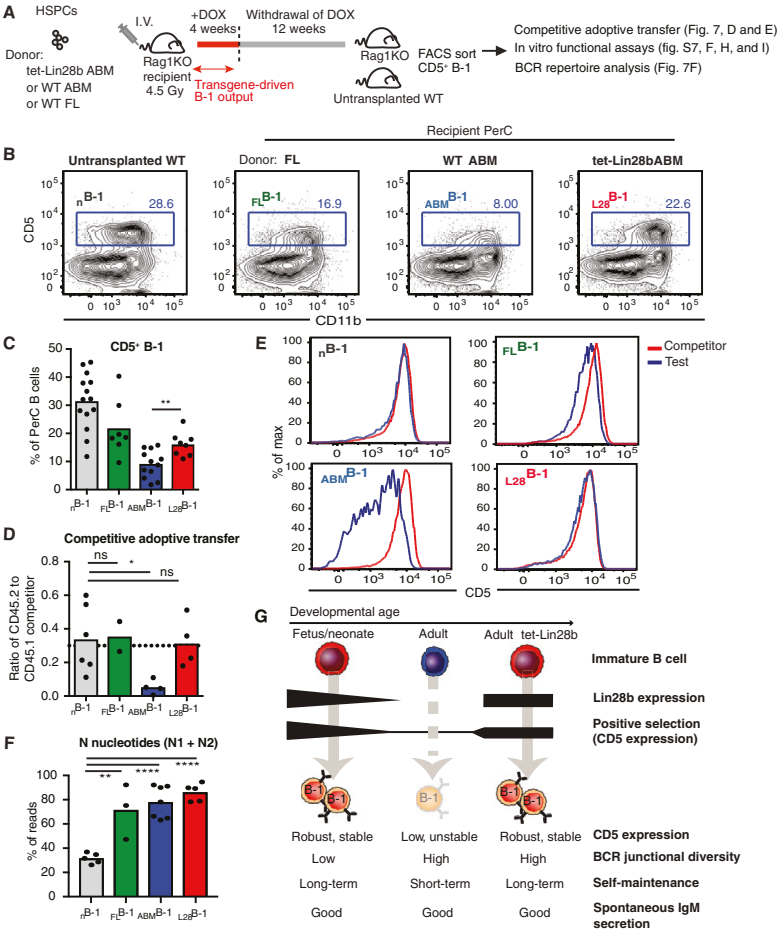

Fig. 7. Tet-Lin28b–induced positive selection during adult B lymphopoiesis produces fully functional CD5$^+$ B-1 cells. (**A**) Schematic showing the DOX-STOP experimental setup. A total of 10,000 LSK HSPCs were sorted from the indicated donors and transplanted into sublethally irradiated Rag1KO recipients. Recipients were kept on a DOX diet for 4 weeks, allowing for transient B-1 cell output by tet-Lin28b HSPCs, followed by a normal diet for 12 weeks (fig. S6). (**B**) Gating strategy for FACS sorting of PerC CD5$^+$ B-1 cells isolated from untransplanted adult (16-week-old) WT mice ($_n$B-1) or the indicated reconstituted recipients 16 weeks after transplantation. (**C**) Frequency of PerC CD5$^+$ B-1 cells 16 weeks after transplantation ($n = 7$ to 14 from three experiments). (**D**) A total of 2×10^4 sorted CD5$^+$ B-1 cells from the indicated mice were competitively transferred by intraperitoneal injection along with congenic $_n$B-1 competitors at a 1:2 ratio. Bar graph shows donor:competitor recovery ratio 12 weeks after transfer ($n = 2$ to 6 from two experiments). (**E**) Histogram showing CD5 expression levels of transferred $_n$B-1, $_{FL}$B-1, $_{ABM}$B-1, and $_{L28}$B-1 cells and their congenic competitors. (**F**) Frequency of CDR3 containing one or more N-nucleotide additions at the N1and N2 VDJ junctions combined. $n = 3$ to 7 biological replicates from three experiments. *$P \leq 0.05$, **$P \leq 0.01$, ****$P \leq 0.0001$. Error bars show the SD of the mean. (**G**) Graphical summary. Our data put forward a unified model for the augmented B-1 cell output early in life. Lin28b-dependent ImmB cell positive selection early in life endows B-1 cells with their hallmark characteristics, including a stable CD5 expression profile and long-term fitness. Ectopic Lin28b in adult life can efficiently induce B-1 cell positive selection on the backdrop of a highly diverse adult type BCR junctional diversity. Adult-derived B-1 cells that develop independently of Lin28b are functionally comparable in terms of IL-10 and spontaneous IgM secretion but display reduced CD5 expression and impaired long-term fitness. We propose that Lin28b-mediated enhancement of B cell tonic signaling licenses self-reactive B-1 cell output during the neonatal period when the risk for harmful autoreactivity is constrained by limited junctional diversity, thereby contributing to an important layer of natural antibody-mediated immunity.

the relative precursor-progeny frequency of B cell selection efficiency. Third, our use of transient tet-Lin28b induction in a transplantation setting allowed us to tease apart transgene effects on B cell positive selection from those on mature B cell function and maintenance. Together, these approaches have allowed us to demonstrate that Lin28b expression during the central tolerance checkpoint is necessary and sufficient for the generation of fully functional long-lived B-1 cells on the backdrop of a highly diverse adult type BCR repertoire. Although the degree and specificity of self-antigen reactivity of tet-Lin28b–induced $CD5^+$ B-1 cells that are not PtC reactive remain to be empirically determined, our findings indicate that the Lin28b-dependent mode of B-1 cell selection into the mature B cell pool is a predictive feature of bone marrow–independent self-renewal.

Despite the many remaining questions, our study establishes an undeniable link between developmental timing and B cell signaling strength. This is a substantial advancement in our understanding of B-1 cell fate determination that reconciles two compelling yet previously disjointed bodies of work emphasizing the importance of early progenitor ontogeny on the one hand (*68*–*71*) and BCR-driven events on the other (*21*, *72*–*75*). Most recently, elegant work from Graf *et al.* (*75*) demonstrating that the Cre recombinase–mediated exchange of BCR transgene identity in mature naïve follicular B-2 cells confers B-1 functionality cemented the instructive power of BCR signaling. However, CD5 expression was not fully restored in these BCR-switched cells, leaving open the possibility that additional developmental determinants are required for complete reprogramming to natural B-1 fate (*75*). To this end, our findings that CD5 levels are set in the ImmB cell stage and that transient Lin28b expression during, but not beyond, bone marrow B cell selection is a requirement for stably maintained CD5 expression provide missing links. Our findings represent a mechanistic explanation to the early-life bias of $CD5^+$ B-1 cell output, providing a unified model for B-1 lineage choice in which Lin28b acts as a developmentally restricted regulator of B cell signaling, which, in turn, instructs B-1 cell fate during positive selection.

The risks for incorporating harmful autoreactivity raise the stakes for Lin28b-dependent enhancement of positive selection early in life. Still, when restricted to a narrow developmental window during ontogeny, this seemingly reckless behavior may confer significant evolutionary gains for the host. First, this may represent a critical mechanism to accelerate the expansion phase of the adaptive immune system during the sensitive neonatal period to mitigate the potential risks of lymphopenia. Second, it represents an opportunity for the incorporation of useful polyreactive, and by definition somewhat self-reactive, specificities into the mature B cell pool that could contribute to tissue homeostasis as well as close any gaps in our immune system exploitable by pathogens. Moreover, continuous encounter of self-antigen primes innate-like B cells for rapid and intense responses before the delayed response of conventional follicular B-2 cells. Given that the lack of TdT expression severely restricts CDR3 diversity early in life, the benefits of Lin28b-dependent positive selection may outweigh the limited risks for generating harmful autoimmunity. The unique role of polyreactive antibodies in humoral immunity is widely recognized in both the broad antimicrobial function of natural antibodies and the highly specific protection responses to thymus-dependent antigens (*76*, *77*). Together, our work provides key insights into the phenomenon of B cell positive selection from a developmental biology perspective and highlights the contribution of the ontogenically restricted expression pattern of Lin28b to the establishment of peripheral B cell heterogeneity and lifelong antibody diversity.

MATERIALS AND METHODS

Mice

Col1a1tm2$^{tetO\text{-}LIN28B}$ mice crossed to R26m2rtTA were obtained from the laboratory of G. Daley (Harvard Medical School) (*38*). Transheterozygous mice are herein referred to as tet-Lin28b. In all experiments where tet-Lin28b mice were used, control mice harboring the R26m2rtTA allele were used and are designated as "WT." The following mouse strains were obtained from the Jackson Laboratory: *Lin28b*$^{-/-}$ (B6.Cg-*Lin28b*$^{tm1.1Gqda}$/J strain number 023917) (*37*), Rag1KO (B6.129S7-*Rag1*^{tm1Mom}/J strain number 002216), CD45.1 (B6.SJL-*Ptprc*^{a} *Pepc*^{b}/BoyJ strain number 002014), *CD19*$^{-/-}$ [B6.129P2(C)-*Cd19*$^{tm1(cre)Cgn}$/J strain number 006785], and EuMYC [B6.Cg-Tg (IghMyc)22Bri/J strain number 002728]. CD45.2 WT mice were from Taconic (B6NTac, Taconic). Adult mice were 10 to 16 weeks of age unless specified differently. DOX diet (200+ mg/kg) was obtained from ssniff GMBH. All animal procedures were performed in accordance with ethical permits approved by the Swedish Board of Agriculture.

HSPC transplantations

For HSPC transplantations, 10,000 LSK HSPCs from CD45.2 E14.5 FL or ABM were FACS-sorted and transplanted into either Rag1KO or congenic $CD45.2^+CD45.1^+$ recipient mice together with 200,000 CD45.1 total BM support cells. Recipient mice were irradiated (1 × 450 cGy for Rag1KO and 2 × 450 cGy for CD45.1) and transplanted by tail vein injection. All mice were given ciproxin (125 mg/liter) containing water for 2 weeks after irradiation. Endpoint analysis was performed 16 to 20 weeks after transplantation as indicated for each experiment. For the DOX-STOP regimen in Fig. 7, recipient mice were fed a DOX diet for 7 days before transplantation with and 4 weeks after transplantation. Mice were analyzed after a DOX-free chase period of 12 weeks.

Lentiviral cellular barcoding and transplantation of pro-B cells

A total of 100,000 pro-B cells were sorted and transduced with Barcode-GFP-LV (*40*), as previously described (*15*). The equivalence of 50,000 sorted and transduced pro-B cells was transplanted per Rag1KO recipient 12 hours after Barcode-GFP-LV transduction. Recipients for cells in the +DOX condition were maintained on a DOX diet starting 7 days before transplantation and throughout the course of the experiment. Splenic mature B cells ($CD19^+CD93^-GFP^+$) were FACS-sorted 2 weeks after transplantation and analyzed for barcode content, as previously described (*15*). Samples were indexed using the Nextera XT Indexing Kit (Illumina) and sequenced using the Illumina NextSeq platform (Illumina). Two technical polymerase chain reaction (PCR) replicates were performed from the genomic DNA of each population, and only barcodes found in both technical replicates were considered for further analysis, as shown in fig. S4.

Flow cytometry

Antibodies are detailed in table S2. BM cells were extracted by crushing the bones from hindlimbs, hips, and spine with mortar and pestle (*78*). Adult, but not neonatal, BM and spleens were subjected to red blood cell lysis. Peritoneal lavage was performed using 10 ml (adult) or 2 ml (10-day neonate) of FACS buffer [Hanks' balanced salt solution

supplemented with 0.5% bovine serum albumin (BSA) and 2 mM EDTA]. Antibody staining was performed in FACS buffer at a density of maximum 1×10^7 cells/100-μl volume for 30 min on ice. For intracellular staining, a maximum of 10×10^6 cells were fixed and permeabilized either in 100 μl of 4% formaldehyde at room temperature (RT) for 15 min and in 0.5% Triton-X in phosphate-buffered saline (PBS) at RT for 15 min or using the Transcription Factor Buffer Set (BD Pharmingen) according to the manufacturer's instructions.

All FACS experiments were performed at the Lund Stem Cell Center FACS Core Facility, Lund University, on FACSAria III, FACSAria IIu, Fortessa, and LSR II instruments (Becton Dickinson). Bulk populations were sorted using a 70- or 85-μm nozzle, 0.32.0 precision mask, and a flow rate of maximally 6000 events/s. For pro-B cell or ImmB cell isolation, total BM cells were pre-enriched by MACS (Miltenyi Biotec) depletion of Lineage$^+$ cells (Ter119$^+$Gr1$^+$CD11b$^+$CD3e$^+$) according to the manufacturer's instructions before FACS sorting.

All analyses were performed using FlowJo 9 or 10. For IQR plots, the 25th percentile, median, and 75th percentile of expression were determined using FlowJo. Values were then plotted using R and the ggplot2 package.

VDJseq

VDJseq on isolated complementary DNA (cDNA) was performed as previously described (*79*). All analyses were performed using R version 3.2.1 (2015) and R version 3.5.2 (2018) (R Core Team; www.R-project.org/). Gini indexes were calculated using the R Reldist package 1.6-6. R scripts are available upon request.

EdU pulse label

Mice were injected intraperitoneally with a single dose of 5 mg of EdU (Abcam). At the indicated time points, 10×10^6 ABM or spleen cells were prepared and stained for surface markers as described above. Next, cells were fixed in 4% paraformaldehyde for 15 min at RT and permeabilized using a solution of 0.5% Triton-X in PBS for 15 min at RT. Subsequently, the Click-iT reaction between EdU and azide–Alexa Fluor 555 was performed according to the manufacturer's protocol (Thermo Fisher Scientific).

Enzyme-linked immunosorbent assay

Enzyme-linked immunosorbent assay (ELISA) plates were coated with an IL-10 antibody in carbonate buffer [0.1 M Na_2CO_3:0.1 M $NaHCO_3$ (pH 9.6) at a 1:3 ratio] overnight at 4°C. Plates were washed with PBS-T (PBS with 0.1% Tween 20) and blocked with 1% BSA in PBS and incubated at RT for 2 hours. After washing with PBS-T, plates were washed before adding appropriate sample dilutions. After washing with PBS-T, anti–IgM–horseradish peroxidase antibody was added for 2 hours at RT. After washing of plates with PBS-T, TMB substrate (Pierce) was added. The reaction was stopped by an equal amount of STOP solution (2 M H_2SO_4).

RNA sequencing

RNA-seq was performed on sorted ABM or 3-day-old NBM ImmB cells (CD19$^+$B220^{lo}CD93$^+$IgM$^+$CD24^{hi}). Libraries were generated using the SMART-Seq v4 Ultra Low Input RNA Library Prep Kit (Clontech) and the Nextera XT DNA Indexing Kit (Illumina) according to the manufacturer's instructions. Libraries were indexed using the Nextera XT v2 Indexing Kit (Illumina) according to the manufacturer's instructions. Libraries were sequenced on an Illumina NextSeq system using a NextSeq V500/550 150-cycle high-output kit. Reads were aligned using STAR aligner v2.7.1 (*80*) and counted using RSEM v.1.28. Differential gene expression analysis was performed using the DESeq2 R package v1.22.2 (*81*) in R 3.5.2. GSEA was performed using the fgsea R package v1.8.8 in R 3.5.2. (*82*) was run on DESeq2 normalized counts using standard parameters with 1000 permutations and the $\log_2$ fold change as ranking metric. H collection MSigDB hallmark gene sets were used for analysis (*45*). Data are made available in the Gene Expression Omnibus repository (GSE135603).

Quantitative PCR

Total RNA was isolated using RNAzol (Sigma-Aldrich). cDNA synthesis was performed using the TaqMan Reverse Transcription Reagent Kit (Life Technologies) according to the manufacturer's instructions. Quantitative PCR (qPCR) analysis was done using probes from Integrated DNA Technologies (IDT) (*Myc* Mm.PT.39a.22214843.g and *Actb* Mm.PT.58.28494642, Lin28b Mm.PT.58.8558661) and master mix from Kapa Biosystems.

Western blot

Cells were lysed in 50 mM tris-HCl (pH 7.8), 150 mM NaCl, 1 mM EDTA, and 1% NP-40. Loading samples were prepared with Laemmli buffer (Bio-Rad) with β-mercaptoethanol (Scharlau Chemicals) and protease inhibitor (Roche). Proteins were separated by SDS–polyacrylamide gel electrophoresis (12% Mini-Protean TGX gel, Bio-Rad) and transferred to a nitrocellulose membrane (Trans-Blot Turbo Mini Nitrocellulose Transfer Packs, Bio-Rad). Membranes were blocked for 1 hour at RT in 5% BSA, 5% skimmed milk, or 5% enhanced chemiluminescence (ECL) blocking solution in tris-buffered saline (TBS)–0.05% Tween 20 depending on the manufacturer's instructions. Antibodies are listed in table S2. The ECL Prime kit (GE Healthcare) was used to detect protein bands with a ChemiDoc XRS+ system (Bio-Rad). All reagents were used according to the manufacturer's instructions.

Statistical analysis

All statistical analysis was performed using GraphPad Prism v7. Statistical significance was tested using a two-sided unpaired *t* test, unless otherwise specified in the figure legend. Statistical analysis of RNA-seq data was obtained through analysis in the cited R packages.

SUPPLEMENTARY MATERIALS

immunology.sciencemag.org/cgi/content/full/4/39/eaax4453/DC1
Fig. S1. Gating strategies for developing B cells.
Fig. S2. Cell cycle analysis of tet-Lin28b ABM pre-B and ImmB subsets.
Fig. S3. Determination of the minimal DOX treatment window during B cell maturation required for efficient CD5$^+$ B-1 cell output from tet-Lin28b ABM.
Fig. S4. Barcode filtering and analysis strategy.
Fig. S5. Differentially expressed genes within top enriched Hallmark gene sets.
Fig. S6. Genetic evidence implicating Lin28b in the CD19/PI3K/c-Myc pathway.
Fig. S7. Transient tet-Lin28b expression of ABM progenitors promotes the output of functionally competent CD5$^+$ B-1 cells.
Table S2. Antibodies used in this study.
Data file S1. Table S1: Raw data supplement.
Data file S2. VDJseq PerC B-1 CD5 slices.
Data file S3. DESeq2 normalized counts for adult tet-Lin28b and WT ImmB RNA-seq.
Data file S4. DESeq2 normalized counts for neonatal Lin28b$^{+/+}$, Lin28b$^{-/-}$ ImmB RNA-seq.

REFERENCES AND NOTES

1. N. Vrisekoop, J. P. Monteiro, J. N. Mandl, R. N. Germain, Revisiting thymic positive selection and the mature T cell repertoire for antigen. *Immunity* **41**, 181–190 (2014).

2. J. Lang, M. Jackson, L. Teyton, A. Brunmark, K. Kane, D. Nemazee, B cells are exquisitely sensitive to central tolerance and receptor editing induced by ultralow affinity, membrane-bound antigen. *J. Exp. Med.* **184**, 1685–1697 (1996).
3. D. Nemazee, Receptor editing in lymphocyte development and central tolerance. *Nat. Rev. Immunol.* **6**, 728–740 (2006).
4. S. Shivtiel, N. Leider, O. Sadeh, Z. Kraiem, D. Melamed, Impaired light chain allelic exclusion and lack of positive selection in immature B cells expressing incompetent receptor deficient of CD19. *J. Immunol.* **168**, 5596–5604 (2002).
5. E. Diamant, Z. Keren, D. Melamed, CD19 regulates positive selection and maturation in B lymphopoiesis: Lack of CD19 imposes developmental arrest of immature B cells and consequential stimulation of receptor editing. *Blood* **105**, 3247–3254 (2005).
6. L. Verkoczy, B. Duong, P. Skog, D. Aït-Azzouzene, K. Puri, J. L. Vela, D. Nemazee, Basal B cell receptor-directed phosphatidylinositol 3-kinase signaling turns off RAGs and promotes B cell-positive selection. *J. Immunol.* **178**, 6332–6341 (2007).
7. L. E. Tze, B. R. Schram, K.-P. Lam, K. A. Hogquist, K. L. Hippen, J. Liu, S. A. Shinton, K. L. Otipoby, P. R. Rodine, A. L. Vegoe, M. Kraus, R. R. Hardy, M. S. Schlissel, K. Rajewsky, T. W. Behrens, Basal immunoglobulin signaling actively maintains developmental stage in immature B cells. *PLoS Biol.* **3**, e82 (2005).
8. N. Baumgarth, B-1 cell heterogeneity and the regulation of natural and antigen-induced IgM production. *Front. Immunol.* **7**, 324 (2016).
9. K. Hayakawa, M. Asano, S. A. Shinton, M. Gui, D. Allman, C. L. Stewart, J. Silver, R. R. Hardy, Positive selection of natural autoreactive B cells. *Science* **285**, 113–116 (1999).
10. R. Wasserman, Y.-S. Li, S. A. Shinton, C. E. Carmack, T. Manser, D. L. Wiest, K. Hayakawa, R. R. Hardy, A novel mechanism for B cell repertoire maturation based on response by B Cell precursors to pre–B receptor assembly. *J. Exp. Med.* **187**, 259–264 (1998).
11. L. W. Arnold, C. A. Pennell, S. K. McCray, S. H. Clarke, Development of B-1 cells: Segregation of phosphatidyl choline-specific B cells to the B-1 population occurs after immunoglobulin gene expression. *J. Exp. Med.* **179**, 1585–1595 (1994).
12. H. Ferry, T. L. Crockford, J. C. H. Leung, R. J. Cornall, Signals from a self-antigen induce positive selection in early B cell ontogeny but are tolerogenic in adults. *J. Immunol.* **176**, 7402–7411 (2006).
13. N. Shyh-Chang, G. Q. Daley, Lin28: Primal regulator of growth and metabolism in stem cells. *Cell Stem Cell* **12**, 395–406 (2013).
14. J. Yuan, C. K. Nguyen, X. Liu, C. Kanellopoulou, S. A. Muljo, Lin28b reprograms adult bone marrow hematopoietic progenitors to mediate fetal-like lymphopoiesis. *Science* **335**, 1195–1200 (2012).
15. T. A. Kristiansen, E. Jaensson Gyllenbäck, A. Zriwil, T. Björklund, J. A. Daniel, E. Sitnicka, S. Soneji, D. Bryder, J. Yuan, Cellular barcoding links B-1a B cell potential to a fetal hematopoietic stem cell state at the single-cell level. *Immunity* **45**, 346–357 (2016).
16. R. G. Rowe, L. D. Wang, S. Coma, A. Han, R. Mathieu, D. S. Pearson, S. Ross, P. Sousa, P. T. Nguyen, A. Rodriguez, A. J. Wagers, G. Q. Daley, Developmental regulation of myeloerythroid progenitor function by the *Lin28b-let-7-Hmga2* axis. *J. Exp. Med.* **213**, 1497–1512 (2016).
17. M. R. Copley, S. Babovic, C. Benz, D. J. H. F. Knapp, P. A. Beer, D. G. Kent, S. Wohrer, D. Q. Treloar, C. Day, K. Rowe, H. Mader, F. Kuchenbauer, R. K. Humphries, C. J. Eaves, The Lin28b-let-7-Hmga2 axis determines the higher self-renewal potential of fetal haematopoietic stem cells. *Nat. Cell Biol.* **15**, 916–925 (2013).
18. J. Wang, E. M. Wissink, N. B. Watson, N. L. Smith, A. Grimson, B. D. Rudd, Fetal and adult progenitors give rise to unique populations of $CD8^+$ T cells. *Blood* **128**, 3073–3082 (2016).
19. M. C. Stolla, S. C. Catherman, P. D. Kingsley, R. G. Rowe, A. D. Koniski, K. Fegan, L. Vit, K. E. McGrath, G. Q. Daley, J. Palis, *Lin28b* regulates age-dependent differences in murine platelet function. *Blood Adv.* **3**, 72–82 (2019).
20. Y. Zhou, Y.-S. Li, S. R. Bandi, L. Tang, S. A. Shinton, K. Hayakawa, R. R. Hardy, Lin28b promotes fetal B lymphopoiesis through the transcription factor Arid3a. *J. Exp. Med.* **212**, 569–580 (2015).
21. R. Berland, H. H. Wortis, Origins and functions of B-1 cells with notes on the role of CD5. *Annu. Rev. Immunol.* **20**, 253–300 (2002).
22. P. Casali, A. L. Notkins, $CD5^+$ B lymphocytes, polyreactive antibodies and the human B-cell repertoire. *Immunol. Today* **10**, 364–368 (1989).
23. H. S. Azzam, A. Grinberg, K. Lui, H. Shen, E. W. Shores, P. E. Love, CD5 expression is developmentally regulated by T cell receptor (TCR) signals and TCR avidity. *J. Exp. Med.* **188**, 2301–2311 (1998).
24. J. N. Mandl, J. P. Monteiro, N. Vrisekoop, R. N. Germain, T cell-positive selection uses self-ligand binding strength to optimize repertoire recognition of foreign antigens. *Immunity* **38**, 263–274 (2013).
25. K. L. Hippen, L. E. Tze, T. W. Behrens, CD5 maintains tolerance in anergic B cells. *J. Exp. Med.* **191**, 883–890 (2000).
26. L. Wen, J. Brill-Dashoff, S. A. Shinton, M. Asano, R. R. Hardy, K. Hayakawa, Evidence of marginal-zone B cell-positive selection in spleen. *Immunity* **23**, 297–308 (2005).
27. E. Y. Chung, J. N. Psathas, D. Yu, Y. Li, M. J. Weiss, A. Thomas-Tikhonenko, CD19 is a major B cell receptor-independent activator of MYC-driven B-lymphomagenesis. *J. Clin. Invest.* **122**, 2257–2266 (2012).
28. J. C. Poe, V. Minard-Colin, E. I. Kountikov, K. M. Haas, T. F. Tedder, A c-Myc and surface CD19 signaling amplification loop promotes B cell lymphoma development and progression in mice. *J. Immunol.* **189**, 2318–2325 (2012).
29. D. Benhamou, V. Labi, R. Novak, I. Dai, S. Shafir-Alon, A. Weiss, R. Gaujoux, R. Arnold, S. S. Shen-Orr, K. Rajewsky, D. Melamed, A c-Myc/miR17-92/Pten axis controls PI3K-mediated positive and negative selection in B cell development and reconstitutes CD19 deficiency. *Cell Rep.* **16**, 419–431 (2016).
30. S. Düber, M. Hafner, M. Krey, S. Lienenklaus, B. Roy, E. Hobeika, M. Reth, T. Buch, A. Waisman, K. Kretschmer, S. Weiss, Induction of B-cell development in adult mice reveals the ability of bone marrow to produce B-1a cells. *Blood* **114**, 4960–4967 (2009).
31. N. E. Holodick, T. Vizconde, T. L. Rothstein, B-1a cell diversity: Nontemplated addition in B-1a cell Ig is determined by progenitor population and developmental location. *J. Immunol.* **192**, 2432–2441 (2014).
32. C. M. Sawai, S. Babovic, S. Upadhaya, D. J. H. F. Knapp, Y. Lavin, C. M. Lau, A. Goloborodko, J. Feng, J. Fujisaki, L. Ding, L. A. Mirny, M. Merad, C. J. Eaves, B. Reizis, Hematopoietic stem cells are the major source of multilineage hematopoiesis in adult animals. *Immunity* **45**, 597–609 (2016).
33. A. B. Kantor, A. M. Stall, S. Adams, L. A. Herzenberg, L. A. Herzenberg, Differential development of progenitor activity for three B-cell lineages. *Proc. Natl. Acad. Sci. U.S.A.* **89**, 3320–3324 (1992).
34. M. Bogue, S. Gilfillan, C. Benoist, D. Mathis, Regulation of N-region diversity in antigen receptors through thymocyte differentiation and thymus ontogeny. *Proc. Natl. Acad. Sci. U.S.A.* **89**, 11011–11015 (1992).
35. H. Wardemann, S. Yurasov, A. Schaefer, J. W. Young, E. Meffre, M. C. Nussenzweig, Predominant autoantibody production by early human B cell precursors. *Science* **301**, 1374–1377 (2003).
36. G. K. Pedersen, M. Àdori, S. Khoenkhoen, P. Dosenovic, B. Beutler, G. B. Karlsson Hedestam, B-1a transitional cells are phenotypically distinct and are lacking in mice deficient in IκBNS. *Proc. Natl. Acad. Sci. U.S.A.* **111**, E4119–E4126 (2014).
37. G. Shinoda, N. Shyh-Chang, T. Y. de Soysa, H. Zhu, M. T. Seligson, S. P. Shah, N. Abo-Sido, A. Yabuuchi, J. P. Hagan, R. I. Gregory, J. M. Asara, L. C. Cantley, E. G. Moss, G. Q. Daley, Fetal deficiency of Lin28 programs life-long aberrations in growth and glucose metabolism. *Stem Cells* **31**, 1563–1573 (2013).
38. H. Zhu, N. Shyh-Chang, A. V. Segrè, G. Shinoda, S. P. Shah, W. S. Einhorn, A. Takeuchi, J. M. Engreitz, J. P. Hagan, M. G. Kharas, A. Urbach, J. E. Thornton, R. Triboulet, R. I. Gregory; DIAGRAM Consortium; MAGIC Investigators13, D. Altshuler, G. Q. Daley, The *Lin28/let-7* axis regulates glucose metabolism. *Cell* **147**, 81–94 (2011).
39. S. H. Naik, T. N. Schumacher, L. Perié, Cellular barcoding: A technical appraisal. *Exp. Hematol.* **42**, 598–608 (2014).
40. R. Lu, N. F. Neff, S. R. Quake, I. L. Weissman, Tracking single hematopoietic stem cells in vivo using high-throughput sequencing in conjunction with viral genetic barcoding. *Nat. Biotechnol.* **29**, 928–933 (2011).
41. R. R. Hardy, K. Hayakawa, M. Shimizu, K. Yamasaki, T. Kishimoto, Rheumatoid factor secretion from human Leu-1+ B cells. *Science* **236**, 81–83 (1987).
42. J. H. Antin, S. G. Emerson, P. Martin, N. Gadol, K. A. Ault, Leu-1+ (CD5+) B cells. A major lymphoid subpopulation in human fetal spleen: Phenotypic and functional studies. *J. Immunol.* **136**, 505–510 (1986).
43. M. Bofill, G. Janossy, M. Janossa, G. D. Burford, G. J. Seymour, P. Wernet, E. Kelemen, Human B cell development. II. Subpopulations in the human fetus. *J. Immunol.* **134**, 1531–1538 (1985).
44. J. Zikherman, R. Parameswaran, A. Weiss, Endogenous antigen tunes the responsiveness of naive B cells but not T cells. *Nature* **489**, 160–164 (2012).
45. A. Liberzon, C. Birger, H. Thorvaldsdottir, M. Ghandi, J. P. Mesirov, P. Tamayo, The Molecular Signatures Database (MSigDB) hallmark gene set collection. *Cell Syst.* **1**, 417–425 (2015).
46. V. B. Sampson, N. H. Rong, J. Han, Q. Yang, V. Aris, P. Soteropoulos, N. J. Petrelli, S. P. Dunn, L. J. Krueger, MicroRNA let-7a down-regulates MYC and reverts MYC-induced growth in Burkitt lymphoma cells. *Cancer Res.* **67**, 9762–9770 (2007).
47. S. Manier, J. T. Powers, A. Sacco, S. V. Glavey, D. Huynh, M. R. Reagan, K. Z. Salem, M. Moschetta, J. Shi, Y. Mishima, C. Roche-Lestienne, X. Leleu, A. M. Roccaro, G. Q. Daley, I. M. Ghobrial, The LIN28B/let-7 axis is a novel therapeutic pathway in multiple myeloma. *Leukemia* **31**, 853–860 (2017).
48. E. Koscianska, V. Baev, K. Skreka, K. Oikonomaki, V. Rusinov, M. Tabler, K. Kalantidis, Prediction and preliminary validation of oncogene regulation by miRNAs. *BMC Mol. Biol.* **8**, 79 (2007).
49. T.-C. Chang, L. R. Zeitels, H.-W. Hwang, R. R. Chivukula, E. A. Wentzel, M. Dews, J. Jung, P. Gao, C. V. Dang, M. A. Beer, A. Thomas-Tikhonenko, J. T. Mendell, Lin-28B transactivation is necessary for Myc-mediated let-7 repression and proliferation. *Proc. Natl. Acad. Sci. U.S.A.* **106**, 3384–3389 (2009).
50. X. Jiang, H. Huang, Z. Li, Y. Li, X. Wang, S. Gurbuxani, P. Chen, C. He, D. You, S. Zhang, J. Wang, S. Arnovitz, A. Elkahloun, C. Price, G. M. Hong, H. Ren, R. B. Kunjamma, M. B. Neilly, J. M. Matthews, M. Xu, R. A. Larson, M. M. Le Beau, R. K. Slany, P. P. Liu, J. Lu,

J. Zhang, C. He, J. Chen, Blockade of miR-150 maturation by MLL-fusion/MYC/LIN-28 is required for MLL-associated leukemia. *Cancer Cell* **22**, 524–535 (2012).
51. N. Shyh-Chang, H. Zhu, T. Yvanka de Soysa, G. Shinoda, M. T. Seligson, K. M. Tsanov, L. Nguyen, J. M. Asara, L. C. Cantley, G. Q. Daley, Lin28 enhances tissue repair by reprogramming cellular metabolism. *Cell* **155**, 778–792 (2013).
52. L. Srinivasan, Y. Sasaki, D. P. Calado, B. Zhang, J. H. Paik, R. A. DePinho, J. L. Kutok, J. F. Kearney, K. L. Otipoby, K. Rajewsky, PI3 kinase signals BCR-dependent mature B cell survival. *Cell* **139**, 573–586 (2009).
53. G. V. Baracho, M. H. Cato, Z. Zhu, O. R. Jaren, E. Hobeika, M. Reth, R. C. Rickert, PDK1 regulates B cell differentiation and homeostasis. *Proc. Natl. Acad. Sci. U.S.A.* **111**, 9573–9578 (2014).
54. A. N. Anzelon, H. Wu, R. C. Rickert, Pten inactivation alters peripheral B lymphocyte fate and reconstitutes CD19 function. *Nat. Immunol.* **4**, 287–294 (2003).
55. P. Engel, L. J. Zhou, D. C. Ord, S. Sato, B. Koller, T. F. Tedder, Abnormal B lymphocyte development, activation, and differentiation in mice that lack or overexpress the CD19 signal transduction molecule. *Immunity* **3**, 39–50 (1995).
56. R. C. Rickert, K. Rajewsky, J. Roes, Impairment of T-cell-dependent B-cell responses and B-1 cell development in CD19-deficient mice. *Nature* **376**, 352–355 (1995).
57. D. C. Otero, A. N. Anzelon, R. C. Rickert, CD19 function in early and late B cell development: I. Maintenance of follicular and marginal zone B cells requires CD19-dependent survival signals. *J. Immunol.* **170**, 73–83 (2003).
58. Z. Hao, K. Rajewsky, Homeostasis of peripheral B cells in the absence of B cell influx from the bone marrow. *J. Exp. Med.* **194**, 1151–1164 (2001).
59. S. Sato, N. Ono, D. A. Steeber, D. S. Pisetsky, T. F. Tedder, CD19 regulates B lymphocyte signaling thresholds critical for the development of B-1 lineage cells and autoimmunity. *J. Immunol.* **157**, 4371–4378 (1996).
60. M. Inaoki, S. Sato, B. C. Weintraub, C. C. Goodnow, T. F. Tedder, CD19-regulated signaling thresholds control peripheral tolerance and autoantibody production in B lymphocytes. *J. Exp. Med.* **186**, 1923–1931 (1997).
61. A. Gonzalez-Martin, B. D. Adams, M. Lai, J. Shepherd, M. Salvador-Bernaldez, J. M. Salvador, J. Lu, D. Nemazee, C. Xiao, The microRNA miR-148a functions as a critical regulator of B cell tolerance and autoimmunity. *Nat. Immunol.* **17**, 433–440 (2016).
62. M. Coffre, D. Benhamou, D. Rieß, L. Blumenberg, V. Snetkova, M. J. Hines, T. Chakraborty, S. Bajwa, K. Jensen, M. M. W. Chong, L. Getu, G. J. Silverman, R. Blelloch, D. R. Littman, D. Calado, D. Melamed, J. A. Skok, K. Rajewsky, S. B. Koralov, miRNAs are essential for the regulation of the PI3K/AKT/FOXO pathway and receptor editing during B cell maturation. *Cell Rep.* **17**, 2271–2285 (2016).
63. S. Sander, D. P. Calado, L. Srinivasan, K. Köchert, B. Zhang, M. Rosolowski, S. J. Rodig, K. Holzmann, S. Stilgenbauer, R. Siebert, L. Bullinger, K. Rajewsky, Synergy between PI3K signaling and MYC in Burkitt lymphomagenesis. *Cancer Cell* **22**, 167–179 (2012).
64. S. Wang, B. Chim, Y. Su, P. Khil, M. Wong, X. Wang, A. Foroushani, P. T. Smith, X. Liu, R. Li, S. Ganesan, C. Kanellopoulou, M. Hafner, S. A. Muljo, Enhancement of LIN28B-induced hematopoietic reprogramming by IGF2BP3. *Genes Dev.* **33**, 1048–1068 (2019).
65. K. Hayakawa, Y.-S. Li, S. A. Shinton, S. R. Bandi, A. M. Formica, J. Brill-Dashoff, R. R. Hardy, Crucial role of increased Arid3a at the pre-B and immature B cell stages for B1a cell generation. *Front. Immunol.* **10**, 457 (2019).
66. E. M. Staley, A. Z. Feldman, R. G. Koenig, B. Hill, CD5 positive B-ALL, a uniquely aggressive subcategory of B-ALL? A case report and brief review of the literature. *Pediatr. Blood Cancer* **66**, e27484 (2019).
67. L. Chen, Y. Sun, J. Wang, H. Jiang, A. G. Muntean, Differential regulation of the c-Myc/Lin28 axis discriminates subclasses of rearranged MLL leukemia. *Oncotarget* **7**, 25208–25223 (2016).
68. E. Montecino-Rodriguez, K. Dorshkind, B-1 B cell development in the fetus and adult. *Immunity* **36**, 13–21 (2012).
69. A. B. Kantor, L. A. Herzenberg, Origin of murine B cell lineages. *Annu. Rev. Immunol.* **11**, 501–538 (1993).
70. K. Hayakawa, R. R. Hardy, L. A. Herzenberg, L. A. Herzenberg, Progenitors for Ly-1 B cells are distinct from progenitors for other B cells. *J. Exp. Med.* **161**, 1554–1568 (1985).
71. E. Ghosn, M. Yoshimoto, H. Nakauchi, I. L. Weissman, L. A. Herzenberg, Hematopoietic stem cell-independent hematopoiesis and the origins of innate-like B lymphocytes. *Development* **146**, dev170571 (2019).
72. S. Casola, K. L. Otipoby, M. Alimzhanov, S. Humme, N. Uyttersprot, J. L. Kutok, M. C. Carroll, K. Rajewsky, B cell receptor signal strength determines B cell fate. *Nat. Immunol.* **5**, 317–327 (2004).
73. K. Rajewsky, The Herzenberg lecture: How to make a B-1 cell? *Ann. N. Y. Acad. Sci.* **1362**, 6–7 (2015).
74. G. Haughton, L. W. Arnold, A. C. Whitmore, S. H. Clarke, B-1 cells are made, not born. *Immunol. Today* **14**, 84–87 (1993).
75. R. Graf, J. Seagal, K. L. Otipoby, K.-P. Lam, S. Ayoub, B. Zhang, S. Sander, V. T. Chu, K. Rajewsky, BCR-dependent lineage plasticity in mature B cells. *Science* **363**, 748–753 (2019).
76. J. J. Bunker, S. A. Erickson, T. M. Flynn, C. Henry, J. C. Koval, M. Meisel, B. Jabri, D. A. Antonopoulos, P. C. Wilson, A. Bendelac, Natural polyreactive IgA antibodies coat the intestinal microbiota. *Science* **358**, eaan6619 (2017).
77. H. Mouquet, M. C. Nussenzweig, Polyreactive antibodies in adaptive immune responses to viruses. *Cell. Mol. Life Sci.* **69**, 1435–1445 (2012).
78. C. Lo Celso, D. Scadden, Isolation and transplantation of hematopoietic stem cells (HSCs). *J. Vis. Exp.*, 157 (2007).
79. D. Su, S. Vanhee, R. Soria, E. J. Gyllenbäck, L. M. Starnes, M. K. Højfeldt, G. K. Pedersen, J. Yuan, J. A. Daniel, PTIP chromatin regulator controls development and activation of B cell subsets to license humoral immunity in mice. *Proc. Natl. Acad. Sci. U.S.A.* **114**, E9328–E9337 (2017).
80. A. Dobin, C. A. Davis, F. Schlesinger, J. Drenkow, C. Zaleski, S. Jha, P. Batut, M. Chaisson, T. R. Gingeras, STAR: Ultrafast universal RNA-seq aligner. *Bioinformatics* **29**, 15–21 (2013).
81. M. I. Love, W. Huber, S. Anders, Moderated estimation of fold change and dispersion for RNA-seq data with DESeq2. *Genome Biol.* **15**, 550 (2014).
82. A. A. Sergushichev, An algorithm for fast preranked gene set enrichment analysis using cumulative statistic calculation. *bioRxiv* 060012 [**Preprint**]. 20 June 2016. https://doi.org/10.1101/060012.
83. V. Agarwal, G. W. Bell, J.-W. Nam, D. P. Bartel, Predicting effective microRNA target sites in mammalian mRNAs. *eLife* **4**, e05005 (2015).

Acknowledgments: We thank J. A. Daniel and T. P. Bender for their critical input. **Funding:** J.Y. was supported by the European Research Council (715313), Wallenberg Academy Fellows, the Swedish Research Council, StemTherapy, and the Wenner-Gren Foundation. J.Y. and E.J.G. were supported by the Swedish Cancer Society. M.S., J.Y., and S.S. were supported by the Knut and Alice Wallenberg Foundation. **Author contributions:** J.Y., S. Vanhee, and E.J.G. designed the study. S. Vanhee, E.J.G., H.Å., T.A.K., S.D., G.M., K.O., A.D., and S. Vergani performed the experiments. S. Vanhee performed the computational analyses together with S.L., S.S., and J.U. C.T.J., G.B., C.B., and M.S. provided critical expertise. J.Y. conceived the study and wrote the paper together with S. Vanhee. **Competing interests:** The authors declare that they no competing interests. **Data and materials availability:** The data for this study have been deposited in the database GSE135603.

Submitted 25 March 2019
Accepted 27 August 2019
Published 27 September 2019
10.1126/sciimmunol.aax4453

Citation: S. Vanhee, H. Åkerstrand, T. A. Kristiansen, S. Datta, G. Montano, S. Vergani, S. Lang, J. Ungerbäck, A. Doyle, K. Olsson, G. Beneventi, C. T. Jensen, C. Bellodi, S. Soneji, M. Sigvardsson, E. J. Gyllenbäck, J. Yuan, Lin28b controls a neonatal to adult switch in B cell positive selection. *Sci. Immunol.* **4**, eaax4453 (2019).

Paper II

frontiers | Frontiers in Immunology

TYPE Original Research
PUBLISHED 17 April 2023
DOI 10.3389/fimmu.2023.1130930

OPEN ACCESS

EDITED BY
Barbara L. Kee,
The University of Chicago, United States

REVIEWED BY
Nichol E. Holodick,
Western Michigan University, United States
Rodney P. DeKoter,
Western University, Canada
Patrick Swanson,
Creighton University, United States

*CORRESPONDENCE
Joan Yuan
joan.yuan@med.lu.se

SPECIALTY SECTION
This article was submitted to B Cell Biology, a section of the journal Frontiers in Immunology

RECEIVED 23 December 2022
ACCEPTED 21 March 2023
PUBLISHED 17 April 2023

CITATION
Åkerstrand H, Boldrin E, Montano G, Vanhee S, Olsson K, Krausse N, Vergani S, Cieśla M, Bellodi C and Yuan J (2023) Enhanced protein synthesis is a defining requirement for neonatal B cell development. *Front. Immunol.* 14:1130930. doi: 10.3389/fimmu.2023.1130930

Enhanced protein synthesis is a defining requirement for neonatal B cell development

Hugo Åkerstrand[1], Elena Boldrin[1], Giorgia Montano[1], Stijn Vanhee[1], Karin Olsson[1], Niklas Krausse[1], Stefano Vergani[1], Maciej Cieśla[2], Cristian Bellodi[2] and Joan Yuan[1]*

[1]Developmental Immunology Unit, Department of Molecular Hematology, Lund Stem Cell Center, Lund University, Lund, Sweden, [2]RNA and Stem Cell Biology Unit, Department of Molecular Hematology, Lund Stem Cell Center, Lund University, Lund, Sweden

The LIN28B RNA binding protein exhibits an ontogenically restricted expression pattern and is a key molecular regulator of fetal and neonatal B lymphopoiesis. It enhances the positive selection of CD5+ immature B cells early in life through amplifying the CD19/PI3K/c-MYC pathway and is sufficient to reinitiate self-reactive B-1a cell output when ectopically expressed in the adult. In this study, interactome analysis in primary B cell precursors showed direct binding by LIN28B to numerous ribosomal protein transcripts, consistent with a regulatory role in cellular protein synthesis. Induction of LIN28B expression in the adult setting is sufficient to promote enhanced protein synthesis during the small Pre-B and immature B cell stages, but not during the Pro-B cell stage. This stage dependent effect was dictated by IL-7 mediated signaling, which masked the impact of LIN28B through an overpowering stimulation on the c-MYC/protein synthesis axis in Pro-B cells. Importantly, elevated protein synthesis was a distinguishing feature between neonatal and adult B cell development that was critically supported by endogenous *Lin28b* expression early in life. Finally, we used a ribosomal hypomorphic mouse model to demonstrate that subdued protein synthesis is specifically detrimental for neonatal B lymphopoiesis and the output of B-1a cells, without affecting B cell development in the adult. Taken together, we identify elevated protein synthesis as a defining requirement for early-life B cell development that critically depends on *Lin28b*. Our findings offer new mechanistic insights into the layered formation of the complex adult B cell repertoire.

KEYWORDS

LIN28B, protein synthesis, B-1 cells, neonatal B cell development, c-MYC

Introduction

B-cell development is centered around alternating stages of cellular proliferation and V(D)J recombination at the immunoglobulin heavy and light chain loci, with the goal of producing a diverse yet self-tolerant B cell repertoire. During the Pro-B cell stage, productive IgH rearrangement results in the expression of a pre-BCR complex and differentiation into the large Pre-B cell stage. The latter is marked by a transient burst of clonal expansion. Cell cycle exit is accompanied by the initiation of light chain recombination and entry into the small Pre-B cell stage. IL-7 signaling is an essential trophic factor during the Pro- and large Pre-B cell stages, promoting cell survival, proliferation, and differentiation, through distinct effects mediated by the Stat5 and mTORC1/c-MYC signaling axes (1, 2). IL-7 signaling wanes as large Pre-B cells move away from IL-7 producing stromal cells *in vivo* and its attenuation is required for the developmental progression into the small Pre-B cell stage and the onset of IgK light chain recombination (3). Generation of a productive immunoglobulin heavy and light chain complex leads to membrane IgM expression and developmental progression into the immature B (Imm-B) cell stage. Here, cells carrying innocuous BCRs are allowed to mature while self-reactive specificities are subject to central tolerance mechanisms including receptor editing and apoptosis to remove potentially harmful recognition of "self" (4). Progression through these stages is accompanied by dramatic fluctuations in bioenergetic states. Although metabolic capacity has been proposed to modulate the central tolerance checkpoint (5), this theory has not been empirically proven.

Much of what we know about B cell development comes from studies in adult mice, which differs significantly from fetal and neonatal life. For example, while B cell development in adult bone marrow strictly requires IL-7 mediated signaling, B cell output can take place in neonatal mice lacking IL-7Ra until around two weeks of age (6). Furthermore, both the pre-BCR and mature BCR checkpoints are less stringent during neonatal life allowing for the positive selection of poly and self-reactive specificities in mice and men (7–9). This correlates with the output of self-reactive CD5+ B-1a cells in mice, which secrete natural antibodies important for the clearance of cellular debris and act as a first line of defense against pathogens (10). Despite these differences, the basis for the developmental switch in B cell output is not well understood.

One molecular program that distinguishes early life lymphopoiesis is centered around the post-transcriptional regulator LIN28B. Along with LIN28A, it is one of two mammalian homologs of the heterochronic *lin-28* RNA binding protein first identified in *Caenorhabditis elegans* (11). In the mammalian hematopoietic system, *Lin28b* expression is abundant during fetal life and gradually silenced within the first two to three weeks of life, critically controlling a neonatal switch in hematopoietic stem cell function and lineage output patterns (12–14). LIN28A/B plays an established role in regulating cellular growth and metabolism in various tissues, most famously through the direct inhibition of the biogenesis of the evolutionarily conserved Let-7 family of microRNAs. Its expression de-represses Let-7 targets which include the proto-oncogenes *Myc*, *Arid3a*, *Hmga2* and *Igf2bp1-3* (15–17). We and others have previously shown that ectopic LIN28A/B expression in the adult is sufficient to reinitiate a fetal-like gene expression signature and promote key aspects of fetal-like lymphopoiesis, including the efficient production of CD5+ B-1a cells (13–15, 18). These studies establish ectopic LIN28B expression as a powerful approach to understand the unique molecular program that governs early life B cell output. Furthermore, studies from both BCR poly-clonal and BCR transgenic mouse models make clear that LIN28B relaxes the central tolerance checkpoint to allow for the positive selection of self-reactive BCR specificities and thereby uniquely shapes the neonatal B cell repertoire (19, 20). Immunophenotypically, this phenomenon is marked by the developmental progression of CD5+ Imm-B cells destined for the B-1a cell lineage (19). The mechanism for this effect is, although not fully understood, at least in part linked to augmentation of c-MYC protein levels in Imm-B cells (19) known to promote B cell positive selection (21).

A less understood mechanism of LIN28B action is through the direct binding of coding mRNAs to either positively or negatively regulate transcript stability and protein translation, in a context dependent manner (22–31). In particular, several studies have demonstrated the ability of LIN28B to promote the translation of ribosomal proteins, through Let-7 independent direct binding to their transcripts in human ES cells (32), transformed human kidney (22) and neuroblastoma (31) cell lines. However, the role of the protein synthesis pathway in LIN28B dependent B cell output is not known. Here we demonstrate that LIN28B can directly interact with ribosomal protein transcripts in primary B cell precursors. Using an inducible mouse model we show that LIN28B expression during adult B cell development elevates protein synthesis during the small Pre-B and Imm-B cell stages. Finally, we show that elevated protein synthesis is a hallmark of neonatal B cell development that depends on endogenous *Lin28b* expression and critically supports the generation of CD5+ B-1a cells early in life. We conclude that LIN28B augments protein synthesis to potentiate the unique features of early life B cell output.

Materials and methods

Mice

tet-LIN28B mice were generated by intercrossing *Col1a*$^{tetO\text{-}LIN28B}$ (JAX: #023911) mice, carrying Doxycyclin (Dox) inducible Flag-tagged human *Lin28b* cDNA under the endogenous *Col1a* promoter, to *Rosa26*^{rtTA*m2} (JAX: #006965) mice and were originally obtained from the laboratory of George Daley (Harvard Medical School) (33). Monoallelic transgene expressing mice were used for experiments. *Rosa26*^{rtTA*m2} heterozygous littermates were used as control mice. For *in vivo* experiments, Doxycycline (Dox) chow (200 mg/kg, Ssniff, cat#A112D70203) was fed to tet-LIN28B and littermates for 10 days before analysis. B6.Cg-*Lin28b*$^{tm1.1Gqda}$/J (*Lin28b* KO) (JAX: #023917), C57BLKS-*Rpl24*^{Bst}/J (Bst) (JAX: #000516) and Nur77-GFP (Jax #016617) were from the Jackson laboratory. Wildtype mice were from Taconic (B6NTAC, Taconic). The *Lin28b*-eGFP knock-in strain was generated as previously described (34). Adult mice were

used at 10 to 16 weeks of age, neonates were analyzed at the indicated days post-birth. Male and female mice were used interchangeably throughout the experiments. Animal husbandry and experimental procedures were performed in accordance with ethical permits issued by the Swedish Board of Agriculture.

Bone marrow cultures

Adult bone marrow B cell precursors from untreated adult mice were expanded and enriched *ex vivo*, as previously described (35). Briefly, single cell suspension of red blood cell lysed bone marrow cells from untreated adult mice were plated in complete RPMI-1640 (Fischer Scientific, cat#21875091) (supplemented with 10% FBS, HEPES, NEAA, Sodium Pyruvate, Penstrep, 2-mercaptoethanol) and incubated for 15 min at 37 °C. The non-adherent cells were isolated and seeded at a cell density of 0.75-1.5 million/mL using complete RPMI-1640, IL-7 (20 ng/mL, Peprotech, cat#217-17), and Dox (0.1 µg/ml, Sigma-Aldrich, cat#D3072). Note that Dox treatment was always initiated *ex vivo* at the start of the culture. The cell culture medium was refreshed every second day.

RNA immunoprecipitation sequencing

Cells from day 5 bone marrow cultures from tet-LIN28B or littermate control mice were used for lysis and RIP using Magna RIP RNA-Binding Protein Immunoprecipitation kit (Millipore, cat#17-700) according to the manufacturer's instructions. Briefly, 10% of the total lysate was kept as input sample. 4 µg of anti-Flag antibody (Sigma) and 50 µl of A/G beads (Millipore, cat#16-663) were added to the lysate and incubated for 3 hours. Beads were washed 6 times with ice-cold RIP wash buffer (Millipore, cat#17-700). RNA was extracted using RNAzol (Sigma-Aldrich, cat#R4533) and Direct-zol RNA MicroPrep kit (Zymo Research, cat#R2060). For RNA quantification and quality control respectively, Qubit with RNA HS kit (Thermofisher Scientific, cat# Q32852) and Agilent Bioanalyzer with RNA Pico kit (Agilent, cat#5067-1513) were used according to the manufacturer's instructions. 20ng of total RNA was used for the cDNA synthesis and amplification with the SMART-Seq v4 Ultra Low Input RNA Kit for Sequencing (Takara, cat#634889) according to instructions. Library tagmentation and indexing was performed using Nextera XT DNA Kit (Illumina, cat#FC-121-1030) and Nextera XT v2 set A Indexing kit (Illumina, cat#15052163). Library quantification and library size were measured using Qubit DNA HS kit (Thermofisher Scientific, cat#Q32851) and BioAnalyzer DNA HS kit (Agilent, cat#5067-4626). The samples were run in NextSeq 550 using NextSeq High output 150 cycles 2x76bp.

The sequencing was aligned to mm10 using the STAR aligner (v2.7.1) and counted using RSEM (v1.28). After mapping, the RSEM result files were loaded into R and their FPKM values were used for the analysis. To filter out lowly expressed genes, the initial data (covering 54,752 genes) was filtered for genes that had at least 50 FPKM value in the input and IP of both tet-Lin28b samples (1,459 genes), which were then used for all the analysis presented in Figure 1. The individual sample FPKM values before and after filtering are included below (Table 1).

Enrichment was calculated as IP over Input FPKM for each of the two tet-LIN28B samples, individually. 238 transcripts had an average enrichment of at least 2-fold and were considered for subsequent analyses. Littermate control sample was not considered when generating this list. Gene ontology analysis was done using the Panther database (pantherdb.org, release 17.0). Comparable results were obtained using the KEGG pathway and BioPlanet. All the sequencing data is accessible through GEO, GSE217788.

Poly-A RNA sequencing

B cell precursor subsets were FACS sorted from adult BM of Dox induced mice of the indicated genotypes. RNA sequencing libraries were generated as previously described (19) and sequenced on Illumina NextSeq and NovaSeq. Note that FSC-A low, small Pro-B cells were excluded from the FACS sorting gate. All data was processed and analyzed as previously described (19). Data is accessible through GSE217788 except for Imm-B cells that was previously generated (19) and is accessible through GSE135603. GSEA used Wald's stat generated by DESeq2 as a ranking metric. MSigDB Mouse collections Hallmark_MYC_target_v1.

Metabolic labeling of nascent proteins

Cells were depleted of endogenous methionine by pre-culturing in methionine free RPMI (Fisher Scientific, cat#A1451701). After 45 minutes, the medium was supplemented with L-azidhomoalanine (AHA, 1 mM final concentration, Fisher Scientific, cat#C10102) and labeled for one hour. AHA uptake was visualized using Click-iT Plus Alexa Fluor 555 Picolyl Azide Toolkit (Fisher Scientific, cat#C10642), following the manufacturer's protocol. Briefly, up to 3 x 10^6 cells were fixed in 400 µL of 4% formaldehyde (Fischer Scientific, cat#28906) for 20 minutes at room temperature, washed, and then permeabilized in equal volume of 0.1% saponin (Sigma, cat#S4521) for 20 minutes. Alexa Fluor 488 Alkyne (Fisher Scientific, cat#A10267) was used in place of Alexa Fluor 555 for FACS analysis.

EdU labeling for cell cycle analysis

Analysis was performed in accordance with the manufacturer's instructions (Invitrogen, cat#C10634). Briefly, single cell suspension of red blood cell lysed bone marrow cells was plated in complete RPMI-1640 (Fischer Scientific, cat#21875091) and labeled with EdU (10 µM) for 30 minutes. Cells were then stained for surface proteins before fixation and permeabilization. The EdU was Click-iT ligated to Alexa Fluor 555 and analyzed with DAPI for separation according to cell cycle phase.

10.3389/fimmu.2023.1130930

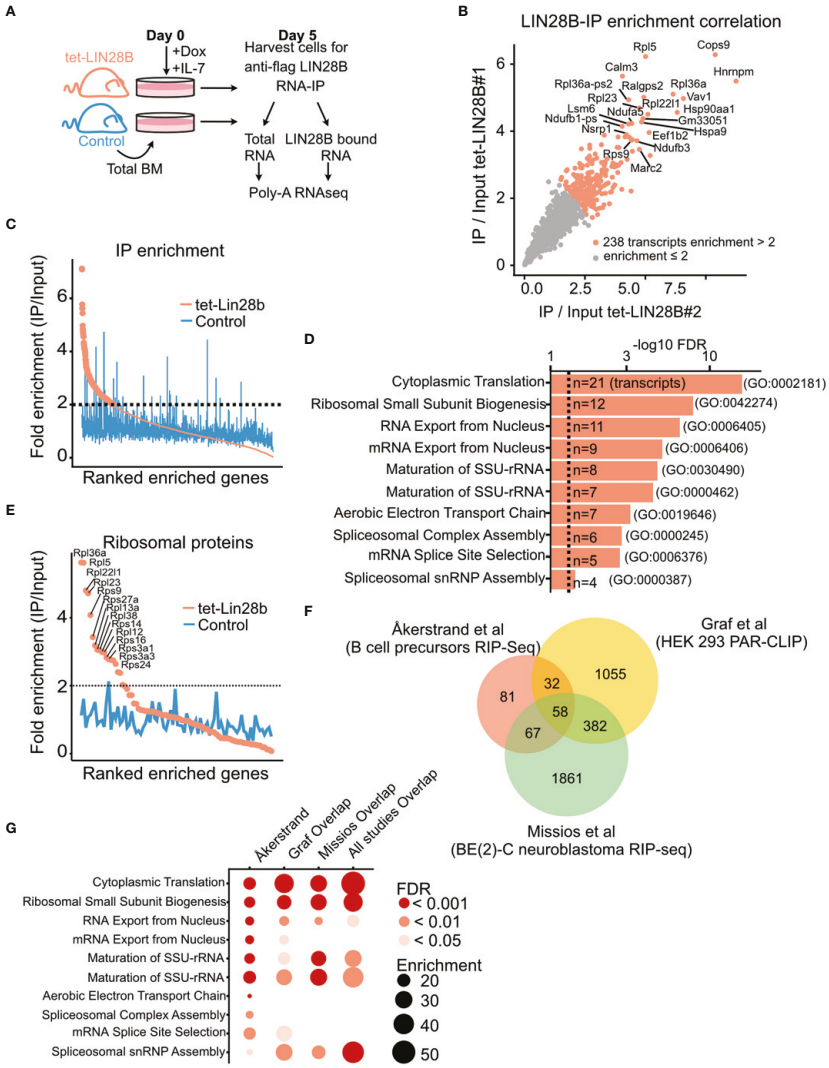

FIGURE 1
LIN28B binds to ribosomal protein transcripts in primary B cell precursors. **(A)** Schematic of experimental setup for the identification of LIN28B-bound mRNA targets in bone marrow (BM) B cell precursors. Uninduced adult total BM of the indicated genotypes were plated in IL-7 (20 ng/mL) and Doxycycline (Dox, 0.1 µg/mL) prior to RNA-IP for five days to allow for Pro-B cell expansion. Co-immunoprecipitated mRNA from two tet-LIN28B and one control mouse were individually subjected to Poly-A RNA-seq. **(B)** IP/input enrichment ratios from the two tet-LIN28B samples were plotted against each other showing high correlation between the two biological replicates. LIN28B IP/input enrichment ratio of greater than two-fold (n=238 transcripts) were used for subsequent analyses. **(C)** Average enrichment ratio ranking of the two tet-LIN28B samples compared to control. **(D)** Top ten gene ontology terms of the 238 enriched transcripts. **(E)** Graph showing the average enrichment ratio of all ribosomal protein coding transcripts ranked by IP/Input. **(F)** Analysis of overlapping genes between the 238 LIN28B enriched transcripts of this study (Åkerstrand et al) and previously published LIN28B-mRNA RIP-Seq and PAR-CLIP data sets (22, 31). **(G)** Gene ontology analyses of overlapping interacting transcripts between the indicated studies.

10.3389/fimmu.2023.1130930

TABLE 1 RIP-seq sample FPKM values.

Sample	Initial reads (FPKM)	Filtered reads (FPKM)
#1 tet-Lin28b input:	1,320,000	1,090,000
#1 tet-Lin28b IP:	1,260,000	1,080,000
#2 tet-Lin28b input:	1,360,000	1,140,000
#2 tet-Lin28b IP:	1,230,000	1,040,000
Ctrl input:	1,380,000	1,140,000
Ctrl IP:	1,140,000	912,000
Sum:	7,690,000	6,402,000

Flow cytometry

Bone marrow cells were extracted by crushing bones from hind- and front limbs, hips, and sternum, using mortar and pestle. Peritoneal cavity was isolated by flushing adult mice with 8 mL of FACS buffer (Hank's Balanced Salt Solution (Gibco, cat#14175-053) supplemented with 0.5% Bovine Serum Albumin (Sigma, cat#A9647) and 2 mM EDTA (Invitrogen, cat#15575-038)), or neonates 1-8 mL depending on the age. Red blood cell lysis was performed on bone marrow and spleens using ACK lysis buffer (Fischer Scientific, cat#A1049201), only for mice that were at least 19 days old. Lineage depletion was carried out before cell sorting by MACS Cell Separation and LS columns (Miltenyi Biotec, cat#130-042-401) to deplete CD3+, TER119+, or Gr-1+ cells, according to manufacturer's instructions.

Antibody staining of surface antigen was performed using FACS buffer, at a cell density of 1 x 10^7 cells per 100 µL of FACS buffer with antibodies, for 30 minutes at 4 °C. Analysis of intracellular antigens was done by using the same fixation and permeabilization as was described under "Metabolic labeling of nascent proteins" or using BD Cytofix/Cytoperm fixation/permeabilization kit (BD Biosciences, cat#554714). Maximum of 3 x 10^6 cells per reaction. All flow cytometry experiments were gated on live CD19+ B cells and the following immunophenotypes: Pro-B cells (CD93+IGM−cKIT+), Pre-B cells (CD93+IGM−cKIT− and FSC-A to separate large from small), Imm-B cells (CD93+IGM+), peritoneal cavity B-1a B cells (CD5+CD23−B220low and CD43+), and peritoneal cavity B-2 B cells (B220high CD23+ and CD43−). All flow cytometry experiments were performed at the Lund Stem Cell Center FACS Core Facility (Lund University, Lund, Sweden) using BD Fortessa, BD Fortessa X20, BD FACS Aria III, or BD FACS Aria II instruments. Cell sorting was performed using a 70 µm nozzle, 0.32.0 precision mask, and a flow rate below 6000 events/s. Analysis was performed using FlowJo version 10. Antibodies are listed in Supplemental Table S1.

Bone marrow HSPC transplantation

4000 bone marrow Lineage$^-$ Sca1$^+$ cKit$^+$ (LSK) donor cells (CD45.1) from day 10 neonatal *Rpl24*$^{WT/Bst}$ or WT mice were FACS sorted and mixed at a 1:2 ratio with 8000 sorted CD45.1 competitor LSK cells and 200,000 CD45.1 total BM support cells. Cells were transplanted into lethally irradiated (2 × 450 cGy) and CD45.1+ CD45.2+ double positive adult recipients by tail vein injection. Endpoint analysis was performed 13–14 weeks after transplantation.

Western blot

Sorted B cells were lysed in RIPA buffer (CST, cat#9806S), protease inhibitor (Roche, cat#4693132001), and PMSF (CST, cat#8553S). Loading samples were prepared with Laemmli buffer (Bio-Rad, cat#1610747) with β-mercaptoethanol (Bio-Rad, cat#1610710). Proteins were separated by SDS–polyacrylamide gel electrophoresis (Any kD Mini-Protean TGX gel, Bio-Rad, cat#4568125) and transferred to a nitrocellulose membrane (Trans-Blot Turbo Mini Nitrocellulose Transfer Packs, Bio-Rad, cat#1704158). Membranes were blocked for 1 hour at RT in 5% skimmed milk. Antibodies are listed in Supplemental Table S1. The ECL Select kit (GE Healthcare, cat#RPN2235) was used to detect protein bands with a ChemiDoc XRS+ system (Bio-Rad). Band intensity was quantified by Image Lab Software v6.1(BioRad). Each lane was automatically detected with manual adjustments to subtract the background and each band was individually selected followed by quantification of peak area of obtained histograms.

For RIPseq, 10% of the each indicated protein extract was collected to validate the immunoprecipitation efficiency. Proteins were separated by SDS–polyacrylamide gel electrophoresis (12% Mini-Protean TGX gel, Bio-Rad, cat#4561043) and transferred to a nitrocellulose membrane (Trans-Blot Turbo Mini Nitrocellulose Transfer Packs, Bio-Rad, cat#1704158). Membranes were blocked for 1 hour at RT in 5% skimmed milk. Antibodies are listed in Supplemental Table S1.

qRT-PCR

50.000 sorted cells were lysed in RNAzol (Sigma-Aldrich, cat#R4533) and total RNA was extracted using Direct-zol RNA MicroPrep kit (Zymo Research, cat#R2060) according to the manufacturer's instructions. Total RNA (8 µl) was used in random primed cDNA synthesis with TaqMan Reverse Transcription Reagents (Applied Biosystem, cat#N8080234). Diluted cDNA 1:2 (4 µl) was used in every qPCR reaction using KAPA probe Fast qPCR kit (Kapa Biosystem, cat#KK4706) with primers targeting 45S (Thermofisher Scientific, cat# Mm03985792_s1) and 18S (Thermofisher Scientific, cat# 4333760T) rRNA transcripts. The relative expression levels of rRNA were evaluated using log2 (2ΔCt) calculation.

Statistical analysis

All statistical analysis was carried out in R (version 4.1.2) and RStudio (version 1.4.1717), using functions from the following packages: tidyverse (version 1.3.1), DESeq2 (version 1.32.0),

rstatix (version 0.7.0), fgsea (version 1.18.0), and ggpubr (version 0.4.0). Statistics for bulk RNA-seq was generated using the DESeq2 package without custom settings. Data from non-sequencing methods were imported into R and statistics calculated using Wilcox or T-test, as indicated by the figure legends. Asterisks indicate the P-value, *<0.05, **<0.01, ***<0.001, ****<0.0001.

Results

The LIN28B mRNA interactome in primary B cell precursors is enriched for ribosomal protein transcripts

Using an inducible tet-LIN28B mouse model expressing Flag-tagged human *Lin28b* cDNA upon doxycycline (Dox) induction (*Col1a*$^{tetO\text{-}LIN28B}$ *Rosa26*^{rtTA*m2}) (33), we and others have previously demonstrated that LIN28B expression is sufficient to re-initiate fetal-like hematopoietic output in adult life (14, 19, 36, 37). To better understand the underlying mechanism, we performed immunoprecipitation of its mRNA interactome in developing B cells. To obtain sufficient cell numbers for interactome profiling, adult B cell precursors from uninduced tet-LIN28B and control mice were expanded for 5 days by culturing whole bone marrow cells in the presence of IL-7 and supplemented with Dox *ex vivo* to induce LIN28B expression. After five days with IL-7, the cultures reached above 80% B cell purity (Supplemental Figure 1A). Cells were harvested and subjected to anti-FLAG RNA immunoprecipitation (IP) coupled with poly-A selected RNA-sequencing (RIP-seq) (Figure 1A). Immunoprecipitation efficiency of LIN28B was validated by western blot analysis (Supplemental Figure 1B). Total RNA sequencing of corresponding input samples was used for calculating RIP-seq enrichment. LIN28B RIP/input ratio of the technical replicates showed a high degree of correlation ($R=0.93$, $p < 2.2e\text{-}16$) (Figure 1B) and were averaged for downstream analyses. 238 transcripts displayed a higher than two-fold RIP/input enrichment in tet-LIN28B samples but showed no trend in the control (Supplemental Table S2; Figure 1C). Gene ontology (GO) analysis revealed a prominent enrichment for ribosomal protein coding transcripts (Figures 1D, E), suggesting that ribosomal function might be a core target pathway of LIN28B during B cell development. Interestingly, similar observations were previously made in other cell types, including 293T cells (22) and BE (2)-C neuroblastoma cells (31). Indeed, cross comparison of our identified targets with these studies yielded cytoplasmatic translation as the predominant overlapping GO term (Figures 1F, G). Our analysis also identified other GO terms involved in RNA splicing and oxidative phosphorylation, consistent with previous LIN28A/B interactome studies in various cell types (23, 38). We conclude that the direct LIN28B mRNA regulon in the context of primary bone marrow B cell progenitor cells is dominated by transcripts implicated in universal biosynthetic pathways, which are shared across a wide range of cell types. In particular, our findings implicate the ribosome as a potential target for LIN28B regulation in B cell progenitors.

LIN28B enhances protein synthesis in the small Pre-B and Imm-B stages of B cell development

LIN28B bound mRNA targets have been linked to both translational increase and decrease in a context dependent manner (22–24, 27, 31, 39). In the case of ribosomal protein transcripts, enhanced protein translation was shown by SILAC (stable isotope labeling using amino acid in cell culture) metabolic labeling (22) as well as polysome profiling (31). To assess ribosomal protein levels during B cell development, we performed western blot analysis on sorted B cell precursors from tet-LIN28B and control mice following 10 days of Dox induction *in vivo* (Supplemental Figure 2A). We selected RPL36, RPL23 and RPS9 from the RIP-seq enriched transcript list and found increased protein expression upon LIN28B induction in the Pro-B and large Pre-B subsets (Figures 2A, B). Differences were less apparent for the small Pre-B and Imm-B subsets (Supplemental Figure 2B), which have lower cellular protein content. Overall, these results are consistent with enhanced translation of LIN28B bound ribosomal protein encoding transcripts.

Given this increase in ribosomal proteins, we expected a corresponding increase in overall ribosomal content upon tet-LIN28B induction. To this end, we measured the 18S rRNAs by qRT-PCR of FACS sorted B cell precursors. To our surprise, Pro and large-Pre-B cells did not exhibit any LIN28B dependent increase in 18S levels. Instead, ribosomal content first began to increase in a LIN28B dependent manner in the quiescent small Pre-B cell stage and reached statistical significance in Imm-B cells (Figure 2C). Additional analysis of the 45S precursor rRNA showed the same trend (Figure 2D). Thus, an increase in ribosome biogenesis takes place subsequent to the observed increase in ribosomal protein expression during LIN28B induced B cell development. To evaluate whether this observation correlated with changes in global protein synthesis rates, we measured newly synthesized proteins in freshly isolated B cell precursors using metabolic labelling with the methionine analog L-azidohomoalanine (AHA) (40). As expected, FACS readout of AHA uptake from Dox induced control and tet-LIN28B mice showed highly dynamic protein synthesis levels during B cell development that peaks in the large Pre-B cell subset (Figure 2E). Pro-B cells exhibited a bimodal profile with respect to protein synthesis that correlated with cell size (AHA^{high} or AHA^{low}, Supplemental Figure 2C). Although there was a tendency towards an increased frequency of AHA^{high} Pro-B cell in tet-LIN28B induced mice, the changes were not statistically significant (Figures 2F, G; Supplemental Figures 2C, D). tet-LIN28B induction increased global protein synthesis was first observed as cells transitioned from the large to the small Pre-B stage and peaked in the Imm-B cell stage (Figures 2F, G), mirroring the observed effects on ribosome biogenesis. This was accompanied by increased cell size as measured by FACS (FSC-A) (Figure 2H), and a moderate increase in the fraction of proliferating cells within the Imm-B subset (Supplemental Figure 2E). These findings are consistent with elevated protein synthesis boosting biomass accumulation

10.3389/fimmu.2023.1130930

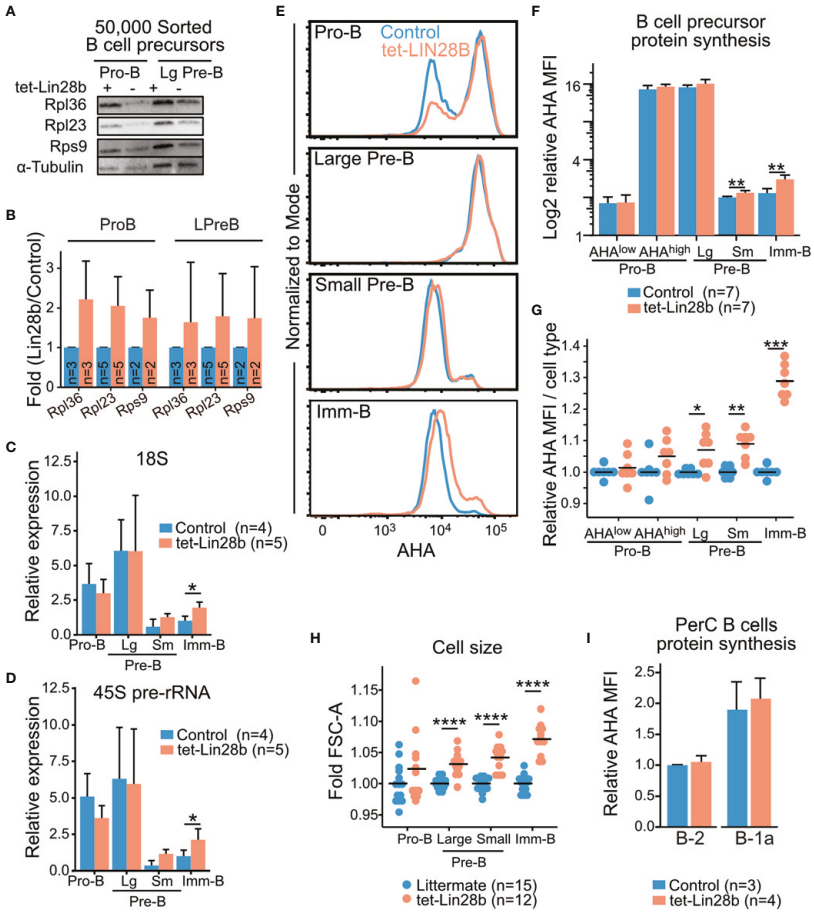

FIGURE 2
LIN28B enhances protein synthesis in small Pre-B and Imm-B cells **(A)** Representative western blot analysis for the indicated ribosomal proteins from 50,000 FACS sorted Pro-B and large Pre-B cells from adult tet-LIN28B or littermate control mice following 10 days of *in vivo* Dox induction. **(B)** Quantification of western blot data from 2-5 biological replicates and three separate experiments (See materials and methods). **(C, D)** qRT-PCR for 18S rRNA or 45S pre-rRNA from 50,000 FACS sorted adult B cell progenitors. Expression values were normalized relative to the littermate control Imm-B cells. Large and small Pre-B cells are indicated as Lg and Sm respectively. **(E)** Representative FACS histogram overlays of L-Azidohomoalanine (AHA) uptake, corresponding to their protein synthesis rates, in the indicated subsets from adult mice. **(F, G)** AHA median fluorescence intensity (MFI) for indicated BM B cell precursor stage as shown in **(E)**. **(F)** Data is presented as relative values to one control small Pre-B cell subset for each experiment. **(G)** Data is normalized per cell type to one control sample for each experiment. **(H)** Measurement of FSC-A MFI. Data is normalized per cell type to one control sample for each experiment. **(I)** AHA MFI for the indicated, peritoneal cavity (PerC) B cell subsets, plotted relative to control B-2 values. Wilcox test was used to calculate p-values **B–D**, **F**, **I**. *p<0.05, **p<0.01, ***p<0.001, ****p<0.0001. Bars show mean, error bars show standard deviation.

and cell cycle entry following the pre-BCR checkpoint. Interestingly, analysis of mature B cells showed that protein synthesis in peritoneal cavity B-1 and B-2 cells were not affected by ectopic LIN28B (Figure 2I). Taken together, we conclude that LIN28B enhances ribosome content and global protein synthesis levels specifically during the later stages of bone marrow B cell development.

Lin28B augments protein synthesis during IL-7 independent B cell maturation

We sought to understand the stage dependent effects of LIN28B expression on protein synthesis by considering the signals that control dynamic changes in cellular metabolism and biosynthesis during B cell development. We have previously shown that Lin28B

enhances the output of CD5+ Imm-B cells, and that CD5 levels correspond to BCR self-reactivity (19). To assess whether enhanced protein synthesis in Imm-B cells is linked to higher signaling levels through the newly selected BCR we compared CD5 expression with AHA uptake by tet-LIN28B induced Imm-B cells. Indeed, we observed a positive correlation between the two readouts suggesting that enhanced protein synthesis is dictated by BCR signaling strength (Figures 3A, B). To strengthen this interpretation, we confirmed that CD5+ Imm-B cells correspond to those with the highest level of Nur77-GFP reporter expression (Figures 3C, D; Supplemental Figure 3), a well-established measurement of antigen receptor stimulation in mice (41, 42). Interestingly, the percentage of CD5+ Nur77-GFP+ cells was already enhanced in tet-LIN28B induced small Pre-B cells where a ~10% increase in protein synthesis was observed (Figure 2F), although the overall MFI was much lower compared to the Imm-B cells. Taken together, our data show that LIN28B induced protein synthesis precedes the positive selection of CD5+ Imm-B cells and is in line with its permissive effect on the developmental progression from the Pre-B cell stage onwards.

The lack of LIN28B induced effects on protein synthesis in Pro-B cells was puzzling given the *Lin28b* dependent increase in ribosomal protein expression at this stage (Figure 2A). Considering that both IL-7 and LIN28B can act through elevating c-MYC expression, and that the c-MYC transcriptional program is a critical driver of cellular protein synthesis (2, 43), we hypothesized that potent IL-7 signaling might mask any LIN28B mediated effects on the c-MYC/protein synthesis axis in Pro-B cells. To test this, we assessed LIN28B induced protein synthesis in Pro-B cells following IL-7 withdrawal *ex vivo*. B cell precursors were expanded from control and tet-LIN28B adult bone marrow under saturating IL-7 conditions for five days, before culturing under limiting doses of IL-7 (Figure 3E) as previously described (3). Two days following IL-7 withdrawal, cells were harvested and FACS analyzed for LIN28B-dependent effects on c-MYC expression and global protein synthesis. Interestingly, although overall c-MYC and protein synthesis levels of Pro-B cells decreased upon IL-7 withdrawal, the decrease was partially alleviated by tet-LIN28B induction (Figure 3F left). A similar trend was observed for protein synthesis (Figure 3F right) at limiting IL-7 concentrations. Thus, LIN28B has the capacity to enhance the c-MYC/protein synthesis axis in Pro-B cells, but only under limiting IL-7 availability. Taken together, our results provide a likely explanation to the stage dependent effects of LIN28B expression on protein synthesis during B cell development (Figure 3G). In Imm-B cells, enhanced protein synthesis is linked to the increased signaling strength of BCR specificities licensed by LIN28B expression. Prior to the Imm-B cell stage, effects on protein synthesis is dictated by IL-7 responsiveness. During the Pro-B cell stage, potent IL-7 mediated protein synthesis masks the milder effects by LIN28B which become apparent upon entry into the small Pre-B cell stage whereby IL-7Ra expression is fully silenced. This scenario is supported by RNAseq data from sorted B cell precursor subsets from tet-LIN28B and control adult bone marrow, which showed a LIN28B induced increase in c-MYC target genes specifically upon entry into the small Pre-B cell stage (Figure 3H). Taken together, our results suggest a critical role for LIN28B in the small Pre-B cell stage as cells loose IL-7 responsiveness and point toward a key role for c-MYC in LIN28B induced protein synthesis.

Elevated protein synthesis is a hallmark of neonatal B cell development

Endogenous LIN28B expression is developmentally restricted. FACS analysis of LIN28B-eGFP reporter mice (34) captured its window of expression as eGFP gradually diminished to background levels after postnatal day 10 in B cell precursors and postnatal day 19 in hematopoietic stem and progenitor cells (HSPCs) (Figure 4A). This time-window correlates with the output of B-1a cells which ceases between day 10 and day 19 during unperturbed hematopoiesis (44). During the same window, protein synthesis in neonatal bone marrow small Pre-B and Imm-B cells was elevated compared to the adult (Figure 4B). This was dependent on endogenous *Lin28b*, as 3-day-old KO neonates had a significantly lower rate of protein synthesis and decreased cell size during the small Pre-B and Imm-B cell stages (Figures 4C, D). These defects were primarily qualitative and not accompanied by changes in subset frequency (Figure 4E). We conclude that *Lin28b* dependent increases in protein synthesis during the small Pre-B and Imm-B cell stages represent a hallmark of early life B cell development.

Neonatal B cell development relies on a heightened level of protein synthesis

To investigate the importance of elevated protein synthesis for neonatal B cell development, we took advantage of the ribosomal protein hypomorphic $Rpl24^{WT/Bst}$ mouse model. This model carries a mutation that disrupts *Rpl24* mRNA splicing and protein expression (45). The resulting defect in ribosome biogenesis causes a moderate reduction in overall cellular protein synthesis which has no apparent impact on normal adult B cell development (40), but can diminish Eμ-MYC driven B lymphomagenesis known to be 'addicted' to heightened ribosomal function (46). Neonatal B cell development has not previously been examined in $Rpl24^{WT/Bst}$ mice. Given our findings of higher protein synthesis rates, we hypothesized that neonatal B cell development would be more sensitive to constraints in protein synthesis capacity (Figure 5A). Indeed, analysis of $Rpl24^{WT/Bst}$ bone marrow revealed a decrease in the overall CD19+ B cell frequency on postnatal day 3 and day 10 that was resolved by day 19 (Figure 5B). This translated into a concomitant decrease in the frequency of B cell precursor subsets in the bone marrow of $Rpl24^{WT/Bst}$ neonates (Figure 5C) and a time-limited decrease in the frequency of mature B cells in both the spleen (Figure 5D) and the peritoneal cavity of neonatal mice (Figure 5E). Thus, neonatal B cell development is more sensitive to constrained protein synthesis with signs of ribosome 'addiction'. To verify that these effects are cell intrinsic during B cell development, we performed competitive transplantations of neonatal $Rpl24^{WT/Bst}$ or littermate bone marrow HSPCs into lethally irradiated congenic recipients (Figure 5F). Analysis of

10.3389/fimmu.2023.1130930

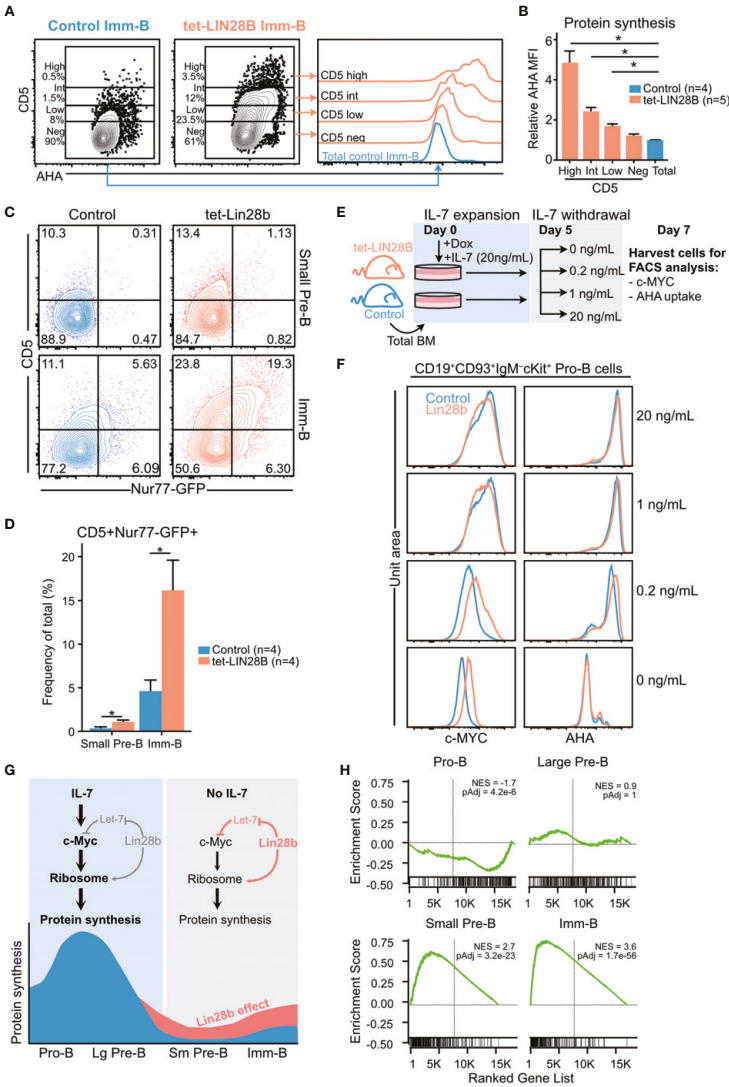

FIGURE 3
Interrogating the stage dependent effects of LIN28B on protein synthesis during B cell development **(A)** (Left) Representative FACS plots showing CD5 expression in adult Imm-B cells from the indicated genotypes and (right) corresponding AHA uptake of the indicated subsets. **(B)** AHA MFI within individual CD5 slices, after normalization to AHA MFI in littermate control Imm-B cells. Wilcox test was used to calculate p-values in **(B)** **p<0.01. Bars show mean ± standard deviation. **(C)** Representative FACS plot showing CD5 surface expression against Nur77-GFP levels for adult small Pre-B and Imm-B cells of the indicated genotypes. **(D)** Quantification of CD5+Nur77-GFP+ cells, as shown in **(C)** Data from four mice per genotype and two separate experiments. **(E)** Experimental setup for measuring the impact of IL-7 availability on sensitivity to LIN28B mediated effects on Pro-B cells. Following 5 days of expanding adult B cell precursors in 20 ng/mL IL-7, the cultures were split into conditions with decreasing concentrations of IL-7. Two days later, the cultures were analyzed by FACS for intracellular c-MYC and AHA uptake. **(F)** Representative FACS histograms for the indicated IL-7 conditions show intracellular staining for c-MYC (left) and AHA uptake (right) in Pro-B cells. **(G)** Schematic illustration of the proposed LIN28B mode of action on protein synthesis during B cell development. **(H)** Gene set enrichment analysis (GSEA) of differentially expressed genes between tet-LIN28B induced and control B cell precursor subsets as identified by RNAseq (See methods). Vertical line indicates Zero cross point. Enrichment for c-MYC target signature version 1 (Hallmark catalog, molecular signature database) is shown. Wilcox test was used to calculate p-values in **(B, D)** *p<0.05. Bars show mean standard deviation.

10.3389/fimmu.2023.1130930

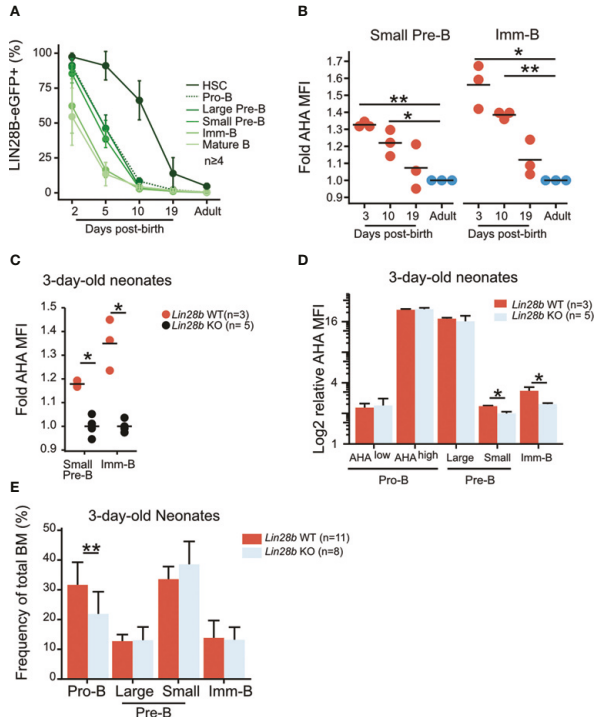

FIGURE 4
Elevated protein synthesis during neonatal B cell development is dependent on LIN28B. **(A)** Analysis of BM hematopoietic stem cells (HSCs: Lineage−, Sca1+, cKit+, CD150+, CD48−, FLT3+) and B cell precursors from *Lin28b*-eGFP mice at the indicated ages. The average frequency and standard deviation of *Lin28b*-eGFP positive cells is shown for each time point. **(B)** AHA MFI from *Lin28b*-WT neonates at the indicated ages are plotted relative to the uptake in WT adult control mice for each subset. **(C)** AHA MFI in 3-day-old neonates of the indicated genotypes. Values are normalized within each experiment to one *Lin28b* KO neonate per cell type. **(D)** Same as in C but normalized to one *Lin28b* KO small Pre-B cell sample within each experiment. **(E)** Frequency of BM B cell precursors in 3-day-old neonates. T-test was used to calculate p-values in B, Wilcox test was used to calculate p-values in C-E. **p<0.001, *p<0.05. Bars show mean standard deviation.

donor versus competitor reconstitution of recipient PerC B cells at 14 weeks post-transplantation showed a selective decrease in B-1a cells from *Rpl24*$^{WT/Bst}$ donors. In contrast, contribution to the B-2 compartment, which relies on continuous HSPC dependent influx, was comparable between the *Rpl24*$^{WT/Bst}$ and wildtype donor HSPCs (Figure 5G). Taken together, these findings demonstrate that neonatal B cell output is selectively sensitive to reduced protein synthesis in a cell intrinsic manner.

The B-1a cell subset is enriched for the VH11 and VH12 encoded reactivity against the self-membrane component phosphatidyl choline (PtC) known to originate early in life. To investigate the qualitative impact of constrained protein synthesis on B-1a cell composition, we analyzed the frequency and absolute number of PtC reactive B-1a cells in 19-day-old Rpl24$^{WT/Bst}$ mice using fluorescently labelled PtC liposomes. This timepoint was selected to minimize influence by peripheral homeostatic expansion (47). Indeed, FACS analysis revealed a dramatic decrease in the frequency and absolute number of PtC reactive B cells in the peritoneal cavity of *Rpl24*$^{WT/Bst}$ neonates (Figures 5H–J). We therefore conclude that elevated protein synthesis is a central distinguishing parameter of neonatal B lymphopoiesis that potentiates the output of CD5+ B-1a cells carrying self-reactive BCRs.

Discussion

In this study, we identified a role for cellular protein synthesis in regulating the unique aspects of early-life B cell development including the time restricted output of self-reactive B-1a cells. Elevated protein synthesis was a defining feature of neonatal B cell development that was mediated at least in part by the endogenous expression of the heterochronic RNA-binding protein LIN28B. As the expression of LIN28B naturally waned during the first weeks of life, protein synthesis became reduced, and ectopic LIN28B expression in the adult was sufficient to recapitulate

10.3389/fimmu.2023.1130930

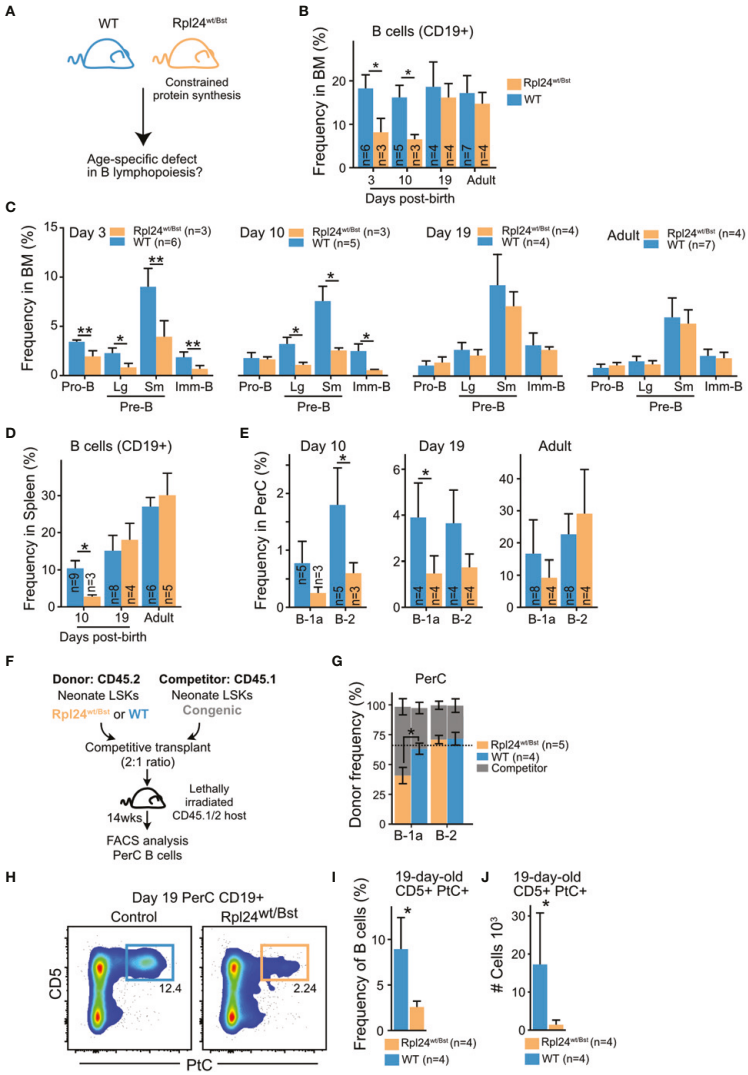

FIGURE 5
Neonatal B cell development relies on enhanced protein synthesis **(A)** *Rpl24*$^{wt/Bst}$ and wildtype littermates were analyzed by FACS at different ages for phenotypic differences during BM B cell development. **(B)** Frequency of CD19+ B cells out of total BM cells at the indicated ages. **(C)** BM B cell precursor subset frequencies at the indicated ages presented as percent of total BM cells. **(D)** Frequency of splenic CD19+ B cells out of total splenocytes at the indicated ages. **(E)** Mature PerC B-1a and B-2 cell frequencies out of total PerC cells at the indicated ages. **(F)** Experimental overview for assessment of cell intrinsic defect of the *Rpl24*$^{wt/Bst}$ mutation. Lineage−, Sca1+, cKit+ (LSK) hematopoietic stem and progenitor cells (HSPCs) from 10-day-old donor and competitor mice of the indicated genotypes were sorted and transplanted into lethally irradiated recipients. 13-14 weeks later, the steady state donor and competitor derived mature PerC B cells were analyzed to assess B-1a and B-2 cell output. **(G)** CD19+ PerC B cells of the indicated subsets were compared for donor versus competitor contribution. The expected frequency based on donor: competitor ratio is indicated by the dashed line. **(H)** Representative FACS plots showing the frequency of CD5+ PtC-liposome reactive B cells in 19-day old littermates. **(I)** CD5+PtC+ frequency out of PerC CD19+ B cells in 19-day-old mice. **(J)** Absolute number of CD5+PtC+ B cells in PerC in 19-day-old mice. Wilcox test was used to calculate p-values. *p<0.05, **p<0.01. Bars show mean ± standard deviation.

elevated protein synthesis small Pre- and Imm-B cells. Consistent with previous reports in other cell types, we showed that LIN28B directly bound to ribosomal protein transcripts in primary B cell precursors, correlating with their enhanced protein expression. Furthermore, an increase in ribosomal biogenesis and protein synthesis coincided with LIN28B induced c-MYC expression in the quiescent small Pre- and Imm-B cell stages. Finally, using *Rpl24*$^{WT/Bst}$ mice as a model for constrained protein synthesis capacity, we showed that neonatal B cell development relied on heightened protein synthesis levels – a hallmark of elevated c-MYC activity. The precise extent and mechanism by which LIN28B cooperates with c-MYC to promote cellular protein synthesis was not disentangled in this study. One likely possibility is that LIN28B may post-transcriptionally act on a c-MYC induced transcriptome to facilitate downstream translation, biomass accumulation and B cell developmental progression.

Protein synthesis is the most energy consuming biosynthetic process in the cell and subject to the constraints imposed by hundreds of components required for ribosome assembly (48). Indeed, protein synthesis rates give an accurate account of the overall cellular metabolism (49). And yet, its ability to control the development and function of immune cells that require rapid expansion and contraction of cellular growth has been an under-explored subject of investigation. Our results using AHA metabolic labelling to measure protein synthesis confirmed dynamic changes in cellular metabolism that underly proliferative bursts following successful BCR checkpoints (1). Importantly, we demonstrated the ability of LIN28B to partially alleviate the biggest drop in protein synthesis upon entry into the small Pre-B cell stage. The restricted metabolism of small Pre-B cells was previously implicated as a mechanism to safeguard the central tolerance checkpoint through enforcing nutrient stress and negative selection upon strong BCR engagement (5). This notion is highly compatible with our observation that LIN28B promoted protein synthesis to augment the output of self-reactive CD5+ B-1 cells early in life. The latter is a hallmark of early life B lymphopoiesis and offers an attractive explanation to the long-known prevalence of self-reactive specificities in neonatal mice and men (7, 50). Our previous findings made clear that LIN28B supports enhanced BCR signaling strength in the Imm-B cell stage (19). Here we report that elevated CD5 and Nur77 expression is visible already in the small pre-B cell stage upon tet-LIN28B induction, suggesting that pre-BCR signaling strength may also be influenced by LIN28B. Consistent with this notion, elevated protein synthesis and cell size is noticeable already in tet-LIN28B large Pre-B cells. Taken together, we propose that the relatively mild increase in protein synthesis mediated by LIN28B provides sufficient relaxation of the metabolic constraints during B cell maturation to qualitatively alter the BCR repertoire output.

In Pro-B cells, IL-7 signaling and downstream mTORC1 activation is the principal driver of c-MYC expression and acts to promote biomass accumulation and proliferation (2). In this study, we showed that both IL-7 signaling and LIN28B expression act on the c-MYC/protein synthesis axis to promote developmental progression during B cell development and that the powerful effects of IL-7 rendered LIN28B function redundant in Pro-B cells. This finding is relevant in the context of understanding the ontogenic differences in IL-7 dependency during B lymphopoiesis. It well-established that the strict requirement for IL-7 mediated signaling, which is characteristic of adult murine B lymphopoiesis, does not apply during fetal and neonatal life (6). We have previously demonstrated that LIN28B over-expression during adult hematopoiesis is sufficient to phenocopy fetal-like behavior by circumventing strict IL-7 dependency (13). Here, our findings that LIN28B partially cushions the impact of IL-7 withdrawal through promoting the shared downstream c-MYC/protein synthesis axis may offer an explanation to the lessened reliance on IL-7 during early life B lymphopoiesis (6).

The RIP-seq experiment presented in this study led us to identify changes in protein synthesis levels as a distinguishing parameter between neonatal and adult B cell development. However, the experiment has several limitations. First, the LIN28B interactome in IL-7 expanded bone marrow Pro-B cell cultures may not exactly reflect that in primary small Pre-B cells. Unfortunately, the amount of material needed for RIPseq is not feasible to obtain from quiescent small Pre-B cells, and data extrapolation should be made with caution. Second, the low number of biological replicates of this experiment prevents statistical analysis and limits the number of enriched transcripts identified. Nevertheless, since our data did detect the same top gene ontology terms as previous datasets from other tissues, they serve as confirmatory evidence in the context of B cell precursors. A recent LIN28B interactome study in hematopoietic progenitors expressing the oncogenic fusion protein MLL-ENL identified both Rps9 and Rpl23 transcripts as direct targets of LIN28B, offering further support to our findings in the hematopoietic system (39). Despite these limitations, our approach resulted in the identification of a relevant regulatory axis for early-life B lymphopoiesis. In the context of neonatal immunity, we and others have previously demonstrated that neonatal antigen exposure produces unique B cell memory clones not generated by adult mice immunized with the same antigen (44, 51). Our current findings that enhanced protein synthesis quantitatively and qualitatively alters neonatal B cell output implicates ribosomal control in the formation of a unique pre-immune repertoire in neonatal mice and has important implications for the layered formation of a complex adaptive immune system (52–54).

Data availability statement

The datasets presented in this study can be found in online repositories. The names of the repository/repositories and accession number(s) can be found in the article.

Ethics statement

The animal study was reviewed and approved by Swedish board of agriculture.

Author contributions

Study was conceptualized by HÅ and JY. Experiments were performed by HÅ, GM, EB, StiV and KO. Critical experimental direction was provided by SteV, MC and CB. EB provided critical input into the overall development the study. Manuscript was written by HÅ and JY. All authors contributed to the article and approved the submitted version.

Funding

JY was supported by the Swedish Research Council, the Swedish Cancer Society, the European Research Council (715313), Knut and Alice Wallenberg Foundation and the Wenner-Gren Foundations.

Acknowledgments

We thank Jonas Ungerbäck and Johanna Tingvall-Gustafsson for help with bioinformatics. We thank Jenny Hansson, Leal Oburoglu, and Svetlana Soboleva for their input. Finally, we also thank the FACS and Bioinformatics core facilities at the Lund Stem Cell Center for their support.

Conflict of interest

The authors declare that the research was conducted in the absence of any commercial or financial relationships that could be construed as a potential conflict of interest.

Publisher's note

Supplementary material

The Supplementary Material for this article can be found online at: https://www.frontiersin.org/articles/10.3389/fimmu.2023.1130930/full#supplementary-material

SUPPLEMENTARY TABLE 1
Antibodies and reagents used for Flow Cytometry, Western Blot, or IP.

References

1. Clark MR, Mandal M, Ochiai K, Singh H. Orchestrating b cell lymphopoiesis through interplay of IL-7 receptor and pre-b cell receptor signalling. *Nat Rev Immunol* (2014) 14(2):69–80. doi: 10.1038/nri3570

2. Zeng H, Yu M, Tan H, Li Y, Su W, Shi H, et al. Discrete roles and bifurcation of PTEN signaling and mTORC1-mediated anabolic metabolism underlie IL-7-driven b lymphopoiesis. *Sci Adv* (2018) 4(1):eaar5701. doi: 10.1126/sciadv.aar5701

3. Mandal M, Okoreeh MK, Kennedy DE, Maienschein-Cline M, Ai J, McLean KC, et al. CXCR4 signaling directs igk recombination and the molecular mechanisms of late b lymphopoiesis. *Nat Immunol* (2019) 20(10):1393–403. doi: 10.1038/s41590-019-0468-0

4. Nemazee D. Mechanisms of central tolerance for b cells. *Nat Rev Immunol* (2017) 17(5):281–94. doi: 10.1038/nri.2017.19

5. Muschen M. Metabolic gatekeepers to safeguard against autoimmunity and oncogenic b cell transformation. *Nat Rev Immunol* (2019) 19(5):337–48. doi: 10.1038/s41577-019-0154-3

6. Kikuchi K, Kondo M. Developmental switch of mouse hematopoietic stem cells from fetal to adult type occurs in bone marrow after birth. *Proc Natl Acad Sci U S A* (2006) 103(47):17852–7. doi: 10.1073/pnas.0603368103

7. Hayakawa K, Asano M, Shinton SA, Gui M, Allman D, Stewart CL, et al. Positive selection of natural autoreactive b cells. *Science.* (1999) 285(5424):113–6. doi: 10.1126/science.285.5424.113

8. Chen JW, Rice TA, Bannock JM, Bielecka AA, Strauss JD, Catanzaro JR, et al. Autoreactivity in naive human fetal b cells is associated with commensal bacteria recognition. *Science.* (2020) 369(6501):320–5. doi: 10.1126/science.aay9733

9. Wong JB, Hewitt SL, Heltemes-Harris LM, Mandal M, Johnson K, Rajewsky K, et al. B-1a cells acquire their unique characteristics by bypassing the pre-BCR selection stage. *Nat Commun* (2019) 10(1):4768. doi: 10.1038/s41467-019-12824-z

10. Baumgarth N. The double life of a b-1 cell: self-reactivity selects for protective effector functions. *Nat Rev Immunol* (2011) 11(1):34–46. doi: 10.1038/nri2901

11. Ambros V, Horvitz HR. Heterochronic mutants of the nematode caenorhabditis elegans. *Science.* (1984) 226(4673):409–16. doi: 10.1126/science.6494891

12. Copley MR, Eaves CJ. Developmental changes in hematopoietic stem cell properties. *Exp Mol Med* (2013) 45:e55. doi: 10.1038/emm.2013.98

13. Yuan J, Nguyen CK, Liu X, Kanellopoulou C, Muljo SA. Lin28b reprograms adult bone marrow hematopoietic progenitors to mediate fetal-like lymphopoiesis. *Science.* (2012) 335(6073):1195–200. doi: 10.1126/science.1216557

14. Kristiansen TA, Jaensson Gyllenback E, Zriwil A, Bjorklund T, Daniel JA, Sitnicka E, et al. Cellular barcoding links b-1a b cell potential to a fetal hematopoietic stem cell state at the single-cell level. *Immunity.* (2016) 45(2):346–57. doi: 10.1016/j.immuni.2016.07.014

15. Zhou Y, Li YS, Bandi SR, Tang L, Shinton SA, Hayakawa K, et al. Lin28b promotes fetal b lymphopoiesis through the transcription factor Arid3a. *J Exp Med* (2015) 212(4):569–80. doi: 10.1084/jem.20141510

16. Copley MR, Babovic S, Benz C, Knapp DJ, Beer PA, Kent DG, et al. The Lin28b-let-7-Hmga2 axis determines the higher self-renewal potential of fetal haematopoietic stem cells. *Nat Cell Biol* (2013) 15(8):916–25. doi: 10.1038/ncb2783

17. Sampson VB, Rong NH, Han J, Yang Q, Aris V, Soteropoulos P, et al. MicroRNA let-7a down-regulates MYC and reverts MYC-induced growth in burkitt lymphoma cells. *Cancer Res* (2007) 67(20):9762–70. doi: 10.1158/0008-5472.CAN-07-2462

18. Wang J, Wissink EM, Watson NB, Smith NL, Grimson A, Rudd BD. Fetal and adult progenitors give rise to unique populations of CD8+ T cells. *Blood.* (2016) 128(26):3073–82. doi: 10.1182/blood-2016-06-725366

19. Vanhee S, Akerstrand H, Kristiansen TA, Datta S, Montano G, Vergani S, et al. Lin28b controls a neonatal to adult switch in b cell positive selection. *Sci Immunol* (2019) 4(39). doi: 10.1126/sciimmunol.aax4453

20. Xu X, Deobagkar-Lele M, Bull KR, Crockford TL, Mead AJ, Cribbs AP, et al. An ontogenetic switch drives the positive and negative selection of b cells. *Proc Natl Acad Sci U S A* (2020) 117(7):3718–27. doi: 10.1073/pnas.1915247117

21. Benhamou D, Labi V, Novak R, Dai I, Shafir-Alon S, Weiss A, et al. A c-Myc/miR17-92/Pten axis controls PI3K-mediated positive and negative selection in b cell development and reconstitutes CD19 deficiency. *Cell Rep* (2016) 16(2):419–31. doi: 10.1016/j.celrep.2016.05.084

22. Graf R, Munschauer M, Mastrobuoni G, Mayr F, Heinemann U, Kempa S, et al. Identification of LIN28B-bound mRNAs reveals features of target recognition and regulation. *RNA Biol* (2013) 10(7):1146–59. doi: 10.4161/rna.25194

23. Wilbert ML, Huelga SC, Kapeli K, Stark TJ, Liang TY, Chen SX, et al. LIN28 binds messenger RNAs at GGAGA motifs and regulates splicing factor abundance. *Mol Cell* (2012) 48(2):195–206. doi: 10.1016/j.molcel.2012.08.004

24. Cho J, Chang H, Kwon SC, Kim B, Kim Y, Choe J, et al. LIN28A is a suppressor of ER-associated translation in embryonic stem cells. *Cell.* (2012) 151(4):765–77. doi: 10.1016/j.cell.2012.10.019

25. Hafner M, Max KE, Bandaru P, Morozov P, Gerstberger S, Brown M, et al. Identification of mRNAs bound and regulated by human LIN28 proteins and molecular requirements for RNA recognition. *RNA*. (2013) 19(5):613–26. doi: 10.1261/rna.036491.112

26. Wang S, Chim B, Su Y, Khil P, Wong M, Wang X, et al. Enhancement of LIN28B-induced hematopoietic reprogramming by IGF2BP3. *Genes Dev* (2019) 33(15-16):1048–68. doi: 10.1101/gad.325100.119

27. Basak A, Munschauer M, Lareau CA, Montbleau KE, Ulirsch JC, Hartigan CR, et al. Control of human hemoglobin switching by LIN28B-mediated regulation of BCL11A translation. *Nat Genet* (2020) 52(2):138–45. doi: 10.1038/s41588-019-0568-7

28. Osborne JK, Kinney MA, Han A, Akinnola KE, Yermalovich AV, Vo LT, et al. Lin28 paralogs regulate lung branching morphogenesis. *Cell Rep* (2021) 36(3):109408. doi: 10.1016/j.celrep.2021.109408

29. Madison BB, Liu Q, Zhong X, Hahn CM, Lin N, Emmett MJ, et al. LIN28B promotes growth and tumorigenesis of the intestinal epithelium *via* let-7. *Genes Dev* (2013) 27(20):2233–45. doi: 10.1101/gad.224659.113

30. Tan FE, Sathe S, Wheeler EC, Yeo GW. Non-microRNA binding competitively inhibits LIN28 regulation. *Cell Rep* (2021) 36(6):109517. doi: 10.1016/j.celrep.2021.109517

31. Missios P, da Rocha EL, Pearson DS, Philipp J, Aleman MM, Pirouz M, et al. LIN28B alters ribosomal dynamics to promote metastasis in MYCN-driven malignancy. *J Clin Invest* (2021) 131(22). doi: 10.1172/JCI145142

32. Peng S, Chen LL, Lei XX, Yang L, Lin H, Carmichael GG, et al. Genome-wide studies reveal that Lin28 enhances the translation of genes important for growth and survival of human embryonic stem cells. *Stem Cells* (2011) 29(3):496–504. doi: 10.1002/stem.591

33. Zhu H, Shyh-Chang N, Segre AV, Shinoda G, Shah SP, Einhorn WS, et al. The Lin28/let-7 axis regulates glucose metabolism. *Cell.* (2011) 147(1):81–94. doi: 10.1016/j.cell.2011.08.033

34. Kristiansen TA, Zhang Q, Vergani S, Boldrin E, Krausse N, Andre O, et al. Developmental cues license megakaryocyte priming in murine hematopoietic stem cells. *Blood Adv* (2022) 6(24):6228–41. doi: 10.1182/bloodadvances.2021006861

35. Holl TM, Haynes BF, Kelsoe G. Stromal cell independent b cell development *in vitro*: generation and recovery of autoreactive clones. *J Immunol Methods* (2010) 354(1-2):53–67. doi: 10.1016/j.jim.2010.01.007

36. Stolla MC, Catherman SC, Kingsley PD, Rowe RG, Koniski AD, Fegan K, et al. Lin28b regulates age-dependent differences in murine platelet function. *Blood Adv* (2019) 3(1):72–82. doi: 10.1182/bloodadvances.2018020859

37. Rowe RG, Wang LD, Coma S, Han A, Mathieu R, Pearson DS, et al. Developmental regulation of myeloerythroid progenitor function by the Lin28b-let-7-Hmga2 axis. *J Exp Med* (2016) 213(8):1497–512. doi: 10.1084/jem.20151912

38. Shyh-Chang N, Zhu H, Yvanka de Soysa T, Shinoda G, Seligson MT, Tsanov KM, et al. Lin28 enhances tissue repair by reprogramming cellular metabolism. *Cell.* (2013) 155(4):778–92. doi: 10.1016/j.cell.2013.09.059

39. Eldeeb M, Yuan O, Guzzi N, Thi Ngoc PC, Konturek-Ciesla A, Kristiansen TA, et al. A fetal tumor suppressor axis abrogates MLL-fusion-driven acute myeloid leukemia. *Cell Rep* (2023) 42(2):112099. doi: 10.1016/j.celrep.2023.112099

40. Signer RA, Magee JA, Salic A, Morrison SJ. Haematopoietic stem cells require a highly regulated protein synthesis rate. *Nature.* (2014) 509(7498):49–54. doi: 10.1038/nature13035

41. Tan C, Mueller JL, Noviski M, Huizar J, Lau D, Dubinin A, et al. Nur77 links chronic antigen stimulation to b cell tolerance by restricting the survival of self-reactive b cells in the periphery. *J Immunol* (2019) 202(10):2907–23. doi: 10.4049/jimmunol.1801565

42. Moran AE, Holzapfel KL, Xing Y, Cunningham NR, Maltzman JS, Punt J, et al. T Cell receptor signal strength in treg and iNKT cell development demonstrated by a novel fluorescent reporter mouse. *J Exp Med* (2011) 208(6):1279–89. doi: 10.1084/jem.20110308

43. Morrow MA, Lee G, Gillis S, Yancopoulos GD, Alt FW. Interleukin-7 induces n-myc and c-myc expression in normal precursor b lymphocytes. *Genes Dev* (1992) 6(1):61–70. doi: 10.1101/gad.6.1.61

44. Vergani S, Muleta KG, Da Silva C, Doyle A, Kristiansen TA, Sodini S, et al. A self-sustaining layer of early-life-origin b cells drives steady-state IgA responses in the adult gut. *Immunity* (2022) 55:1829–42. doi: 10.1016/j.immuni.2022.08.018

45. Oliver ER, Saunders TL, Tarle SA, Glaser T. Ribosomal protein L24 defect in belly spot and tail (Bst), a mouse minute. *Development.* (2004) 131(16):3907–20. doi: 10.1242/dev.01268

46. Barna M, Pusic A, Zollo O, Costa M, Kondrashov N, Rego E, et al. Suppression of myc oncogenic activity by ribosomal protein haploinsufficiency. *Nature.* (2008) 456(7224):971–5. doi: 10.1038/nature07449

47. Yang Y, Wang C, Yang Q, Kantor AB, Chu H, Ghosn EE, et al. Distinct mechanisms define murine b cell lineage immunoglobulin heavy chain (IgH) repertoires. *Elife.* (2015) 4:e09083. doi: 10.7554/eLife.09083.033

48. Buttgereit F. Brand MD. a hierarchy of ATP-consuming processes in mammalian cells. *Biochem J* (1995) 312(Pt 1):163–7. doi: 10.1042/bj3120163

49. Arguello RJ, Combes AJ, Char R, Gigan JP, Baaziz AI, Bousiquot E, et al. SCENITH: A flow cytometry-based method to functionally profile energy metabolism with single-cell resolution. *Cell Metab* (2020) 32(6):1063–75 e7. doi: 10.1016/j.cmet.2020.11.007

50. Meffre E, Salmon JE. Autoantibody selection and production in early human life. *J Clin Invest* (2007) 117(3):598–601. doi: 10.1172/JCI31578

51. New JS, Dizon BLP, Fucile CF, Rosenberg AF, Kearney JF, King RG. Neonatal exposure to commensal-Bacteria-Derived antigens directs polysaccharide-specific b-1 b cell repertoire development. *Immunity.* (2020) 53(1):172–86 e6. doi: 10.1016/j.immuni.2020.06.006

52. Herzenberg LA. Toward a layered immune system. *Cell.* (1989) 59(6):953–4. doi: 10.1016/0092-8674(89)90748-4

53. Vergani S, Yuan J. Developmental changes in the rules for b cell selection. *Immunol Rev* (2021) 300(1):194–202. doi: 10.1111/imr.12949

54. Tabilas C, Smith NL, Rudd BD. Shaping immunity for life: Layered development of CD8(+) T cells. *Immunol Rev* (2023) 315. doi: 10.1111/imr.13185

Paper III

Article Title: Lin28b regulates glucose metabolism during neonatal B cell development
Running Title: Increased glucose uptake during neonatal B lymphopoiesis

Hugo Åkerstrand[1], Elena Boldrin[1], Leal Oburoglu[2], Giorgia Montano[1], Stijn Vanhee[1], Joan Yuan[1*]

[1] Developmental Immunology Unit, Department of Molecular Hematology, Lund Stem Cell Center, Lund University, Lund, Sweden

[2] Hematopoietic Stem Cell Development Unit, Department of Molecular Medicine and Gene Therapy, Lund Stem Cell Center, Lund University, Lund, Sweden

*** Correspondence**:
Joan Yuan
joan.yuan@med.lu.se

Manuscript length
Number of words: 4579
Number of Figures: 4
Number of Supplemental Figures: 0
Number of Supplemental Tables: 1

Keywords
Lin28b, glucose metabolism, CD5, B-1a cell, Pro-B cell, neonatal B cell development

Abstract

LIN28B is a key regulator of glucose metabolism and naturally expressed by B cell progenitors during early life. During this period, B cell development is characterized by an increase in Pro-B cells and the production of CD5+ (B-1a) B cells, both of which can be re-introduced in adult mice through ectopic LIN28B re-expression. However, although it is well known that Lin28b regulates glucose metabolism in various cell types, any elevation in B cell progenitor glucose metabolism and its importance for early-life B cell development remains unknown. In this study, we provide initial insights into an increased glucose uptake by early-life B cell progenitors that is dependent on Lin28b expression. *Ex vivo* experiments find that LIN28B-mediated expansion of Pro-B cells is correlated with glucose availability, but no impact was observed for the output of CD5+ Imm-B cells, which are the putative B-1a progenitors. We also find that the additional glucose does not yield an increase in ATP and further work is needed to determine its metabolism.

Introduction

B cell development revolves around the stringent control of the B cell receptor (BCR) recombination to create a diverse repertoire for immunological protection while avoiding clones with harmful self-reactivity. Still, a certain degree of self-reactive immunoglobulin (Ig) is readily detected in the serum from both healthy human and mice (*1*), with several specificities being enriched in the murine B-1a subset. Since B-1a cells are primarily generated early in life, there must be underlying exemptions from the strict censoring of the self-reactive BCR during this time. However, although the tolerance mechanisms for BCR selection in adult mice has been extensively studied (*2*), much work remains to understand the early-life counterpart and its role in B-1a development.

The RNA-binding protein LIN28B is expressed by B cell progenitors in early life but not adulthood and re-introduces B-1a output in adult mice upon its ectopic expression (*3*). The B-1a output can be discerned already at the bone marrow Imm-B cell stage by the surface expression of CD5 on a subset of Imm-B cells that give rise to B-1a cells when transferred into recipient animals (*4*). Additionally, ectopic LIN28B enables the development of self-reactive Imm-B cells in the Ig HEL- mice (*5*). Thus, Lin28b controls the positive selection of self-reactive Imm-B cells. Initial investigation into the underlying mechanism(s) identified the transcription factor Arid3a (*6*), increased CD19/PI3K/c-MYC signaling pathway activity (*4*), and heightened rates of protein synthesis (Åkerstrand et al 2023). Additionally, Lin28b is also a key regulator of glucose metabolism in various cell types outside of the B cell development (*7*). Interestingly, it was recently hypothesized how low glucose metabolism in B cell progenitors leads to chronic energy starvation and a catastrophic mismatch between energy supply and demand in clones expressing a self-reactive BCR (*8*). However, any early-life increase in glucose metabolism that depends on Lin28b and its role in the output of self-reactive Imm-B cells needs to be experimentally tested.

In this study, we find that Lin28b does indeed increase the glucose uptake into B cell progenitors. To investigate its importance, we turned to *ex vivo* cultured B cell progenitors that faithfully recapitulates *in vivo* Lin28b phenotypes with increased Pro-B cells and a remarkably efficient output of CD5+ Imm-B cells. By following the progenitors over culture days, we find that LIN28B

increased glucose uptake synchronously throughout the B cell development, which argues for a common LIN28B mechanism shared between the progenitor stages although it has not been resolved in this study. Further, by culturing the progenitors under limiting glucose we found that the Pro-B cell expansion but not CD5+ Imm-B cell output followed the availability of glucose in the cullture media. Finally, we focused on understanding the underlying glucose metabolism by investigating ATP generation but found it unchanged up until an increase at the Imm-B cell stage. Further investigation will be required to fully understand the glucose metabolism and its implications for early-life B cell development.

Materials and methods

Mice

tet-LIN28B mice were generated by intercrossing *Col1a*$^{tetO\text{-}LIN28B}$ (The Jackson Laboratory, #023911) to *Rosa26*^{rtTA*m2} (The Jackson Laboratory, #006965) mice and were originally obtained from the laboratory of George Daley (Harvard Medical School) (*9*). Monoallelic transgene expressing mice were used for experiments. *Rosa26*^{rtTA*m2} heterozygous littermates were used as control mice. For *in vivo* experiments, Doxycycline (Dox) chow (200 mg/kg, Ssnif, cat#A112D70203) was fed to tet-LIN28B and littermates for 10 days before analysis. B6.Cg-*Lin28b*$^{tm1.1Gqda}$/J (*Lin28b* KO) (The Jackson Laboratory, #023917) and C57BLKS-*Rpl24*^{Bst}/J (Bst) (The Jackson Laboratory, #000516) were originally purchased from the Jackson laboratory. Wildtype mice were originally purchased from Taconic (B6NTAC, Taconic). The *Lin28b*-eGFP knock-in strain was generated as previously described (*10*). Adult mice were used at 10 to 16 weeks of age, neonates were analyzed at the indicated days post-birth. Male and female mice were used interchangeably throughout the experiments. Animal husbandry and experimental procedures were performed in accordance with ethical permits issued by the Swedish Board of Agriculture.

Bone marrow cultures

Adult bone marrow B cell precursors from untreated adult mice were expanded and enriched *ex vivo*, as previously described (*11*). Briefly, a single cell suspension of red blood cell lysed bone marrow was plated in pre-warmed RPMI-1640 (Fischer Scientific, cat#21875091) and incubated for 15 min at 37 ^{o}C. The non-adherent cells were isolated and seeded at a cell density of 0.75-1.5 million/mL using fully supplemented RPMI-1640, IL-7 (20 ng/mL, Peprotech, cat#217-17), and Dox (0.1 µg/ml, Sigma-Aldrich, cat#D3072). For glucose titration, the fully supplemented culture medium was mixed in similar prepared media but for glucose-depleted RPMI (Gibco, cat#11879020). Dox treatment for bone marrow cultures was always initiated at the start of the culture, never *in vivo*. The cell culture medium was refreshed every second day.

2-NBDG uptake

2-NBDG (Cayman Chemical, cat#11046) was resuspended at a final concentration of 50 µg/mL in complete RPMI (see Bone marrow cultures for formulation) diluted 50:50 with glucose-free RPMI. B cell progenitors were labeled at a cell density of 750,000 cells per mL for three hours at 37 degrees before washed in FACS buffer, surface stained and analyzed on the flow cytometer.

Flow cytometry

Bone marrow cells were extracted by crushing bones from hind- and front limbs, hips, and sternum using mortar and pestle. The peritoneal cavity was isolated by flushing adult mice with 8 mL of FACS buffer (Hank's Balanced Salt Solution (Gibco, cat#14175-053) supplemented with 0.5% Bovine Serum Albumin (Sigma, cat#A9647) and 2 mM EDTA (Invitrogen, cat#15575-038), or neonates 1-8 mL depending on the age. Red blood cell lysis was performed on bone marrow and spleens using ACK lysis buffer (Fischer Scientific, cat#A1049201), only for mice that were at least 19 days old. Lineage depletion was carried out before cell sorting by MACS Cell Separation and LS columns (Miltenyi Biotec, cat#130-042-401) to deplete CD3+, TER119+, or Gr-1+ cells, according to manufacturer's instructions.

Antibody staining of surface antigen was performed using FACS buffer, at a cell density of 1 x 10^7 cells per 100 µL of FACS buffer with antibodies, for 30 minutes at 4 °C. Analysis of intracellular antigens was done by using the same fixation and permeabilization as was described under "Metabolic labeling of nascent proteins", or using BD Cytofix/Cytoperm fixation/permeabilization kit (BD Biosciences, cat#554714). Maximum of 3 x 10^6 cells per reaction. All flow cytometry experiments were gated on live CD19+ B cells and the following immunophenotypes: Pro-B cells (CD93+IGM–cKIT+), Pre-B cells (CD93+IGM–cKIT– and FSC-A to separate large from small), Imm-B cells (CD93+IGM+). All flow cytometry experiments were performed at the Lund Stem Cell Center FACS Core Facility (Lund University, Lund, Sweden) using BD Fortessa, BD Fortessa X20, BD FACS Aria III, or BD FACS Aria II instruments. Cell sorting was performed using a 70 µm nozzle, 0.32.0 precision mask, and a flow rate below 6000 events/s. Analysis was performed using FlowJo version 10. Antibodies are listed in Supplemental table S1.

ATP levels

ATP levels were determined using CellTiter Glo. 2.0 Cell Viability Assay (Promega, cat#G9241) following the manufacturer's protocol. Briefly, equal amounts of B cell progenitors (at a minimum 5,000 cells) were FACS sorted, re-suspended in room temperature warm RPMI-1640 (Fischer Scientific, cat#21875091) and left at bench to equilibrate. After 30 minutes, an equal volume of Assay reagent (50 µL for 96 well plate analysis) was added and the plate was put on an orbital shaker for 2 minutes, incubated on bench for 10 minutes, and then analyzed using Promega GloMax® Discover. The assay reagent was protected from light at all time.

Seahorse analysis

Extracellular acidification rate was measured using the Agilent Seahorse XF Glycolysis Stress Test (Agilent Technologies, cat#103020-100). Briefly, B cell progenitors were sorted from *ex vivo* cultured bone marrow and 150,000 cells and triplicate technical repeats were analyzed. The sorted cells were resuspended in pre-warmed (37 degrees) XF Glycolysis Stress Test medium (prepared according to kit) that had been supplemented with doxycycline (0.1 µg/mL) and IL-7 (20 ng/mL). Cells were seeded at 150,000 cells per 50 µL of media into plates that had been pre-coated with BD Cell-tak (BD Biosciences, cat#354240), spun down (200G for 1 minute, no deacceleration), and incubated for 30 minutes at 37 degrees in a non-CO2 incubator. Cartridge was prepared with glucose (25 mM final, Sigma, cat#G6152), Oligomycin (4 µM final, Sigma, cat#O4876), and 2-DG (50 mM final, Sigma, cat#D6134). Cartridge was incubated for 20 minutes at 37 degrees in a non-CO2 incubator. Cartridge was then added warm assay medium (130 µL) along the side of each well and kept in the non-CO2 incubator until the run (but not more than 30 minutes).

EdU labeling for cell cycle analysis

Analysis was performed in accordance with the manufacturer's instructions (Invitrogen, cat#C10634). Briefly, single cell suspension of IL-7 cultured B cell progenitors was plated in complete RPMI-1640 (Fischer Scientific, cat#21875091) and labeled with EdU (10 µM) for 30 minutes. Cells were then stained for surface proteins before fixation and permeabilization. The

EdU was Click-iT ligated to Alexa Fluor 555 and analyzed with DAPI for separation according to cell cycle phase.

Statistical analysis

All statistical analysis was carried out in R (version 4.1.2) and RStudio (version 1.4.1717), using functions from the following packages: tidyverse (version 1.3.1), DESeq2 (version 1.32.0), rstatix (version 0.7.0), and ggpubr (version 0.4.0). Bar graphs show the mean with standard deviation. Line graphs show the mean with standard deviation. Statistical tests used are noted in the figure legends.

Results

A Lin28b-dependent elevation in glucose uptake across all stages of B cell development

We recently reported on increased protein synthesis and biomass accumulation in small Pre-B and Imm-B cells by LIN28B, with a particularly strong increase in the positively selected CD5+ Imm-B cells (Åkerstrand et al 2023). Here, we considered glucose metabolism as an additional LIN28B-mechanism to support the biomass accumulation in the B cell progenitors for an output of CD5+ Imm-B cells. To test this, we first quantified glucose uptake by FACS using the fluorescent glucose analog 2-(*N*-(7-nitrobenz-2-oxa-1,3-diazol-4-yl)amino)-2-deoxyglucose (2-NBDG). We first measured the effect of endogenous LIN28B in neonatal B cell progenitors using the B6.Cg-*Lin28b*$^{tm1.1Gqda}$/J mouse model that previously identified the role of Lin28b on glucose metabolism outside of B cell development (*12*). As expected, large Pro-B cells had the maximum 2-NBDG uptake by and the minimum was measured for small Pre-B cells. This fluctuation in 2-NBDG uptake was observed in both neonates and adults, but neonatal progenitors had consistently increased 2-NBDG uptake across all progenitor stages. Further analysis of *Lin28b* knockout neonates found that the 2-NBDG levels decreased compared to wildtype littermates, in line with glucose metabolism in neonates being affected by endogenous *Lin28b* (Figure 1A-B). Next, we analyzed if ectopic re-expression of LIN28B in adult mice phenocopied the increased glucose uptake in neonates. To this end, we used the doxycycline inducible tet-Lin28b mouse model (*Col1a*$^{tetO\text{-}LIN28B}$ *Rosa26*^{rtTA*m2}) that was previously used to study glucose metabolism outside of the B cell development (*9*) and is capable of re-introducing B-1a output in adult mice (*4*). Indeed, following 10 days of doxycycline induction for ectopic re-expression of LIN28B in the adult B cell progenitors, 2-NBDG uptake was increased in tet-Lin28b mice relative to littermate controls (Figure 1C-D). Thus, as for many other cell types (*7*), LIN28B increases glucose uptake across all stages of bone marrow B cell development.

An *ex vivo* culture system of B cell progenitors recapitulates the *in vivo* Lin28b phenotypes

The elevated 2-NBDG uptake was in line with a role for augmented glucose metabolism in LIN28B-dependent B lymphopoiesis. However, testing its role *in vivo* is challenging due to the broad effects of glucose-starved diets across cell types and tissues. In addition, limited numbers of B cell progenitors *in vivo* make it challenging to conduct metabolic assays that require many cells, such as extracellular flux assays using the Seahorse system. To overcome these limitations, we turned to *ex vivo* expansion of bone marrow B cell progenitors under saturating levels of IL-7 (*11*). Such cultures greatly expand the available number of B cell progenitors and affords careful control over the glucose levels in the culture media.

We first established the suitability of using the cultures by analyzing them for Pro-B cell expansion and CD5+ Imm-B output, two hallmark features of LIN28B-induced B cell development *in vivo* (*4*) (Åkerstrand et al 2023). To this end, we *ex vivo* induced bone marrow from untreated mice with doxycycline (0.1 µg/mL) and expanded them under saturating IL-7 (20 ng/mL) for five days before phenotypic analysis of the B cell development (Figure 2A). Following five days, the B cells had become highly enriched in the cultures with overall comparable progenitor frequencies between tet-Lin28b and littermate controls (Figure 2B). However, as expected, Pro-B cells was always more frequent in tet-Lin28b cultures (Figure 2C). As *in vivo* (Åkerstrand et al 2023), no Lin28b-

increase in proliferation of Pro-B cells was detected by cell cycle analysis, which indicates an alternative mechanism for how Lin28b enriches the Pro-B cells (Figure 2D). Since there was significant variation in total cell numbers across experiments it foregoes the usefulness of pooling data on total cell numbers (data not shown). Finally, we analyzed the frequency of CD5+ Imm-B cells, which is the *in vivo* B-1a progenitor and the result of positive selection by LIN28B (*4*). Remarkably, far more CD5+ Imm-B cells were isolated from the *ex vivo* cultures than *in vivo*, with up to 70% of the total Imm-B cells being CD5 positive (Figure 2E-F). In summary, we find that *ex vivo* cultures of tet-Lin28b bone marrow B cell progenitors under saturating levels of IL-7 recapitulate *in vivo* phenotypes and even exceed them when it comes to the output of CD5+ Imm-B cells. These cultures are therefore suitable for investigating Lin28b-induced B cell development, including the role of increased glucose uptake.

LIN28B increases glucose uptake simultaneously across B cell development *ex vivo*

Having established how the *ex vivo* culture was a good model system for Lin28b-induced B cell development, we next asked if it also recapitulated the increase in glucose uptake. To this end, we measured 2-NBDG uptake by control and tet-Lin28b progenitors on culture day five. Indeed, all stages of B cell progenitors took up more 2-NBDG in tet-Lin28b cultures and therefore recapitulated its effect *in vivo* (Figure 3A-B).

Next, we considered the importance of an increased glucose uptake for LIN28B induced B cell development. Since glucose uptake was uniformly increased by LIN28B across all stages, it precedes the effect on protein synthesis, c-MYC, and BCR signaling in the small Pre-B and Imm-B cells (*4*) (Åkerstrand et al 2023). Therefore, we wondered if increased glucose metabolism in Pro-B and large Pre-B cells was a prerequisite for the positive selection of the self-reactive BCR. To get an insight into this, we analyzed the timing for LIN28B-induced increase of 2-NBDG uptake into the different B cell progenitors. We reasoned that if 2-NBDG uptake increased first in the upstream progenitors it would indicate that it is a prerequisite for the output of self-reactive clones, whereas if it increased synchronously in all progenitors it would argue for a common Lin28b-dependent mechanism independent from its effect on BCR selection. Following immediate *ex vivo* induction of LIN28B upon plating, analysis of Pro-B cells found that the 2-NBDG uptake increased in tet-Lin28b cultures around culture day 3 and then grew progressively stronger up until termination on culture day 5 (Figure 3C). The same kinetic of increased 2-NBDG uptake in tet-Lin28b cultures was also found for the other progenitor stages (Figure 3D). Thus, we find that LIN28B increases 2-NBDG uptake synchronously across B cell development, likely by a shared mechanism in all the progenitors.

Finally, we also tested the role of glucose in Lin28b-induced B cell development by culturing the progenitors in glucose-starved media. Whole bone marrow from tet-Lin28b or control mice were plated in normal concentrations of IL-7 and doxycycline but under decreasing glucose concentration. The cultures were then analyzed for Pro-B cell expansion and CD5+ Imm-B output at culture day five (Figure 3E). Our analysis found that the availability of glucose impacted on the Pro-B cell frequencies in the tet-Lin28b cultures (Figure 3F) but without any correlation to the CD5+ Imm-B output (Figure 3G). Taken together, we find that 2-NBDG uptake *ex vivo* was increased synchronously across the progenitor stages around culture day three by LIN28B, which

is in line with a common LIN28B mechanism the B cell progenitor stages. Additionally, titration of available glucose in cell culture media found a sensitivity for LIN28B-induced Pro-B cell expansion but not the CD5+ Imm-B output.

Progenitor stage specific effect on glucose metabolism by LIN28B

Glucose can be metabolized in several ways, including the generation of ATP through aerobic glycolysis or oxidative phosphorylation, or it can be used for other anabolic pathways such as the pentose phosphate pathway (*13*). We focused on the impact of glucose metabolism for the generation of ATP, as it has been suggested to limit the development of self-reactive clones (*8*). To this end, we performed Seahorse analysis on sorted B cell progenitors from day 5 *ex vivo* cultures. Surprisingly, and despite the increased 2-NBDG uptake, analysis of aerobic glycolysis found it decreased in LIN28B Pro-B cells and not statistically significant different in large Pre-B cells (Figure 4A-B). Analysis of an equal amount of small Pre-B or Imm-B cells did not generate any signal (data not shown). Thus, extracellular flux assay found no indication that the increased glucose uptake into LIN28B-expressing Pro-B or large Pre-B cells is used for aerobic glycolysis, suggesting an alternative metabolism. In line with this, *in vivo* analysis of ATP levels from sorted B cell progenitors found no increase in tet-Lin28b mice before the Imm-B cell stage (Figure 4C). We conclude that although tet-Lin28b B cell progenitors take up more glucose, our investigations into aerobic glycolysis and ATP levels suggest that such an increased uptake has progenitor stage specific effects with no increased ATP before the Imm-B stage.

Discussion

The purpose of this study was to investigate on one hand the Lin28b capacity for increased glucose metabolism and on the other the Lin28b mechanism supporting B-1a output. Our hypothesis was that Lin28b may depend on augmented glucose metabolism during B lymphopoiesis to increase its biomass and overcome the central tolerance checkpoint (*8*). Indeed, LIN28B elevated 2-NBDG uptake across all stages of bone marrow B cell development *in vivo* that was in line with augmented glucose metabolism. As it was synchronously increased across all stages of development following induction of tet-Lin28b progenitors *ex vivo*, we believe that a common mechanism for increased glucose uptake is shared across all progenitors stages. However, analysis of previously published RNA-seq data (Åkerstrand et al 2023) did not identify any common transcriptional increase of glucose transporters, signaling pathways, or single genes that could explain a shared LIN28B mechanism (data not shown) and further work is warranted.

To understand the importance of glucose metabolism, we turned to *ex vivo* cultures of adult tet-Lin28b or littermate control bone marrow B cell progenitors. While such an approach recapitulated the *in vivo* phenotypes and therefore affords studying the LIN28B mechanisms in B cell progenitors, it also has its limitations. For example, IL-7 results in blocked B cell development around the Pro-B and large Pre-B cell stage, which become metabolically hyperactivated by IL-7 and nutrient replete cell culture media (*14*). Additionally, since complete culture media contains a super-physiological amount of glucose, its concentration might saturate the smaller CD5+ Imm-B cells even when glucose was titrated down and thereby give the false impression that they are impervious to the glucose levels *in vivo*. To this end, the use of chemically defined media that more accurately resemble the physiological availability of nutrients *in vivo* will be informative for studying its impact on CD5+ Imm-B cells. Furthermore, 2-NBDG is an imperfect representation of glucose uptake (*15*) and a limitation of the current study. Additional experiments using isotope-labeled glucose to assess both uptake and fueling of various anabolic pathways, including the pentose phosphate pathway, will be necessary to better understand the role of increased glucose in Lin28b induced B cell progenitors.

Strikingly, the tet-Lin28b cultures had high levels of CD5+ Imm-B cells that far exceeded the normal output *in vivo* and in line with elevated levels of positive selection *ex vivo*. While we cannot rule out a direct LIN28B effect on CD5+ Imm-B cells in culture, they did not proliferate and are therefore not enriched by expansion at this stage. Instead, we consider two alternative B cell development-dependent mechanisms that could explain the super-physiological CD5+ Imm-B frequencies: 1) that B-1a development is favored over B-2 development in culture and/or 2) that a B-1a biased Pro-B cell is favorably enriched in IL-7 cultures and therefore dominates the output of Imm-B cells. Previous work supports both these ideas and warrant their further exploration. For example, early-life B-1 development differs from adult B-2 in response to the pre-BCR checkpoint (*16, 17*) that censors the output of self-reactive clones (*18*). Such a difference might be accentuated under IL-7 culture conditions that enriches for cells around this developmental stage. Additionally, premature kappa recombination in Pro-B cells has been reported for B-1a development in the fetal liver (*16*). If such premature light chain recombination also happens to a high degree in IL-7 cultured Pro-B cells *ex vivo,* it could enable them to overcome the block in B cell development and explain why CD5+ Imm-B dominates the output

(*19*). It is tempting to speculate that a Pro-B cell dependent mechanism might underlie the CD5+ Imm-B output, since they are the primarily expanded population in IL-7 cultures and we previously found that LIN28B expression in Pro-B cells is critical for the B-1a output *in vivo (4)*. Finally, our lab previously found that B-1a output from adult bone marrow is restricted to a fraction of the total B cell producing progenitors (*20*) and perhaps such a B-1a biased progenitor becomes favorably enriched in these cultures. However, how such a favorable enrichment might come about is not known. Further work will be necessary to understand the underlying reason for elevated CD5+ Imm-B cells in culture with important implications for our understanding on B-1a development *in vivo* and how LIN28B affords it.

Acknowledgments
We thank Jonas Ungerbäck and Johanna Tingvall-Gustafsson for their help with bioinformatics. We thank Jenny Hansson and Svetlana Soboleva for their input. Finally, we also thank the FACS and Bioinformatics core facilities at the Lund Stem Cell Center for their support.

Funding
J.Y. was supported by the Swedish Research Council, the Swedish Cancer Society, the European Research Council (715313), Knut and Alice Wallenberg Foundation and the Wenner-Gren Foundations.

References

1. A. Bendelac, M. Bonneville, J. F. Kearney, Autoreactivity by design: innate B and T lymphocytes. *Nat Rev Immunol* **1**, 177-186 (2001).
2. D. Nemazee, Mechanisms of central tolerance for B cells. *Nat Rev Immunol* **17**, 281-294 (2017).
3. J. Yuan, C. K. Nguyen, X. Liu, C. Kanellopoulou, S. A. Muljo, Lin28b reprograms adult bone marrow hematopoietic progenitors to mediate fetal-like lymphopoiesis. *Science* **335**, 1195-1200 (2012).
4. S. Vanhee *et al.*, Lin28b controls a neonatal to adult switch in B cell positive selection. *Sci Immunol* **4**, (2019).
5. X. Xu *et al.*, An ontogenetic switch drives the positive and negative selection of B cells. *Proc Natl Acad Sci U S A* **117**, 3718-3727 (2020).
6. Y. Zhou *et al.*, Lin28b promotes fetal B lymphopoiesis through the transcription factor Arid3a. *J Exp Med* **212**, 569-580 (2015).
7. N. Shyh-Chang, G. Q. Daley, Lin28: primal regulator of growth and metabolism in stem cells. *Cell Stem Cell* **12**, 395-406 (2013).
8. M. Muschen, Metabolic gatekeepers to safeguard against autoimmunity and oncogenic B cell transformation. *Nat Rev Immunol* **19**, 337-348 (2019).
9. H. Zhu *et al.*, The Lin28/let-7 axis regulates glucose metabolism. *Cell* **147**, 81-94 (2011).
10. T. A. Kristiansen *et al.*, Developmental cues license megakaryocyte priming in murine hematopoietic stem cells. *Blood Adv*, (2022).
11. T. M. Holl, B. F. Haynes, G. Kelsoe, Stromal cell independent B cell development in vitro: generation and recovery of autoreactive clones. *J Immunol Methods* **354**, 53-67 (2010).
12. G. Shinoda *et al.*, Fetal deficiency of lin28 programs life-long aberrations in growth and glucose metabolism. *Stem Cells* **31**, 1563-1573 (2013).
13. K. Voss *et al.*, A guide to interrogating immunometabolism. *Nat Rev Immunol* **21**, 637-652 (2021).
14. Y. Dong, R. Tu, H. Liu, G. Qing, Regulation of cancer cell metabolism: oncogenic MYC in the driver's seat. *Signal Transduct Target Ther* **5**, 124 (2020).
15. L. V. Sinclair, C. Barthelemy, D. A. Cantrell, Single Cell Glucose Uptake Assays: A Cautionary Tale. *Immunometabolism* **2**, e200029 (2020).
16. J. B. Wong *et al.*, B-1a cells acquire their unique characteristics by bypassing the pre-BCR selection stage. *Nat Commun* **10**, 4768 (2019).
17. D. Kitamura *et al.*, A critical role of lambda 5 protein in B cell development. *Cell* **69**, 823-831 (1992).
18. R. A. Keenan *et al.*, Censoring of autoreactive B cell development by the pre-B cell receptor. *Science* **321**, 696-699 (2008).
19. D. Melamed, J. A. Kench, K. Grabstein, A. Rolink, D. Nemazee, A functional B cell receptor transgene allows efficient IL-7-independent maturation of B cell precursors. *J Immunol* **159**, 1233-1239 (1997).
20. T. A. Kristiansen *et al.*, Cellular Barcoding Links B-1a B Cell Potential to a Fetal Hematopoietic Stem Cell State at the Single-Cell Level. *Immunity* **45**, 346-357 (2016).

Table S1. Antibodies and reagents used for Flow Cytometry *or* Western Blot

Antigen	Fluorochrome	Clone	Manufacturer	Reference#
7-AAD	-	-	BD Bioscience	559925
B220	APC Cy7	RA3-6B2	BioLegend	103224
B220	PE CF594	RA3-6B2	BD Biosciences	562313
CD117	BV421	2B8	BD Biosciences	562609
CD117	PE	2B8	Invitrogen	12-1171-82
CD19	APC Cy7	1D3	BD Biosciences	557655
CD19	BV786	1D3	BD Biosciences	563333
CD25	PE eFluor610	PC61.5	Invitrogen	61-0251-82
CD3	PE Cy5	145-2C11	BioLegend	100310
CD5	BV421	53-3.3	BD Biosciences	562739
CD5	PE	53-7.3	BioLegend	100608
CD93	APC	AA4.1	BioLegend	136510
CD93	BV786	AA4.1	BD Biosciences	740941
c-MYC	Unconjugated	Y69	Abcam	Ab32072
Gr-1	PE Cy5	RB6-8C5	BioLegend	108410
IgM	FITC	11/41	BD Biosciences	553437
IgM	PE Cy7	RMM-1	BioLegend	406514
Alkyne, 5-isomer	AF488	-	Invitrogen	A10267
Ter119	PE Cy5	TER-119	BioLegend	116210
Tubulin alpha			CST	2125
FLAG M2			Sigma	F1804
LIN28B			CST	4196

Captions

Figure 1. Lin28b-dependent increase in glucose uptake into B cell progenitors

(A) Representative histograms showing the 2-NBDG uptake by B cell progenitors from 3-day-old neonates of indicated genotypes or an adult wildtype control mouse. (**B**) Quantification of 2-NBDG median fluorescence intensity (MFI) for indicated bone marrow B cell progenitor stages. The MFI was normalized to the signal in small Pre-B from adult mice. Data from five separate experiments. **(C)** Representative histograms showing the 2-NBDG uptake by B cell progenitors from an adult tet-Lin28b or littermate control mouse. **(D)** Quantification of 2-NBDG MFI for indicated bone marrow B cell progenitor stages. The MFI was normalized to the littermate control for each separate cell type. Data from four separate experiments. Wilcox test was used to calculate p-values for B and D. *p<0.05, **p<.001. Bars or crossbar show mean and error bars show the standard deviation.

Figure 2. E*x vivo* cultured tet-Lin28b B cell progenitors recapitulates the *in vivo* phenotypes

(A) Schematic of experimental setup for *ex vivo* cultures of bone marrow B cell progenitors. Whole bone marrow from adult tet-Lin28b or littermate control mice were expanded in the presence of IL-7 (20 ng/mL) and doxycycline (dox, 0.1 µg/mL) for five days, before analysis. **(B)** Representative FACS analysis and gating strategy used throughout the study. Frequencies on culture day five from a littermate control (left) or tet-Lin28b mouse (right) is shown. **(C)** Quantification of the B cell progenitor frequencies out of the expanded B cells on culture day five. Data from 14 separate experiments. **(D)** Quantification of cell cycle analysis as was measured using EdU and DAPI uptake to separate the cells into the respective phase. Data from three separate experiments. **(E)** Representative histograms showing CD5 expression on culture day five Imm-B cells from the adult littermate control (left) or tet-Lin28b (right). **(F)** Quantification of the CD5 MFI data. Data from 14 separate experiments. Wilcox test was used to calculate p-values in C, D, and F. *p<0.05, ***p<0.001, ****p<0.0001. Bars show mean and error bars show standard deviation.

Figure 3. LIN28B increases glucose uptake simultaneously across B cell development *ex vivo*

(A) Representative histograms showing the 2-NBDG uptake by adult B cell progenitors on culture day five of tet-Lin28b a littermate control mouse. **(B)** Quantification of 2-NBDG median fluorescence intensity (MFI) for the B cell progenitor stage. The MFI was normalized to the signal in small Pre-B from littermate control mice. Data from four separate experiments. **(C)** Representative histograms showing 2-NBDG uptake by Pro-B cells of the indicated genotype on culture day 2-5. **(D)** Quantification of 2-NBDG median fluorescence intensity (MFI) on each day of the culture. The measured 2-NBDG MFI is presented relative to the signal in the littermate control on each day. Data from three separate experiments. **(E)** Schematic of experimental setup glucose titrated *ex vivo* cultures of bone marrow B cell progenitors. Whole bone marrow from adult tet-Lin28b or littermate control mice were expanded in the presence of IL-7 (20 ng/mL), doxycycline (dox, 0.1 µg/mL) and decreasing concentration of glucose. At culture day five, the frequency of Pro-B cells (F) and CD5+ Imm-B output (G) was analyzed for any correlation to glucose levels. **(F)** Graph showing frequency of Pro-B cells against the level of glucose in the culture media. **(G)** Graph showing frequency of CD5+ Imm-B cells against the level of glucose in the culture media. Wilcox test was used to calculate p-values in B and D. *p<0.05, **p<0.01.

Correlation analysis was performed using Pearson's test in D. Bars (B) or dots (D) show mean, error bars show standard deviation.

Figure 4. Stage-specific effect on glucose metabolism by LIN28B
(A) Representative line graphs showing the measured extracellular acidification rate (ECAR) by the Seahorse flux analyzer. B cell progenitors were FACS sorted from day five cultures of adult bone marrow of the indicated genotype that had been expanded under standard culture conditions. **(B)** Quantification of aerobic glycolysis using the ECAR as measured in A. Data from three separate experiments. **(C)** ATP levels in FACS sorted adult bone marrow B cell progenitors at the indicated developmental stage and genotype. Data from four separate experiments. Wilcox test was used to calculate p-values in B and C. *$p<0.05$.

Figure 1

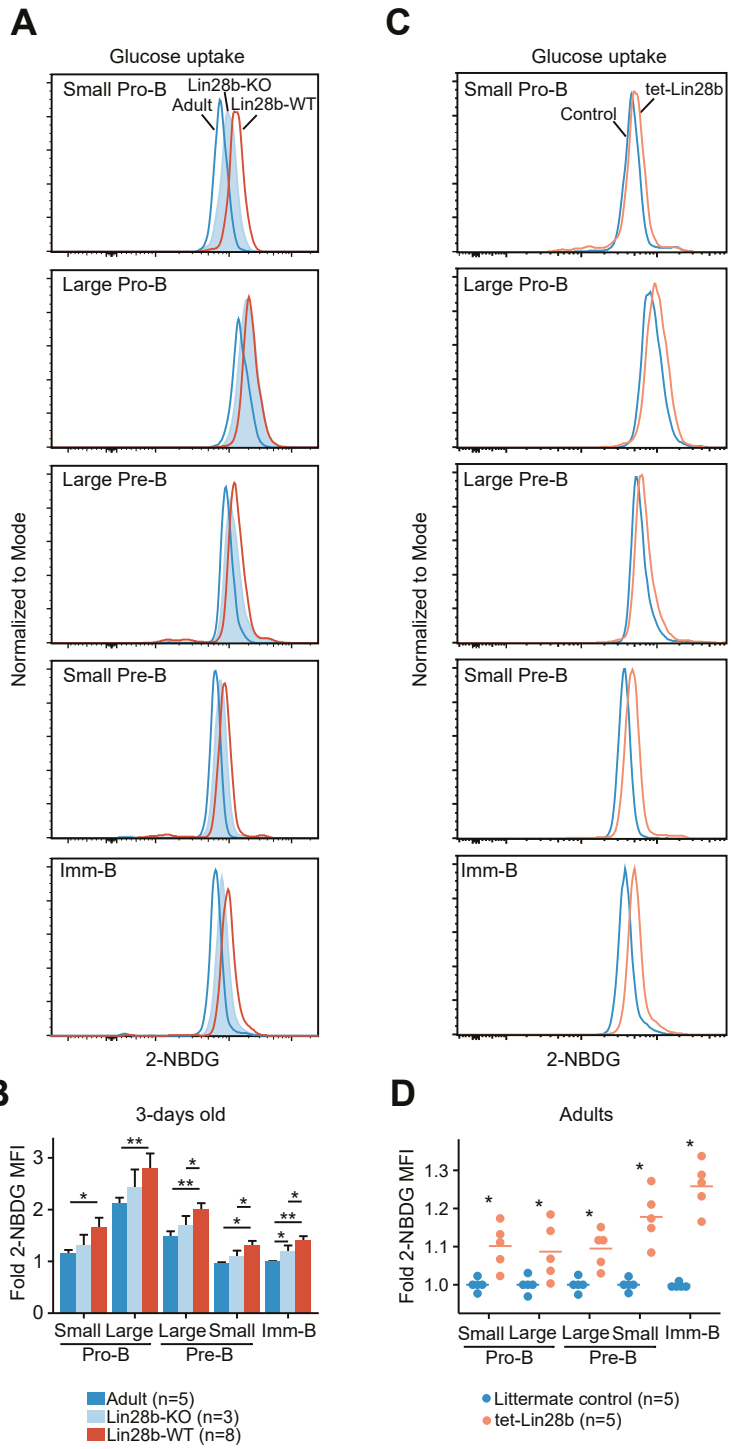
A
Glucose uptake
Small Pro-B
Lin28b-KO
Adult
Lin28b-WT
Large Pro-B
Large Pre-B
Small Pre-B
Imm-B
Normalized to Mode
2-NBDG
C
Glucose uptake
Small Pro-B
tet-Lin28b
Control
Large Pro-B
Large Pre-B
Small Pre-B
Imm-B
Normalized to Mode
2-NBDG
B
3-days old
Fold 2-NBDG MFI
Small Large Large Small Imm-B
Pro-B Pre-B
Adult (n=5)
Lin28b-KO (n=3)
Lin28b-WT (n=8)
D
Adults
Fold 2-NBDG MFI
Small Large Large Small Imm-B
Pro-B Pre-B
Littermate control (n=5)
tet-Lin28b (n=5)

Figure 2

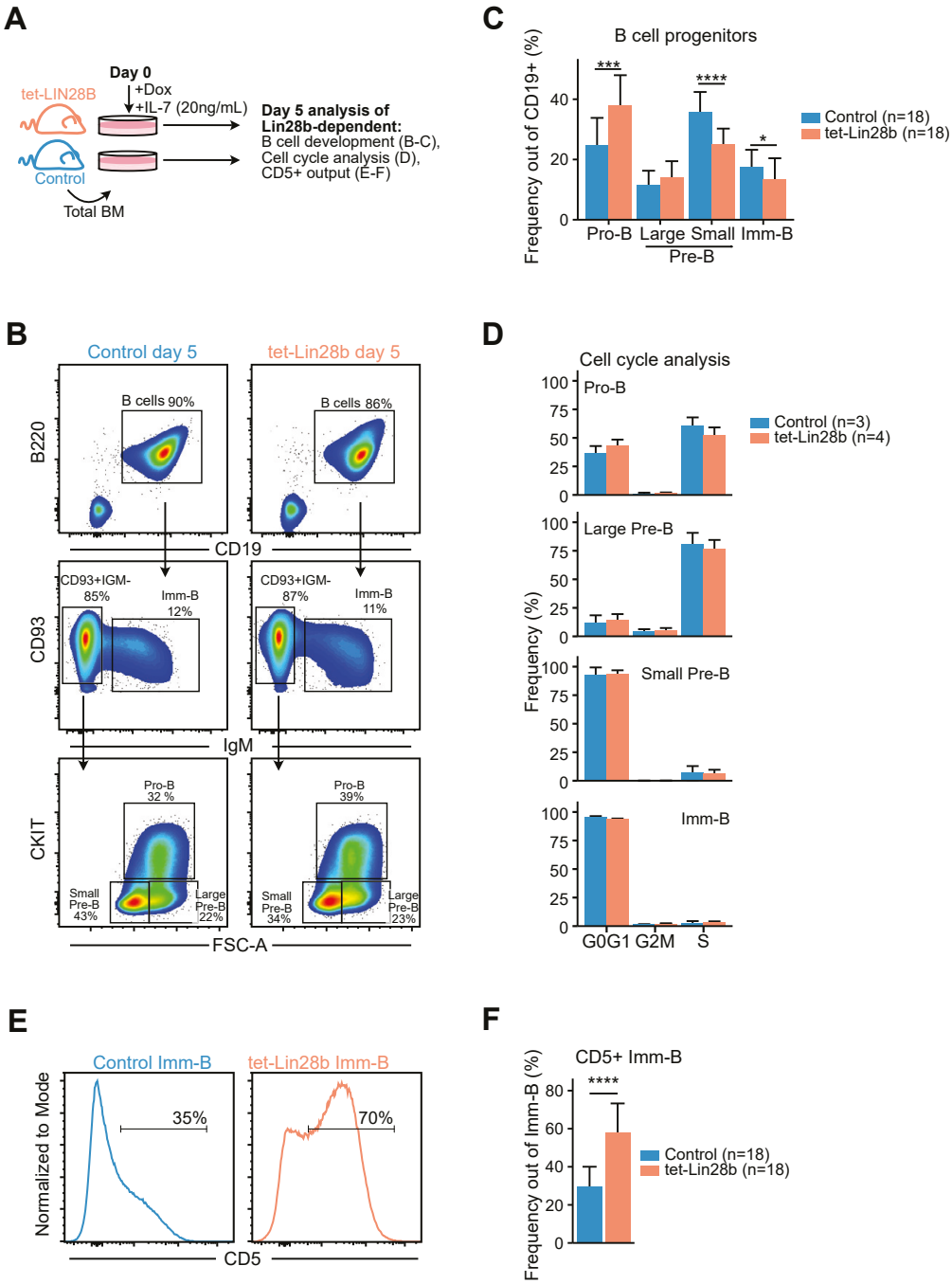
A
Day 0
+Dox
+IL-7 (20ng/mL)
tet-LIN28B
Control
Total BM
Day 5 analysis of Lin28b-dependent:
B cell development (B-C),
Cell cycle analysis (D),
CD5+ output (E-F)
C
B cell progenitors
Frequency out of CD19+ (%)
Pro-B
Large Pre-B
Small Pre-B
Imm-B
Control (n=18)
tet-Lin28b (n=18)
B
Control day 5
tet-Lin28b day 5
B220
CD19
B cells 90%
B cells 86%
CD93
CD93+IGM- 85%
Imm-B 12%
CD93+IGM- 87%
Imm-B 11%
IgM
CKIT
Pro-B 32 %
Small Pre-B 43%
Large Pre-B 22%
Pro-B 39%
Small Pre-B 34%
Large Pre-B 23%
FSC-A
D
Cell cycle analysis
Pro-B
Large Pre-B
Small Pre-B
Imm-B
Frequency (%)
Control (n=3)
tet-Lin28b (n=4)
G0G1
G2M
S
E
Control Imm-B
tet-Lin28b Imm-B
Normalized to Mode
35%
70%
CD5
F
CD5+ Imm-B
Frequency out of Imm-B (%)
Control (n=18)
tet-Lin28b (n=18)

Figure 3

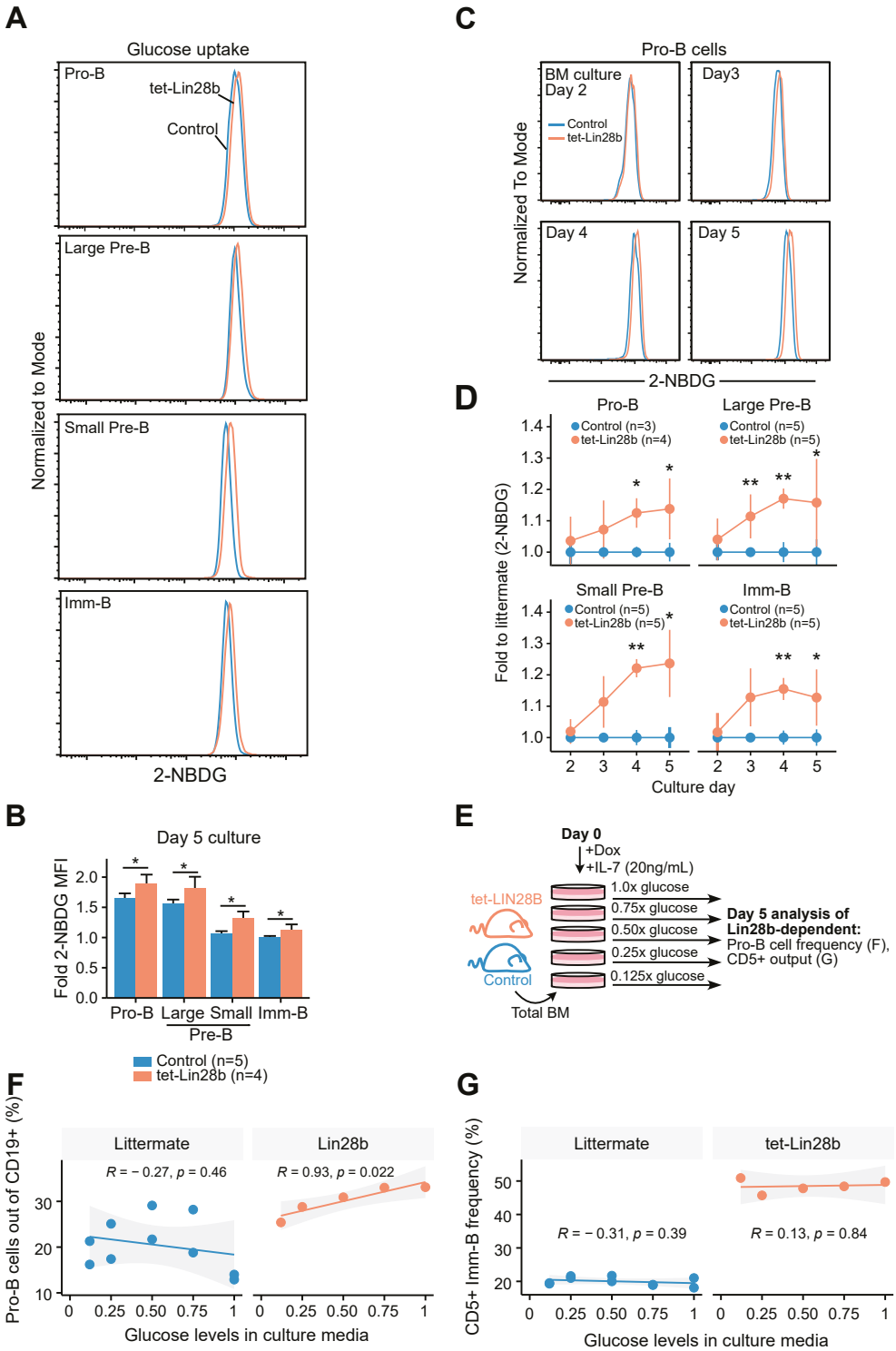
A
Glucose uptake
Pro-B
tet-Lin28b
Control
Large Pre-B
Small Pre-B
Imm-B
Normalized to Mode
2-NBDG
B
Day 5 culture
Fold 2-NBDG MFI
Pro-B
Large Pre-B
Small Pre-B
Imm-B
Control (n=5)
tet-Lin28b (n=4)
C
Pro-B cells
BM culture Day 2
Day3
Day 4
Day 5
Control
tet-Lin28b
Normalized To Mode
2-NBDG
D
Pro-B
Large Pre-B
Small Pre-B
Imm-B
Control (n=3)
tet-Lin28b (n=4)
Control (n=5)
tet-Lin28b (n=5)
Fold to littermate (2-NBDG)
Culture day
E
Day 0
+Dox
+IL-7 (20ng/mL)
tet-LIN28B
Control
Total BM
1.0x glucose
0.75x glucose
0.50x glucose
0.25x glucose
0.125x glucose
Day 5 analysis of Lin28b-dependent:
Pro-B cell frequency (F),
CD5+ output (G)
F
Littermate
Lin28b
R = − 0.27, p = 0.46
R = 0.93, p = 0.022
Pro-B cells out of CD19+ (%)
Glucose levels in culture media
G
Littermate
tet-Lin28b
R = − 0.31, p = 0.39
R = 0.13, p = 0.84
CD5+ Imm-B frequency (%)
Glucose levels in culture media

Figure 4

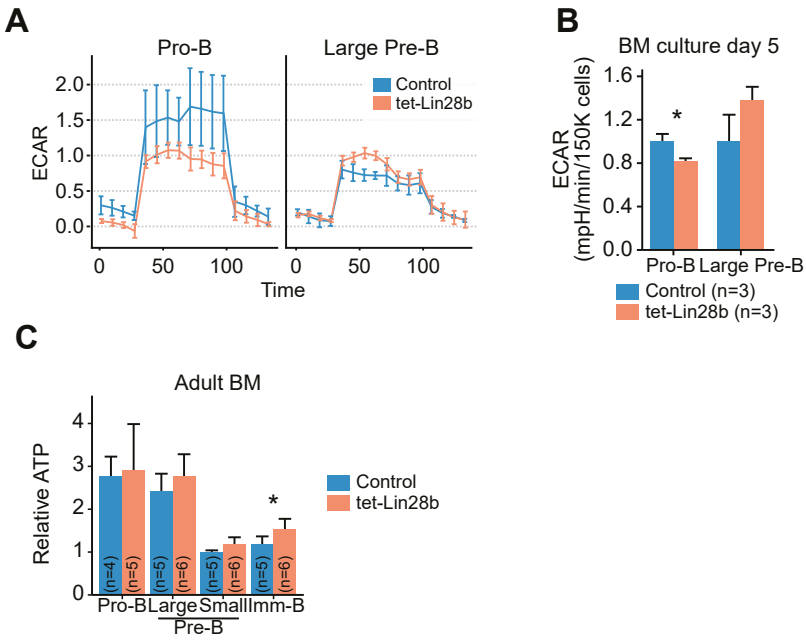
A
Pro-B
Large Pre-B
Control
tet-Lin28b
ECAR
2.0
1.5
1.0
0.5
0.0
0
50
100
Time
B
BM culture day 5
ECAR
(mpH/min/150K cells)
1.6
1.2
0.8
0.4
0.0
*
Pro-B Large Pre-B
Control (n=3)
tet-Lin28b (n=3)
C
Adult BM
Relative ATP
4
3
2
1
0
*
(n=4)
(n=5)
(n=5)
(n=6)
(n=5)
(n=6)
(n=5)
(n=6)
Pro-B
Large
Small
Imm-B
Pre-B
Control
tet-Lin28b